MATHEMATICAL ANALYSIS OF PRESSURE CHAMBER EFFLUX EXPERIMENTS

Richard L. Stroshine, Ph.D.

Cornell University 1980

The Scholander pressure chamber is one of several devices used to study the water relations of green plants. For field work it can be used to rapidly measure leaf water potential, and for laboratory studies it can be used to determine the turgor and osmotic components of plant water potential.

A series of experiments were conducted on wheat leaves. A leaf was cut from the plant and placed in the cylindrical chamber so that its cut end protruded through an air-tight seal. When the chamber was pressurized to several atmospheres, water appeared at the cut end. When the pressure was increased several more atmospheres, water flowed from the cut end of the leaf for 10 to 40 minutes. The total efflux was dependent on the water potential of the leaf. Efflux curves for the experiments were drawn by plotting the total water expressed as a function of time after the pressure increase. The total efflux was dependent on the water potential of the leaf. This dissertation is an experimental and mathematical analysis of the efflux curves. The specific objectives of the study were:

(i) To develop a mathematical model relating relevant physiological and anatomical properties of the leaf to its efflux curve.

(ii) To determine the major sources of resistance to water flow through the wheat leaf.

(iii) To use the model as a tool to explore the influence of the experimental procedures on experimental results.

Efflux experiments were performed on wheat leaves of varying length. Fifteen minutes after application of an overpressure, there was no measurable water flow from shorter leaves. Measurable water flow from longer leaves continued for up to 40 minutes.

Leaf anatomy was studied using scanning and transmission electron microscopes, and a light microscope. Cross sections taken from leaves which had been tested in the chamber showed that the cells were undamaged and that the relative volume of airspace in the leaf decreased. A model of xylem deformation suggested that the vessels could collapse when subjected to pressures normally used in the experiments. However, the vessels in the leaf cross sections were in tact. Sections taken in the vicinity of the chamber seal showed distortion and disruption of epidermal and mesophyll cells but no damage to xylem vessels.

Two models were developed to describe the changes in leaf cell water potential during an efflux experiment. Both assumed that water flowed from cells to the nearest xylem element through which it flowed from the leaf. The first model neglected the xylem resistance of the leaf and assumed that water flowed from one cell vacuole to the next. Models in which water flowed through one, two, three, or five cells

gave distinct efflux curves. Decreasing the membrane permeability in the one cell model made its efflux curve nearly identical to the efflux curve of a two cell model having a higher membrane permeability.

The second model combined the efflux resistances of the flow through xylem vessels and through a single membrane. Xylem resistance was estimated using Poiseuille's law. Results from this model suggested that only the bundles which have small diameter vessels offer enough resistance to water flow to appreciably affect water efflux from the leaf.

The second model has implications for the use of the pressure chamber. During most pressure chamber experiments, the chamber pressure is increased for several minutes and then reduced. In most cases, when the pressure is reduced, water is still flowing from the cut end. The model suggests that such a technique may introduce an experimental error because the cells in the leaf may not have attained equilibrium.

MATHEMATICAL ANALYSIS OF PRESSURE CHAMBER EFFLUX CURVES

A Thesis

Presented to the Faculty of the Graduate School

of Cornell University

in Partial Fulfillment for the Degree of

Doctor of Philosophy

by

Richard L. Stroshine

May, 1980

BIOGRAPHICAL SKETCH

Richard L. Stroshine was born in 1947 and reared on a grain farm in Oregon, Ohio. He earned a Bachelor of Science in Agricultural Engineering from Ohio State University in June, 1971 and a Master of Science in Agricultural Engineering in August of 1971. His Master's Thesis, entitled Development of a Test to Measure Soil Oxygen Demand, was in the area of agricultural waste management.

In June 1972 he graduated from U.S. Naval Officer Candidate School at Newport, Rhode Island. He served aboard the USS Raleigh, LPD-1 from August of 1972 to June of 1975.

In August of 1975 he was awarded a Liberty Hyde Bailey Research Assistanceship and began his doctoral studies at Cornell University. He joined the faculty of Purdue University as an assistant professor of Agricultural Engineering in February, 1980.

ACKNOWLEDGEMENTS

This research would not have been possible without the help of many people. Dr. J. Robert Cooke was my committee chairman and Dr. Richard Rand of Theoretical and Applied Mechanics and Dr. Tom Sinclair of Agronomy served on my committee. I extend my thanks to them. The encouragement and support of Dr. Cooke during these past 4 years have been of inestimable value. His advice has been both wise and trustworthy. Dr. Richard Rand is to be especially thanked for his suggestions about the mathematical approaches to the problem formulation and solution. My discussions with him taught me much about modeling. At times when they were most needed, Dr. Tom Sinclair's questions motivated me to try approaches I might otherwise have overlooked.

During the course of my work on this topic, I had helpful discussions with many researchers including Dr. Herman Wiebe of the Utah State University, Dr. Peter Kaufman of the University of Michigan, Dr. Park Nobel of the University of California at Los Angeles, Dr. Ted Hammel of Scripps Institute of Oceanography, and Dr. Betty Klepper of the Columbia Plateau Research Center at Pendleton, Oregon.

Many people here at Cornell also gave me assistance. Dr. Peter Steponkus made available the laboratory and greenhouse space. Dr. Jay Cutler, Mr. Kevin Shahan, and Mr. Jeff Melkonian helped with pressure chamber experiments. My discussions with Dr. Cutler about the theory

and use of the pressure chamber were especially helpful. Dr. Cutler and Mr. Shahan performed the first group of efflux experiments reported in this thesis. Dr. Jean Chabot helped me with the anatomy studies by fixing and staining samples, preparing slides, and performing the transmission electron microscopy. She also helped me interpret the results of the anatomy. Dr. M. Parthasurathy and his staff made available the scanning electron microscope and schooled me in its use. Discussions with Dr. Dominick Paolillo were valuable when I was learning about the anatomy of wheat plants.

I typed most of my thesis using Cornell's IBM 370/168 computer and the Waterloo Script text formatting program. However, several people helped me with other portions of this thesis. Miss Sue Roedel typed the tables and Mrs. Millie Kabrick typed the formulas and figure labels. Dr. Richard Muck assisted me in finishing many of the details such as the inking of the final copies of the figures. I appreciate their help immensely.

While I have been studying here at Cornell I have benefited greatly from the encouragement of family and friends. The support and encouragement of my parents and brother were particularly helpful. I am grateful to Mr. Hugh Gauch of the Ecology and Systematics Department. His natural inquisitiveness about science has helped me to learn the same attitude and his friendship has been invaluable. I have also benefited from the sustained encouragement of Mr. David Pinnow. Finally, I am thankful for the support of my friends at Bethel Grove Bible Church and for the friendship and support of the Reverend Merold Stern.

TABLE OF CONTENTS

LIST OF TABLES

LIST OF FIGURES

CHAPTER 1

INTRODUCTION

The pressure chamber is one of several devices used to study the water relations of green plants. For field work it can be used to rapidly measure leaf water potential, and for laboratory studies it can be used to determine the magnitudes of the components of water potential.

The importance of the pressure chamber is illustrated by some of its present and potential uses. It was popularized by Scholander, et al. (1964, 1965) who developed it as a means of comparing the xylem potential of plants adapted to various habitats. (The xylem potential has since been shown to be approximately equal to the water potential.) Cutler, et al. (1980) and Shahan (1980) used the pressure chamber to study the drought adaptation of rice. Clark and Hiler (1973) and Hiler, et al. (1972) demonstrated its usefulness as a tool for quantifying plant water stress. Hiler et al. (1972) applied it to their studies of irrigation scheduling. The modeling of Stegman, et al. (1976) suggested that irrigation scheduling on the basis of plant water stress could reduce water use.

As energy conservation becomes more critical, and as water supplies in water-deficient states diminish, applications such as the above will be important. For example, Dr. William Splinter past president of the American Society of Agricultural Engineers, recently pointed out (Splinter, 1979) that "...pumping water for irrigation accounts for 35 per cent of the total energy used in production

agriculture in the U.S. while total irrigated acreage accounts for only 20 per cent of the total cropland." In 1975 an estimated 68 per cent of the ground water and 46 per cent of the total water withdrawn from water supplies was used for irrigation (U.S. Bureau of the Census, 1978). Research into drought adaptation, plant water stress, and irrigation scheduling may increase the efficiency of agricultural production by reducing costs. The pressure chamber will no doubt play an important role in such studies.

Figure 1.1 shows a cross section of a pressure chamber. The water potential is measured on a leaf detached from the plant and placed in the chamber such that its severed end protrudes into the atmosphere. Tightening the sealing knob on the head of the chamber compresses a grommet which presses against the leaf and forms a seal. When the chamber is pressurized, water appears at the cut end of the leaf. If the chamber pressure is further increased, water will flow from the cut end. The mathematical and experimental studies described in this dissertation investigate the physiological and anatomical features of the plant which influence the rate at which water can be forced from the leaf.

Water in a living plant is held in continuous columns which start in the root and extend through the vascular system to evaporation sites in the leaves. Detachment of the leaf breaks these columns. Water in cells has a potential less than that of pure water exposed to the atmosphere. Hammel and Scholander (1976, p 28,36) have proposed that the water in the xylem is under negative pressure or tension. If their theory is correct, detachment of a leaf will release

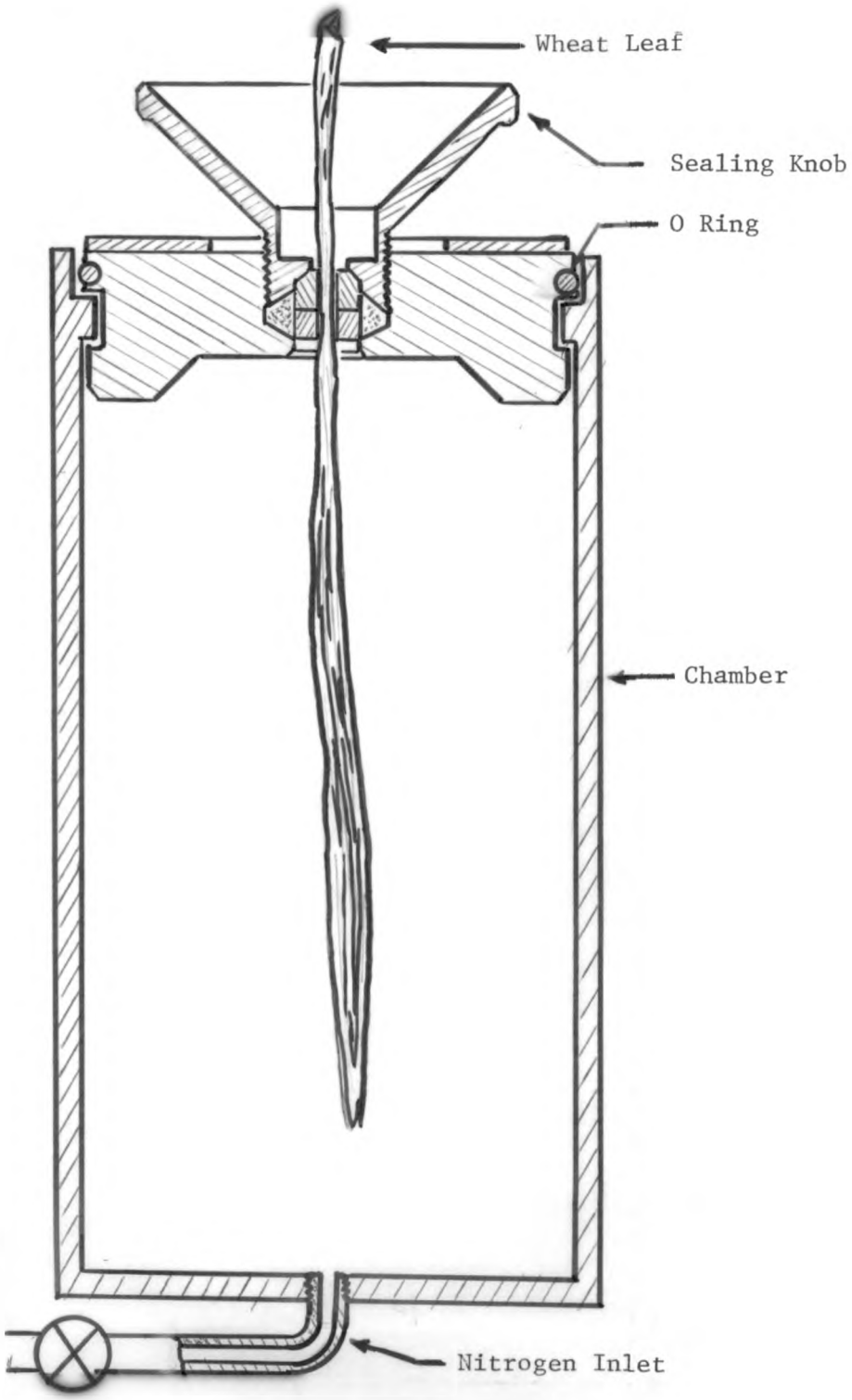

Figure 1.1 Cross sectional view of a pressure chamber manufactured by the Soil Moisture Equipment Corporation, Santa Barbara, California. (The drawing is not to scale.)

this tension, and the water in the xylem will be pulled into the individual leaf cells. Water will remain in those pores with diameters small enough to allow surface tension to hold it against the forces drawing it into the cells. If the chamber containing the severed leaf is pressurized, water will then be forced out of the cells and appear at the cut end of the stem protruding from the chamber. The minimum chamber pressure needed to make the water appear at the cut surface is called the balance pressure.

The following is a brief summary of the historical development of the pressure chamber. Refer to Ritchie and Hinkley (1975) for a more detailed account. Dixon (1914,pg 142) used a device similar to a pressure chamber in his studies of osmotic pressure of plant cells. He placed a tree branch with eight or more leaves in a large glass chamber (50 centimeters long, 10 centimeters in diameter and one centimeter thick). The container was sealed with the cut end of the branch protruding from one end of the chamber through a rubber stopper fitted into the container's bottom. The protruding end was placed in a glass vessel containing a weighed quantity of water. Dixon's use of a glass cylinder allowed him to observe the wilting of the leaves as he increased the pressure in the chamber and forced the water from the branch. He measured the increase in the weight of the water in the glass vessel to determine how much was expressed. However, after two explosions he abandoned this method in search of another.

Fifty years after Dixon's work, Scholander and his coworkers (Scholander, et al.,1964,1965) developed the pressure chamber method for use in their studies of the "sap pressure" in desert and forest

plants, and halophytes. They developed the following method for measuring the osmotic component of water potential. First they determined the balance pressure. Secondly, they increased the pressure several atmospheres and collected and measured the sap expressed from the leaf. They continued incrementing the pressure and collecting the sap until they had obtained nine or more measurements. Using these measurements they constructed a pressure^{-1}-volume curve by plotting the reciprocal of pressure as a function of the amount of water expressed. Using this curve they could estimate the osmotic potential of the leaf cells.

Tyree and Hammel (1972) developed a model which they used in the analysis of pressure^{-1}- volume curves. Their method of analysis gives values of volume-averaged turgor and osmotic potentials and parameters which can be used to relate cell volume to cell turgor pressure.

More recently the pressure chamber has been used to generate "kinetic" or efflux curves. At the suggestion of Dr. Hammel, Tyree and Dainty (1973) performed experiments which measured the "kinetics" of water efflux from hemlock leaves placed in a pressure chamber. After detaching the leaves from the tree, and placing them in the chamber, they increased the chamber pressure until they reached the balance pressure. They then increased the pressure several atmospheres and collected and measured the amount of water expressed from the leaf at various times after the pressure increase. With a chamber pressure 3 bars above the initial balance pressure, as much as 30 minutes elapsed before water stopped flowing from the cut end of the stem.

In efflux experiments the rate at which water is forced from the leaf depends on the resistance encountered by the flowing water. In a recent article Tyree and Cheung (1977) used results of the efflux experiments to discuss possible pathways of water movement through the leaf and to estimate the resistances of these pathways. The research described in this dissertation extends the work of Tyree and Cheung by using mathematical and experimental techniques to relate anatomical features to efflux.

CHAPTER 2

OBJECTIVES AND OVERVIEW

Water traveling from plant roots to the evaporation sites in leaves encounters various resistances to flow through the roots, stems, and leaves. Although the leaf resistance is often assumed to be negligible, some recent research suggests that, at least in some plants, there is a gradient in water potential along the length of a rapidly transpiring leaf (Rawlins, 1963, Wiebe and Prosser, 1977, Denmead and Millar, 1976). When water is forced from a leaf placed in a pressure chamber, it may encounter resistances similar to those encountered by water flowing in the transpiration stream. Thus if the xylem vessels affect the rate of water flow through leaves in the pressure chamber, they may also be responsible for establishing a water potential gradient along the length of a transpiring leaf. Therefore, the study of pressure chamber efflux experiments can add insight into the significance of leaf resistances. In addition, it can help clarify sources of error arising from experimental procedures, and thereby aid researchers in obtaining more accurate results.

The specific objectives of this research are:

(i) To develop a model which relates water efflux from a wheat leaf placed in a pressure chamber to relevant anatomical and physiological properties of the leaf.

(ii) To determine major sources of resistance to water flow through the leaf.

(iii) To use the model as a tool to explore the influence of experimental procedures on experimental results obtained with the pressure chamber.

Using wheat leaves, I conducted the efflux experiments described in chapter 4. The experiments were similar to those which Tyree and Dainty performed on hemlock. The relatively simple structure of the wheat's vascular system combined with its agronomic importance made it a logical choice. In addition, I studied the anatomy of the leaves by determining cell diameters, leaf volume, and number and diameter of xylem vessels. The results of the anatomical studies are included in chapter 5.

In attempts to model efflux of water from wheat leaves, I progressed through a series of three models. The first and simplest model neglected the leaf cells and assumed that expressed water came from the compression of the xylem by the gas in the chamber. I modeled xylem elements as thick-walled cylinders and predicted deformation of the xylem using the theory of elasticity. The results are described in chapter 6. The decrease in volume of the xylem can vary from less than 1 per cent to more than 24 per cent depending on assumptions made about the modulus of elasticity of the xylem wall. Furthermore, under the right conditions, the xylem could collapse. However, no collapsed vessels were found in leaf cross sections made

from leaves which had been removed from the chamber after a test.

I ignored the xylem in the second model, and assumed that compression of the individual cells caused the water to flow from one cell to the next until it reached the xylem vessels. I assumed the xylem resistance was insignificant and neglected water flow through cell walls by assuming that all of the water expressed from a given cell was forced into an adjacent cell and continued traveling from cell to cell until it reached the xylem. This model is presented in chapter 7. The model showed that the curve of efflux per unit volume from a single cell with a low membrane permeability looks like the curve for a series of cells each having higher permeabilities. The model predicted efflux curves similar in shape to experimental curves, but the assumption that xylem resistance was insignificant was difficult to justify. Therefore, I developed a third and more general model.

For the third model, which I describe in chapter 8, I assumed that water flows from individual cells to the nearest xylem vessel, and then flows through the xylem vessel until it reaches the cut end of the stem. I further assumed that water flowing from cells to the atmosphere along this pathway encounters only two major resistances: the resistance to flow from the interior to the exterior of the individual cell, and the resistance to flow through the xylem vessels.

Results of the third model agree reasonably well with experiments. Preliminary results of this model showed that, when xylem resistance is significant, the time required for all of the water to be forced from a leaf should be dependent upon leaf length.

To test this idea, I performed additional experiments which are reported in chapter 4. Analysis of the results of these experiments showed that leaf length affects the total amount of time required to force water from a leaf.

The conclusions drawn from this research are discussed in chapter 9. Briefly, this work has shown that the resistance of the small vascular bundles can significantly limit the water efflux rate from a leaf. Since the rate of transpirational flow is as high as the flow rates encountered in pressure chamber efflux, this work has helped establish the importance of xylem resistance to the development of water potential gradients in transpiring plants. Finally, the model is a tool for the analysis of pressure chamber experimental data and can be used to estimate the effect of leaf size and shape on the efflux of water.

CHAPTER 3

LITERATURE REVIEW

The modeling of water efflux from wheat leaves requires an understanding of both the anatomy of the plant, and the pathway which water takes as it travels from individual cells to the cut end of the leaf. A variety of models have been developed which describe water flow through plant tissue, and several have been designed specifically for pressure chamber experiments. This chapter reviews wheat anatomy, describes several experimental studies of water movement in leaves, and summarizes modeling of both water flow through plant tissue and pressure chamber experiments.

3.1 Wheat Leaf Anatomy

The following summary of wheat leaf anatomy covers aspects relevant to water transport and is by no means exhaustive. An extensive study on the wheat plant was done by Percival (1921). Additional information is available in the plant anatomy book by Esau (1977) and papers by Kuo, O'Brien, and Zee (1972), Kuo, O'Brien and Canny (1974), Kuo and O'Brien (1974), O'Brien and Carr (1970), O'Brien and Kuo (1975), and Patrick (1972).

Wheat leaves are parallel-veined. Mature leaves are typically 165-300 millimeters (7-12 inches) long and 10-16 millimeters (3/8- 5/8 inch) wide. The parallel veins are approximately 0.19 to 0.30 millimeters apart. A sketch of the top view of a leaf illustrating

the pattern of veination is shown in figure 3.1 and tracings of cross-sections of wheat leaves showing vascular bundles are shown in figures 3.2 and 3.3. At intervals of two or three millimeters the parallel longitudinal veins are connected by transverse veins consisting of one xylem vessel and one phloem sieve tube (Kuo, et al.,1972). The number of bundles in a mature leaf varies with both position on the plant and location in the leaf. There are fewer bundles near the tip of the leaf because some of the bundles found at the widest portion divide in two and combine with adjacent bundles while others simply join with adjacent bundles (see figure 3.1). As shown in figures 3.2 and 3.3, the bundles are surrounded by two rings of bundle sheath cells, the inner or mestome bundle sheath, and the outer bundle sheath. Schlerenchyma cells are associated with each of the bundles. In small bundles, they are located near the epidermis but in large bundles they extend from the vascular bundle to the epidermis. The mesophyll cells are slightly elongated and thin-walled. They are more or less randomly oriented around vascular bundles, but near the upper and lower epidermis they are often oriented with their long axes at right angles to the plane of the epidermis. The epidermal cells are elongated and thick-walled. Stomates penetrate the epidermis and are located in rows near the vascular bundles. Substomatal cavities located beneath the stomates form relatively large air pockets in the mesophyll.

The anatomy of the vascular bundles is important to the a study of water flow. Such information can be used to determine whether water flowing through xylem vessels encounters a significant resistance to flow. Vascular bundles are found in several sizes. Percival

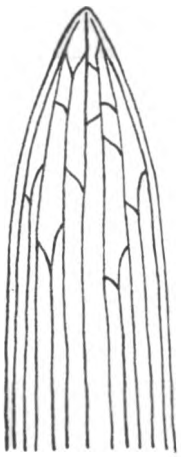

Figure 3.1 Top view of a wheat leaf showing the arrangement of vascular bundles near the tip. The diagram is redrawn from a sketch which appeared in the book The Wheat Plant by Percival (1921).

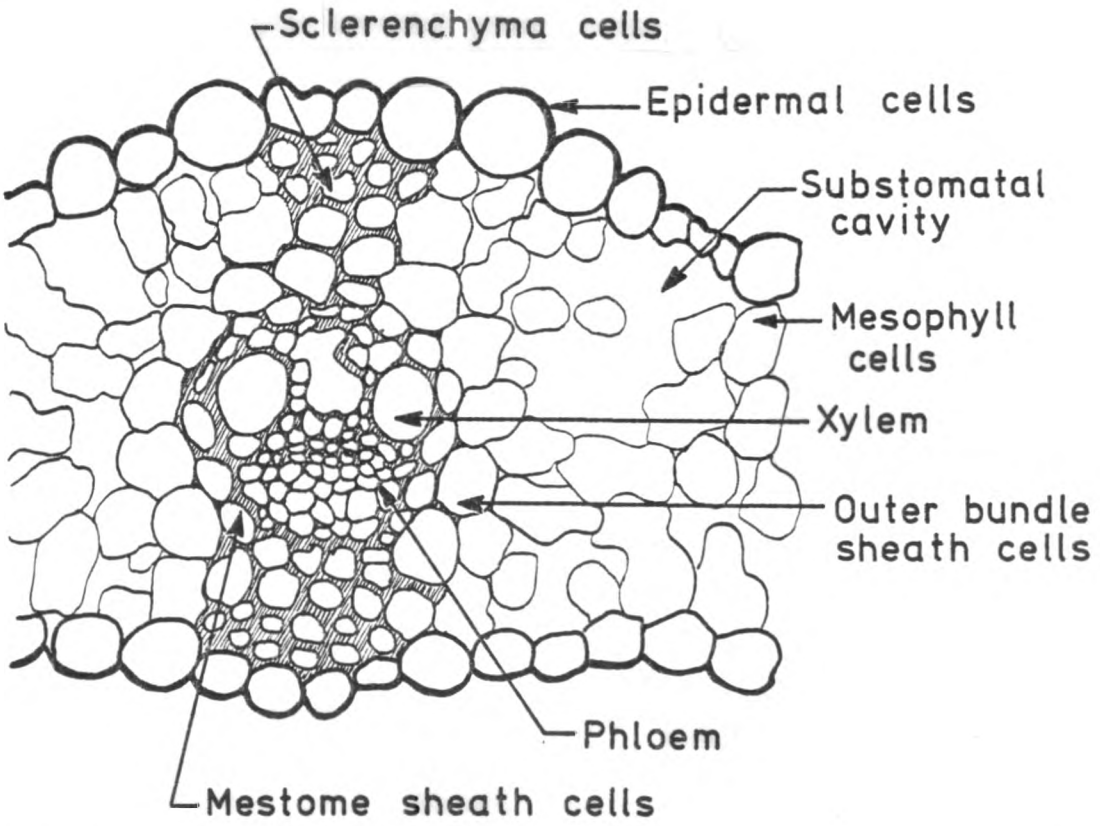

Figure 3.2. A tracing of a cross section of a wheat leaf showing the arrangement of cells in a large vascular bundle. Magnification 400 X.

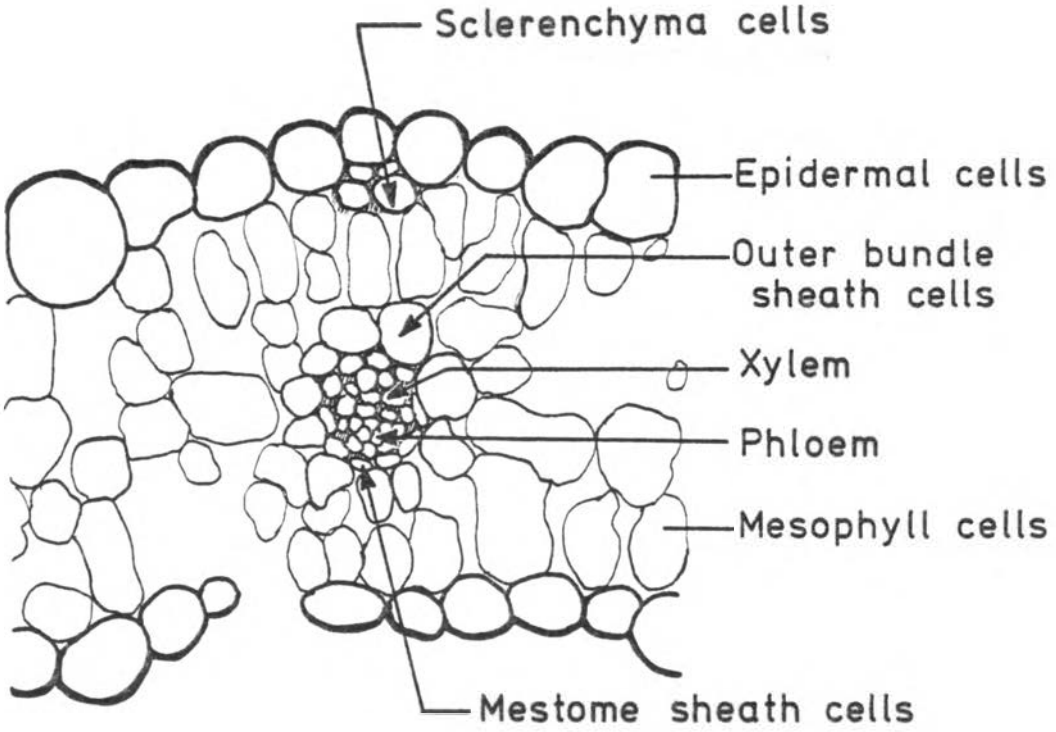

Figure 3.3 Tracing of a cross section of a wheat leaf showing the arrangement of cells in a small vascular bundle. Magnification 400 X.

classified bundles as being either stout bundles or fine intermediates. Patrick (1972) used three classifications: large and small laterals and intermediates. Kuo, O'Brien, and Canny (1974) reported measurements on five bundle types: the midrib, large and small laterals, and large and small intermediates. Percival found that the number of bundles varied with the position of the leaf on the plant. His data for Triticum vulgare is shown in table 3.1. Kuo and his co-workers studied the third leaf from the base of Triticum aestivum L. cv. Heron grown in a greenhouse. Their data is summarized in table 3.2. The total number of bundles in their leaf, 37, differed by 7 from the number given by Percival for the third leaf from the base of Triticum vulgare.

Another anatomical feature reported in the literature may be relevant to water flow. O'Brien and Carr (1970) discovered that the middle lamella of the mestome sheath cell is suberized. This layer encircles each cell and is connected with the the layer in adjacent cells. Therefore, the layers form a collar which envelopes the vascular bundle. They speculated that this layer may regulate water transfer from bundle sheath to mesophyll cells. The transverse veins lack a bundle sheath and have no suberized layer (Kuo,et al.,1972).

3.2 Experimental Studies on Water Flow through Leaves

Many experimental studies have investigated water movement through leaves. Some of these have used dyes or tracers. Such studies are helpful in identifying pathways through which water most readily flows through plant tissues during evaporative water loss. However,

Table 3.1. Number of bundles in the broadest part of the leaves on a full-grown plant of Triticum vulgare (Percival, 1921, p. 59).

Leaf	Stout Bundles			Fine Intermediate Bundles	Total
	Left Half	Midrib	Right Half		
5th (uppermost)	6	1	6	66	79
4th	6	1	6	42	55
3rd	6	1	6	31	44
2nd	4	1	4	28	37
1st (near base of plant)	4	1	4	18	27

Table 3.2. Sizes of vascular bundles and vessles in wheat plants (Triticum aestivum L.cv. 'Heron') grown in a greenhouse. Data is for the third leaf to develop. (From Kuo, et al., 1974, tables 5 and 7).

Bundle type	Number in leaf section	Radius of mestome sheath (mm)	Vessel elements	
			Radius (mm)	Number of vessels with this radius
Midrib	1	.067	.015 .0036	2 9
Large lateral	6	.044	.012 .0060 .0020	2 1 6
Small lateral	4	.035	.0097 .0027	2 3
Large intermediate	13	.014	.0026 .0013	4 2
Small intermediate	10	.0105	.0019	2

these pathways are not necessarily the same pathways for water flow during pressure-induced flow in a wheat leaf placed in a pressure chamber. Since water may permeate membranes which block the passage of the labeling compounds, these techniques show where water readily flows, but do not necessarily show all the portions of the leaf through which water travels.

Armacost (1944) studied the flow of iodine green, eosin, and trypan red in detached twigs of Iowa woody plants. These dyes rapidly penetrated the vascular bundles and border parenchyma cells and then spread into the epidermal cells by first passing through vein rib cells. Presumably these vein rib cells correspond to the schlerenchyma cells. He observed that the dye did not penetrate to the mesophyll cells for several hours.

Weatherly (1963) experimented with rapidly transpiring leaves in which the transpiration was abruptly halted by immersion in water or paraffin. He found that the water uptake rate dropped sharply as soon as transpiration was stopped. It decreased rapidly during the next ten minutes, and then dropped off less rapidly during the next 60 minutes. He defined the inner space in the leaves as the portion of the cells surrounded by a relatively impermeable membrane. It corresponded to either the vacuole or the vacuole and surrounding cytoplasm. The outer space of the leaf he defined as the remaining portion of the leaf capable of absorbing water. When he plotted data for the logarithm of the rate of water uptake against time, he found two straight lines. The data points from the first ten minutes fell on the first line, while the remaining points fell on the second. He reasoned that the

first drop in uptake corresponded to the filling of the outer space in the leaf while the second corresponded to the filling of the inner space. He concluded that the pathway of water movement during transpiration was through the outer space of the leaf. In a later article Weatherly (1965) again discussed possible pathways of water movement and interpreted other experimental results as supporting this view.

Crowdy and Tanton (1970) used lead chelate fixed with hydrogen sulfide to study flow in wheat plants and several species of broad leaves. They defined the free space of leaves as the volume into which solutes can freely diffuse from an outside medium. When they immersed plant roots (including roots of wheat seedlings) in a lead chelate solution, the transpiration stream carried the chelate into the leaves. They fixed the chelates with hydrogen sulfide and sectioned the tissue. On the basis of their experiments, they concluded that 3 to 5 percent of the leaf volume is free space and that the free space is located primarily in the middle lamella. The pectin in the middle lamella was permeable to water and solution. The cellulose was slightly permeable to water, and they suggested its fibrous structure impeded water flow. The results of a study on roots by Tanton and Crowdy (1972a) suggested that the apoplasm (cell wall) was the predominant pathway for water movement in the root. They also found that the water in the roots could freely and passively enter the mature xylem elements. In a third study on the transpiration stream in leaves Tanton and Crowdy, (1972b) found chelate in the free spaces of the mesophyll. Their results suggested that evaporative loss of

water in leaves is both cuticular and peristomatal and that movement to the evaporation site is through the free space. Citing O'Brien and Carr's article on the suberized layer in the mestome sheath of the primary vascular bundles, they suggested that water moves into the free space in the mesophyll through the secondary veins. One disadvantage of a study with chelates was pointed out by Meidner (1975). Cell wall materials and especially the pectin-rich regions of the cuticle preferentially adsorb chelates. However, he further noted that the chelate must have been near these areas in order to be adsorbed.

Meidner (1975) questioned the relative importance of water flow through the mesophyll during transpiration. He proposed that much of the transpired water evaporates from the surface of the epidermal and guard cells which form a portion of the substomatal cavity wall. In his proposed pathway for water movement during transpiration, water traveled from the bundles to the closest epidermal cells and then traveled through the epidermis to the evaporation site. By measuring transpiration rates from strips of epidermis removed from leaves of Tradescantia virginiana he demonstrated that transpirational water loss from the strips could be replenished by flow of water from the bundle sheath cells of the main veins. He also pointed out that the mesophyll cells were in contact with less than 50 percent of the epidermal cell surface and therefore would be unable to replace the transpired water.

Articles such as those by Molz and Ikenberry (1974) (discussed in section 3.3), Weatherly (1963,1965), Crowdy and Tanton (1970), and Tanton and Crowdy (1972a,1972b) support the view that water flow through the cell wall predominates during transpiration. However, there is some evidence that the pathway of movement in the pressure chamber may be different. Tyree and Cheung (1977) assumed that water flowed through the mesophyll to the nearest bundle sheath, and then into the vessels. They analyzed the effect which cell to cell and cell wall pathways would have on the rate of water efflux from the leaves. Their experiments suggested that "water driven out of living cells (or infiltrated airspaces) will travel in and out of cells passing through several membranes and the thinnest part of the cell walls between the cells.." Their work is further discussed in section 3.5.

3.3 Modeling Water Flow in Plant Tissue

During the past two decades several models have been developed to describe water flow through plant tissue. Models developed for use in plant sciences quantify solute and water movement in response to gradients in solute concentration and water potential. This section summarizes these models and discusses those of particular importance to water movement in leaves. The engineering models, which are summarized in section 3.4, describe the deformation of plant materials. Specific models developed for the pressure chamber are discussed in sections 3.5 and 3.6.

Philip (1958a) developed one of the first models of water and solute movement in cell tissues. He started with relations for turgor pressure and osmotic pressure as functions of cell volume, simplified them, and combined them into a single differential equation which described the flow of water into and out of a single cell as a result of a gradient in potential across the cell membrane. By adding an expression for solute movement, he described the behavior of a cell placed in a solution containing water and a diffusible solute. He used the model to analyze water uptake by roots growing in soil in which salts were accumulating. His model predicted that water uptake by roots would continue even when salt was accumulating at a linear (in time) rate around the roots. Diffusion of the solute into the root cells increased their water potential in proportion to the salt build-up. His model suggested that the plant could continue to remove water from the soil even when soil salt concentration increases. This result contradicts the theory of physiological drought.

In a second paper, Philip (1958b) extended his treatment to aggregates of cells. He wrote an equation for flow between two adjacent cells in a tissue with unequal water potentials. This gave him the finite difference approximation of the first spatial derivative. Using the values of water potential in three adjacent cells, he wrote the finite difference equivalent of the second spatial derivative. After assuming that there were a large number of cells in the aggregate and that the length of a single cell was small with respect to the length of the aggregate, he replaced the finite difference with the derivative. That gave him the following diffusion

type equation:

$$\frac{\partial \eta}{\partial t} = D\nabla^2\eta \qquad (3.1)$$

where η is a variable such as water potential, turgor pressure, osmotic potential, or cell volume change. D is a diffusivity and has units appropriate to those of η. Philip pointed out that the above equation is of the same form as the well known heat equation and has an analytic solution. He also showed how his model could be used for cell volume changes when turgor and osmotic potentials are non-linear functions of cell volume. Philip demonstrated how his equation could be extended to two or three dimensions.

In his third paper in the series (1958c, 1958d) Philip applied equation 3.1 to diffusion of water into sheets, cylinders, and spheres of tissue. Assuming a uniform initial water potential for the tissue, he used boundary conditions equivalent to immersion of the tissue in a solution of nondiffusible solute of a differing water potential. He defined half-time of osmosis for a cell as the time required for the water potential of the cell to reach a value equal to the mean of the initial and final values. For a whole tissue, he defined the half time as the time required for the tissue to absorb one half the total amount of water which it is capable of absorbing. Using the solutions to the diffusion equation for the slab, cylinder, and sphere, he studied the internal gradients which developed within the tissues. Tissue half times were inversely proportional to the square of half the thickness (for the slab) or the square of the radius (for the

sphere and cylinder). His analysis demonstrated the importance of geometry to the modeling of water and solute flow.

The basic approach used by Philip has been used repeatedly by researchers modeling water and solute flow. Boyer (1969, 1971) applied Philip's theory to water flow in whole plants. He used the following equation, given by Philip, for the relationship between $t_{\frac{1}{2}}$, the half time (sec) for water flow through slabs of cell aggregates, D, diffusivity (cm^2/sec) of water through tissue, and a, the slab half thickness (cm):

$$\frac{Dt_{\frac{1}{2}}}{a^2} = 0.195 \qquad (3.2)$$

Boyer reasoned that the aggregate of cells in a leaf was arranged in two slabs - one above, and the other below the xylem vessels. He defined the resistance, r, as:

$$r = \frac{\ell}{D} \qquad (3.3)$$

ℓ = the length of the diffusion pathway for water from the xylem pathway to the leaf surface (cm)

D = the diffusivity of water through the slab (cm^2/sec)

By solving equation 3.2 for diffusivity, D, and substituting D into the above equation, he used the half time and the leaf thickness to determine r. He calculated root and stem resistances by measuring the half time for recovery of leaves with only stems and with both stems

and roots attached. Using the resistances calculated from the half times he subtracted the leaf resistance from the resistance of the leaf and stem to give a value for the stem resistance. Similarly, he subtracted the resistance of the root, stem and leaf from the resistance of the stem and leaf and determined root resistance.

Molz (1972) criticized Boyer's work on two points. First he pointed out that Boyer's analysis assumed the diffusivities of water flow (as predicted by volume changes of cells) and water potential were identical. This is not an established fact, although in a reply to Molz, Boyer (1972) presented evidence that they were the same. Secondly, Molz observed that, although Philip's equation is applicable to flow in a slab of cells such as is found in the leaves, it is not valid for flow in other parts of the plant. Therefore,he contended that the resistances to water flow calculated by Boyer for stems and roots cannot be compared to resistances to flow through leaves. Boyer's reply to this criticism was that resistances of stems determined by the recovery method compared favorably with resistances measured by other means. However, Molz's second criticism remains valid and raises a question about that portion of Boyer's analysis.

Murase and Merva (1979) used the following diffusion type equation to estimate the conductance of potato tissue:

$$\frac{\partial \psi}{\partial t} = D_e \frac{\partial^2 \psi}{\partial x^2} \qquad (3.4)$$

D_e = the diffusivity of free energy (cm/bar-sec)

ψ = the water potential (bars)

He used this diffusion equation in two coordinate systems with appropriate boundary conditions. The first, the one-dimensional cartesian co-ordinate system, was appropriate to diffusion into a sheet of tissue. The second, the radial co-ordinate system, was appropriate to diffusion into a cylinder. The resulting solutions gave him a relationship between D, ψ, and t at various distances from the surface of the slab or the axis of the cylinder. He measured the value of water potential with a thermocouple psychrometer, and used this value in the expression for water potential to determine the value of D. Using a previously developed relationship between energy diffusivity and the diffusivity of water he determined the diffusivity of water. His value of 3×10^{-12} m^2/sec-bar is comparable to other values reported in the literature.

Molz and Klepper (1972) applied the equations developed by Philip (1958b) to the water relations of cotton stems. They wrote Philip's equation for water flux in cylindrical co-ordinates and assumed radial symmetry. In the cotton stem the xylem tissue forms a "tube" surrounding the center. This xylem tissue is in turn surrounded by a "tube" of phloem tissue. Molz and Klepper modeled changes in stem diameter by assuming that the phloem changed in volume as water from it flowed into or out of the xylem in response to changes in xylem water potential. The numerical solution of the equation gave them the water potential distribution in the phloem which they in turn used to calculate the flow across the boundary between xylem and phloem. They related this flow to changes in tissue volume and stem diameter. Although they did not have an accurate value for the diffusivity of

water through the phloem tissue, they were able to adjust the value to give stem diameter changes which were quite similar to measured values. In a second paper Molz, Klepper, and Browning (1973) experimentally measured the diffusivity and found that it was 16.2 x 10^{-7} cm^2/sec, approximately twice the value of 8.0 x 10^{-7} cm^2/sec needed to make their model agree with experimental measurements of changes in stem diameter. In a third paper Molz and Klepper (1973) concluded that no simple relationship could be developed which would allow water potential to be determined from stem diameter measurements.

In a more recent paper, Molz and Hornberger (1973) used an approach similar to Philip's. Figure 3.4 shows the linear aggregation of cells for which they wrote one-dimensional equations for solute flux, J, and mass flux, ϕ. By suitable substitution they developed a pair of equations to describe time and space variations in C, diffusible solute concentration and θ, where θ is defined as:

$$\theta = \Delta\tau - \Delta\overline{\pi} \qquad (3.5)$$

$\Delta\tau$ = turgor pressure difference across the membrane separating two cells (bars)

$\Delta\overline{\pi}$ = difference in concentration of nondiffusible solutes between two adjacent cells (bars)

They nondimensionalized their equations in time and space and solved them numerically to get variations in θ and C for a slab of tissue as a function of nondimensional time. They used boundary conditions which corresponded to a slab placed in a diffusible solute and an

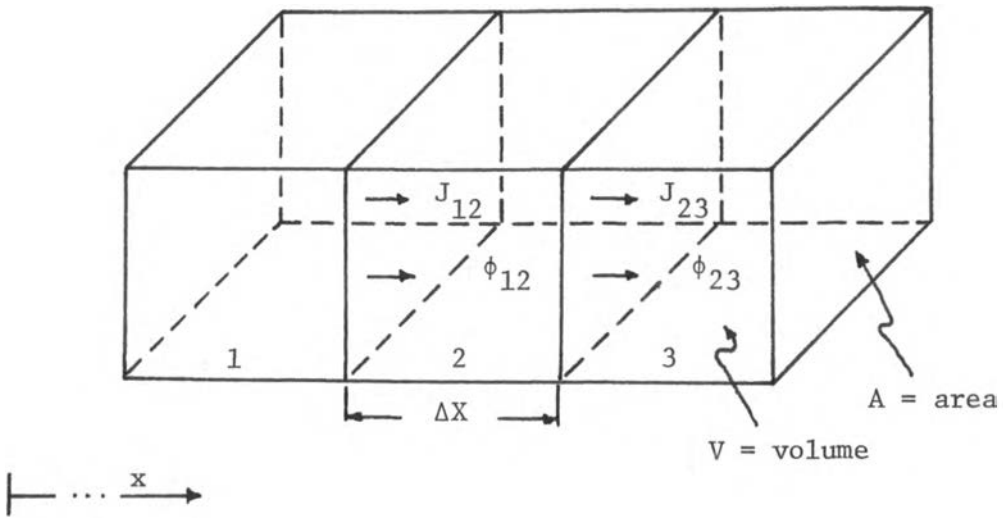

Figure 3.4. A model of water and solute flow through plant tissue as proposed by Molz and Hornberger (1973). J_{ij} is the water flux across the membrane separating the ith and jth cells. ϕ_{ij} is the solute flux across the membrane. The figure is redrawn from Figure 1 in Molz and Hornberger's article.

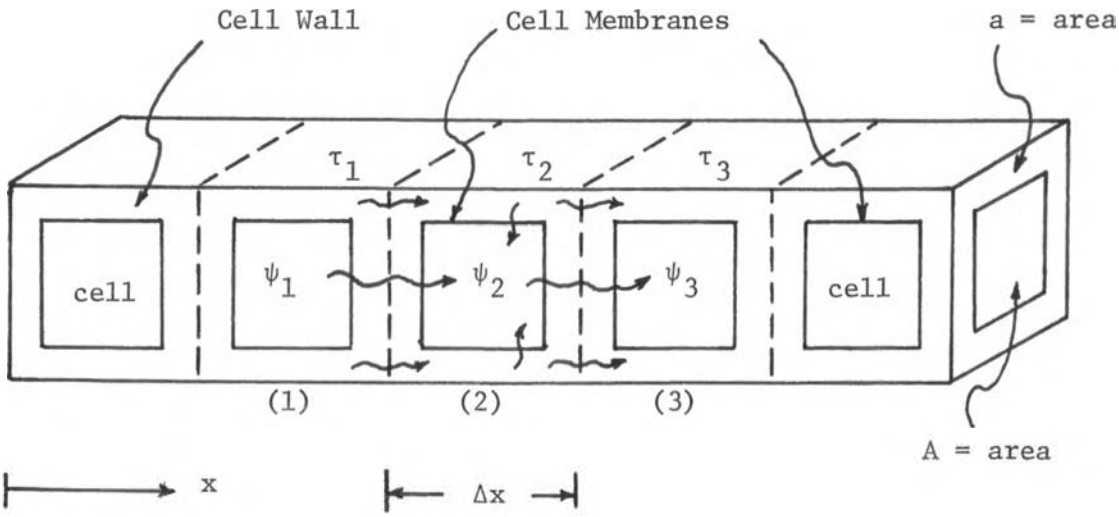

Figure 3.5. A model of water flow in a linear aggregation of plant cells proposed by Molz and Ikenberry (1974). The ith cell has water potential ψ_i and the cell wall surrounding it has water potential τ_i. A is the cross sectional area of the cell vacuoles. The cross sectional area of the cell walls, a, has been exaggerated. The figure is redrawn from Figure 1 in Molz and Ikenberry's model.

initial condition of a uniform water potential in the tissue. By integrating the flow of solute and water across the tissue-solution interface, they determined the quantity of water and solute absorbed by the tissue as a function of time. Their results showed a gradual penetration of solutes into the central portion of the slab of tissue. The initial distribution of θ was uniformly zero. When the tissue was immersed in the solution, their equations predicted that water would flow out of the tissue and that θ would become more negative. The negative value of θ penetrated into the tissue in wave-like fashion. As solute began to flow into the tissue, θ began to return to zero throughout.

Many researchers consider the cell wall an important pathway for water flow (Weatherly 1963, 1965, Tanton and Crowdy, 1972a, 1972b). For example, estimates of the relative magnitude of flow through the cell to cell and cell wall pathways for tomato root tissue have been 3:1 (Weatherly, 1963) and 2:1 (Tyree, 1969). The cell wall pathway was added to the Molz and Hornberger model by Molz and Ikenberry (1974) who described cell wall flow along with flow from cell vacuole to cell vacuole. They divided the cells into two compartments - the cell wall and the vacuole - and wrote differential equations to describe water flow through the two pathways and the exchange of water between them. Figure 3.5 is a diagram of their model. Molz and Ikenberry used their equations to describe variations in water potential in a sheet of tissue with one face permeable to water and the other impermeable. Initially water potential of the cells in the tissue was assumed to vary linearly with distance from the permeable

face. They used the Fourier series method to solve their equations analytically. The resulting series solution described the distribution of water potential in the tissue as a function of time as it gradually assumed a value of zero.

On the basis of their model, Molz and Ikenberry concluded that the cell vacuole and its surrounding cell wall were in local equilibrium with respect to water potential. Furthermore, their estimate of the ratio of water flow from cell vacuole to cell vacuole, to water flow through the cell wall was 5 to 1. They compared this with the values of Weatherly and Tyree and found their model predicted a slightly higher proportion of flow through the vacuole. Molz and Ikenberry concluded their analysis by demonstrating how the pair of equations could be combined into one equation of the form:

$$\frac{\partial \phi}{\partial t} = D \frac{\partial^2 \phi}{\partial x^2} \qquad (3.6)$$

ϕ = water potential at a distance x from some reference point (bars)

D = a diffusivity which combines the effects of flow through the cell wall and the cell vacuoles (cm^2/sec)

Molz based his analysis on an assumption that the water capacity of the vacuolar pathway was 50 to 100 times larger than the water capacity per cell of the cell wall pathway. In a comment on his own paper Molz (1975a) cited evidence that this ratio could be 10 to 1 for some plants. However, he concluded that even with the change in ratio

the cell vacuoles and their surrounding cells would remain in equilibrium.

In another article Molz (1976b) applied his analysis to describing the flow through the apoplasm and symplasm. A diagram of his model is shown in figure 3.6. He assumed that the tonoplast, cytoplasm, and plasmalemma formed a single compound resistance membrane which separated apoplasm from symplasm. The symplasmic connections between cells were plasmodesmata filled with cytoplasm which offered a resistance to water flow equivalent to that of a membrane. Molz's development was quite similar to the one he used in his paper with Ikenberry. It gave him a set of coupled differential equations which he nondimensionalized and solved analytically. He also demonstrated how his two equations could be combined into one. By performing a sensitivity analysis on his parameters, he was able to determine what conditions were needed for the symplasm and apoplasm of individual cells to have identical values of water potential. This "local equilibrium" occurred when there were a large number of cells in series, when the symplasm pathway had a high resistance with respect to flow between symplasm and apoplasm, and when the water capacity of the symplasm and apoplasm were such as to make their respective products of water capacity and resistance nearly equal.

The models developed by Molz and his co-workers have been applied to modeling water flow in roots, leaf disks, and shoots. Molz's root models combined the 1974 equation which he and Ikenberry developed with the Darcy-Richards equation describing water flow in soil. Both equations were written in polar co-ordinates. His steady

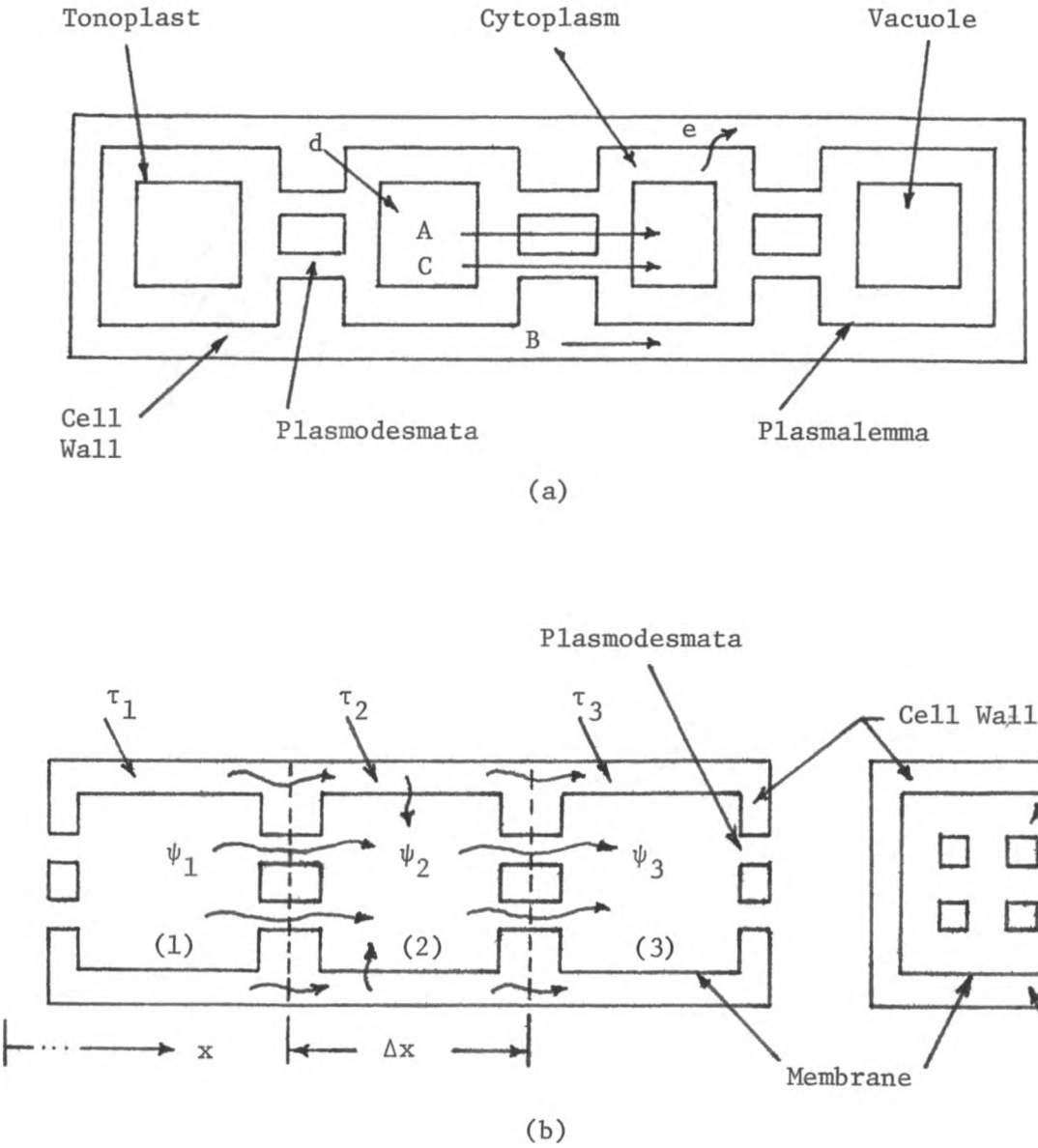

Figure 3.6. Model of a linear aggregate of plant cells used by Molz (1976) to describe flow through the symplasm and apoplasm. Part a shows the flux, A, of water moving out of one vacuole, through the cytoplasm, into the adjacent cell wall, and then into the vacuole of the adjacent cell. B is the flux through the cell wall and C is the flux through the symplasm. Water exchange between vacuoles and cell walls is represented by d and e. Molz idealized the model as shown in part b. The symplasm of the ith cell has water potential ψ_i and the apoplasm adjacent it has water potential τ_i. The figure is redrawn from Figure 1 in Molz's article.

state solution (Molz, 1975b) assumed specific values for both the water potential and water potential gradient at the root endodermis. He matched flow into the root across the root-soil boundary with flow from the soil to the root and equated the water potentials of the soil and root at their interface. Solution of the equations gave Molz the water potential distributions through the soil and root. As a result of his work, he concluded that, providing the soil is still relatively wet, large gradients in water potential develop in the root whereas relatively small gradients develop in the soil. Molz later analyzed the transient case using the time dependent form of the equations (Molz, 1976a). For boundary conditions he again assumed the water potentials at the root-soil interface equal, and matched flow from the soil with flow into the root. He specified that the gradient in soil water potential was zero at some distance from the root and specified a value for water potential at the root epidermis. As an initial condition he specified a uniform potential in the root and soil. Numerical solution of the equations gave Molz the water potential distributions in the root and soil as a function of time. His conclusions were similar to those reached with the steady state model. He found that in the upper 90 per cent of soil moisture availability, the water potential gradients in the root were much greater than those in the soil. In both papers Molz concluded that models predicting the pattern of water removal by roots should account for the limiting effect of the roots on water uptake from the soil.

Molz's models have also been applied to water uptake by leaf disks. Water is absorbed by leaf disks cut from a leaf and floated on

water. Water uptake can be measured by weighing the disks at various times after floating. Normally a disk taken from a water-stressed leaf absorbs water rapidly during the first several hours. After this, absorption continues at a slow but steady rate. The first phase is thought to correspond to water uptake for cell rehydration and the second to water uptake for cell growth. By assuming that water can enter the leaf disk only through the cut edges and not through the cuticle, Molz, Klepper, and Peterson (1973) modeled the disks as cylinders of tissue absorbing water. They applied the radial form of the equations used for water uptake by stems (Molz and Klepper, 1972). Later Molz, Truelove, and Peterson (1975) added a term to the radial equation to describe water uptake due to growth. They assumed that a graph of water uptake (growth) as a function of water potential would give a series of straight line segments. Growth stopped when the water potential went below -4 bars. They set the initial uniform potential of the stem tissue at -10 bars. The water potential around the outside of the disk was set equal to zero along with the water potential gradient at the disk center. They used these boundary conditions in the steady state and transient equations. Solving the equations numerically, they detemined the water potential distribution in the leaf disks at various times after immersion in water. They gave curves for both the cumulative and instantaneous water uptake by the disk.

In his 1972 study Molz concluded that water uptake varied inversely with disk radius. This meant that the water potential at the center of a large disk would not change as rapidly as the water potential at the center of a small diameter disk. In their 1975 study,

Molz, Truelove, and Peterson concluded that the outer portion of the disks are rehydrated more rapidly and enter the growth phase of water uptake before the cells in the center of the disk can be rehydrated. For example, with the particular set of parameters used, Molz found that after 2.8 hours, 11 per cent of the water uptake was used for growth by the cells in the outer periphery of the disk. After 4 hours, 20 per cent of the uptake was used for growth and the portion of the periphery in which growth was occurring had enlarged. His results also predicted that the center of the disk would always have a negative potential. In the specific case solved, the model predicted a water potential at the disk center of between -3 and -4 bars. These results compared favorably with experiments where measurement of the average water potential of the disk gave values slightly less than -4 bars.

In an analysis of water potentials in elongating soybean hypocotyls, Molz and Boyer (1978) applied the radial, steady-state form of Molz's 1974 equation and included a growth term. They assumed that water entered the hypotcotyl through the ring of xylem and flowed both inward toward the pith of the hypocotyl and outward through the cortex. Growth occurred by elongation of the hypocotyl rather than by increase in diameter. Molz and Boyer found the radial water potential distribution in the cortex by assuming a value of -0.3 bars for the water potential at the xylem-cortex interface and equating the gradient of water potential to zero at the epidermis. They found the water potential distribution in the pith by using a value of -0.3 bars for the water potential at the xylem and equating the water potential

gradient at the center of the pith to zero. Water potential measurements with a thermocouple psychrometer agreed with the water potentials predicted by their equations.

All of the above models are applicable to movement in cell aggregates. They neglect flow through xylem. Dimond (1966) studied water flow in the vascular bundles of the stems and petioles of a tomato plant. He determined the number and location of the vascular bundles in the stem, and measured the sizes of their vessels. He assumed that within a bundle, water could pass laterally between vessels, that water potential within each individual leaf was uniform throughout, and that the resistance of the junctions where bundles joined could be neglected. These assumptions allowed him to find the resistance per unit length of bundle using the formula:

$$R = \frac{8\eta}{\pi \sum_{i=1}^{n} nr_i^4} \qquad (3.7)$$

R = resistance per unit length of bundle, (atm/mm^2)

η = the viscosity of the liquid flowing through the bundles (atm-sec)

r = the radius of the i th vessel (mm)

n = the number of vessels with radius r

A tomato plant has both large and small bundles. Dimond found that, in the lower portion of the stem, the resistance of the small bundles was 50 to 100 times that of the large bundles. The resistance of the small bundles remained relatively constant along the entire

length of the stem. However, the resistance of the large bundles was greater in the upper portion of the stem so that they had a resistance per unit length nearly equal to the resistance of the small bundles.

The amount of water carried through the vessels in the vascular bundles varied greatly. By substituting the above formula for resistance into Poiseuille's law, Dimond calculated that the largest and six largest vessels in a bundle conducted, respectively, 23 and 60 per cent of the total water. Conversely, the 10 smallest vessels conducted only about 0.05 per cent of the total. Dimond conjectured that the large vessels, when operative, supply water to rapidly transpiring leaves with little difficulty. However, their large size makes them susceptible to cavitation and other types of damage. When such damage occurs, water flow continues because water is conducted by the small vessels. However, the resistance to flow greatly increases.

Dimond's results can be compared to those of Kuo, O'Brien, and Zee (1972). Using the same data which has been cited in table 3.2 of this thesis, Kuo calculated the relative resistances to flow through the various sized bundles in a wheat leaf and found the relative percentage of flow through each. The percentages for the midrib, 6 large laterals, 4 small laterals, 13 large intermediates, and 10 small intermediates were, respectively, 23.6, 59.1, 16.5, 0.57, and 0.06.

Dimond's model considers resistance to flow through the xylem and does not treat resistance to flow through intercellular spaces. Both of these resistances were included in a model proposed by Aifantis (1977) who applied continuum theory to the description of

water flow. He used a theory which described flow in a media with interstitial spaces of two different sizes. The large diameter spaces were called fissures and the small diameter spaces pores. He modeled the flow in a cylindrical co-ordinate system with the xylem modeled as fissures oriented along the axis of the cylindrical system and the intercellular spaces modeled as pores in a plane perpendicular to the axis. This approach gave Aifantis a set of constitutive equations which he suggested could easily be applied to modeling water flow in stems. However, he did not apply his equations to a particular set of conditions. Although his approach gives a detailed description of the flow of water through the plant material, it does not treat flow through membranes. Such a treatment seems essential to understanding the water potential distribution in plant tissue.

The models mentioned in this section have described water flow in either tissue or xylem. The applications of Molz's models have shown promising results which illustrate the model's usefulness as a tool for investigating plant water relations. In most of the examples mentioned water flow occurs in aggregates of tissue comprised of many cells. However in many leaf tissues, the cells furthest from the xylem are seldom separated from it by more than two or three cells. Therefore, as Molz mentions (Molz, 1974) his model may not be applicable to water flow in leaves. Molz's model of water absorption by leaf disks does not take into account the presence of xylem as a pathway for water movement, and therefore may be subject to error. The model proposed by Dimond demonstrated the importance of the xylem flow. His results suggest that any treatment of water flow in leaves

placed in a pressure chamber would have to include the effect of xylem resistance unless it can be shown as insignificant in comparison to the other resistances to water flow.

3.4 Modeling Deformation of Plant Tissue

The models mentioned in section 3.3 concentrated on modeling water potential distribution and water and solute movement. Since such parameters are important to modeling water flow from leaves placed in a pressure chamber, those models were discussed in detail. Some research has been done which concentrates on the deformation of plant tissue under applied loads. Such information is related to pressure chamber modeling, but not crucial. Therefore, I have included the following brief overview of the work. The deformation of plant material is difficult to model because plant material is often composed of a variety of types of tissue. In addition, it contains solid materials, liquids, and gases.

Recognizing the inhomogeneity of plant materials, Akyurt, Zachariah, and Haugh (1972) proposed two approaches to modeling deformation. Their first approach was to describe the plant tissue as an aggregate of boxes rigidly connected to one another as shown in figure 3.7. They proposed that micro-elastic theory be used to model deformation of the entire aggregate of tissue. Their second approach was to model the deformation of individual cells using the finite element method. Each cell would be an element in the model, and the deformation of an aggregate of tissue would be determined by adding the deformations of the individual cells. The deformation of plant

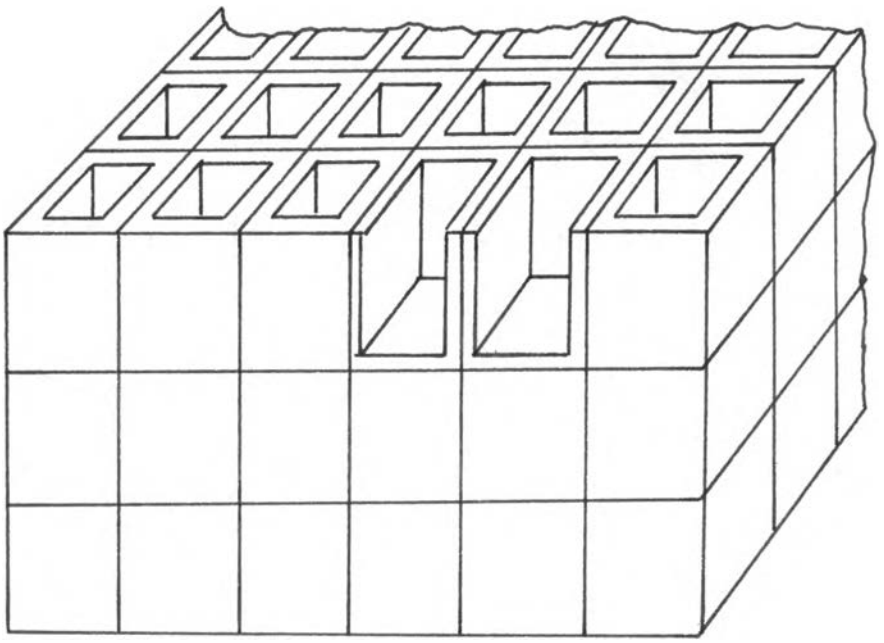

Figure 3.7. A model of plant tissue proposed by Akyurt, et al. (1972). The cells are represented as square boxes whose adjacent sides are rigidly connected.

material comprised of several tissue types would be determined by modeling each type of tissue and then by using the methods of composite media to determine the total deformation. They outlined the development of a set of equations based on microelastic theory and discussed how viscoelastic effects could be treated. However, they did not attempt to apply their theories to specific problems.

Other researchers have looked at plant material as a composite of liquids, solids, and gases. Gustafson, Mase, and Segerlind (1977) developed constitutive equations to describe the deformation of biological materials. Their equations included six material coefficients and they proposed a series of tests which could be used to determine them. They did not analyze the deformation of individual cells, but used bulk material properties which required only "statistical homogeniety of action in the bulk material sense, not uniformity of cell shape and composition." In a second paper Gustafson and Segerlind (1977) used the finite element method to solve these equations for the stress distribution in apples. They modeled the apple as a spherical body (the apple flesh) enclosed by a thin layer of material with a higher elastic modulus (the skin). Assuming a pressure increase was equivalent to an increase in turgor pressure of the flesh, they investigated the stresses produced when the pressure of the liquid phase was increased. Simulating flat plate loading of the apple, they solved their equations a second time. Their results agreed qualitatively with experiments in that they predicted that the restraining effect of the apple skin caused internal stresses to develop in the apple flesh. In a similar approach, Murase and Merva

(1977a) developed constitutive equations to describe the deformation of vegetative tissue pressurized in a pressure chamber. They reported measurements of appropriate parameters for tomato tissue.

In the last several years, researchers have discovered that the water potential of plant materials affects the amount of deformation caused by a given stress. Applying a fixed amount of strain to a sample of tomato epidermis, Murase and Merva (1977b) measured the effect of water potential on the ratio of stress to strain. They found that this ratio varied with water potential and was a minimum at the value of water potential corresponding to zero turgor. DeBaerdemaeker, Segerlind, Murase, and Merva (1978) conducted compression and tension tests on apple and potato flesh and found that the stresses required to cause failure of the tissue varied with the tissue water potential. The tensile strength increased with increasing water potential while the compressive strength decreased. The authors pointed out the necessity of reporting water potential data when conducting deformation tests.

Since tissue deformation occurs in leaves placed in the pressure chamber, these models of tissue deformation may be applicable to studying the way in which pressure applied in the chamber causes water to be forced from the individual cells. However, they presently cannot describe variations in water potential and osmotic potential within the tissue. Their suitability for modeling the efflux of water from leaves placed in pressure chambers is therefore limited.

3.5 Modeling Pressure^{-1} - Volume Curves

The pressure chamber has been used as a tool for measuring the osmotic and turgor potentials and the modulus of elasticity of leaf cells. This section summarizes the development of methods for measuring these parameters. In the last part of the section I have discussed a model of the pressure^{-1}-volume curve developed by Tyree and Cheung and used by them as a tool to investigate sources of error in the analysis of the curve. I have not discussed the theories of the state of water in plant tissue. They are discussed in detail in the references by Scholander and in the book by Hammel and Scholander (1976).

Scholander and his co-workers (Scholander, Hammel, Hemmingsen, and Bradstreet, 1964) developed the pressure chamber to study the osmotic potential of plants. After removing a shoot from a tree or bush, they placed it in an air-tight chamber with the stem protruding. The chamber was similar to the one shown in figure 1.1 but had a rubber compression gland which formed an air-tight seal around the protruding stem. They found the initial balance pressure for the sample by increasing chamber pressure until sap appeared at the cut surface of the stem but did not flow from it. By connecting a plastic tube to the stem, they collected the extruded sap as they increased the pressure above the equilibrium value. They generated a set of data points by increasing the chamber pressure, collecting the expressed water, reducing the pressure, and observing the new balance pressure.

Scholander and his co-workers analyzed the data in the following manner. They plotted the reciprocal of the balance pressure as a function of water expressed. All of the points, with the exception of the first several, fell on a straight line. Their curve was similar to the one shown in figure 3.8. They apparently applied the Boyle-Van't Hoff relationship to the solutes inside the cells, and reasoned that the solute concentration should be proportional to the externally applied pressure. As a result they derived the following relationship between chamber pressure and volume of water expressed:

$$X - V = \frac{K}{P} \qquad (3.8)$$

K = the proportionality constant

X = the total amount of water in the cell

V = the volume of water expressed

P = the pressure in the chamber

The relationship between volume of expressed water and the reciprocal of balance pressure is linear, and the line describing it has a negative slope.

In a second paper Scholander, Hammel, Bradstreet, and Hemmingsen (1965) reported pressure^{-1}-volume plots for both conifers and flowering plants. They noted that the first several data points fell above the straight line fitted through the remainder of the points, and attributed this non-linearity to the effect of turgor pressure.

Several years later Hammel (1967) developed a method for analyzing pressure^{-1}-volume curves. A typical curve is shown in figure

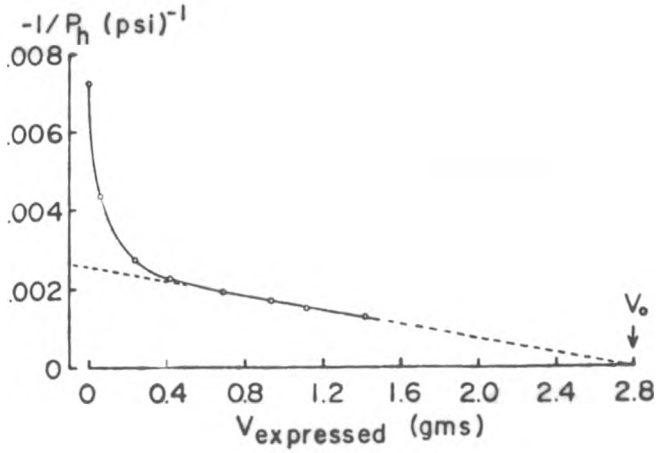

Figure 3.8. A diagram of a pressure^{-1}-volume curve for a hemlock twig showing the reciprocal of balance pressure as a function of grams of sap expressed (taken from Hammel (1967)). V_o is the amount of water which, theoretically, can be expressed from the shoot. The balance pressure is opposite in sign to the hydrostatic pressure in the xylem, P_h. Hammel assumed that the water in the xylem was under tension so that P_h is less than zero. Therefore, the reciprocal of the balance pressure is the negative of the reciprocal of P_h. This is Figure 5A in Hammel's article.

3.8. Hammel pointed out that after approximately 0.5 grams of water was expressed, the curve became linear. He reasoned that, since the cell osmotic potential is a linear function of the volume of water expressed, when the pressure^{-1}-volume curve is linear, the turgor pressure must be zero. By extrapolating the linear portion of the curve to zero volume of water expressed, he found the initial osmotic potential of the cell contents. In figure 3.8 this value is 1.0 divided by 0.0028 or 24.2 bars (357 psi). Similarly, by extending the linear portion to infinite pressure (an ordinate of zero) Hammel determined the total amount of expressible water. He reasoned that this infinite pressure should force out all of the water except that which was bound in portions of the cell.

Hammel also developed a method to measure turgor pressure using the pressure^{-1}-volume curve. For a given volume of sap expressed, Hammel determined the osmotic potential from the extension of the linear portion of the curve. After assuming the matrix component of potential to be zero, he determined the turgor component by subtracting the osmotic component from the total. Using the value of V determined from the pressure^{-1}-volume curve, he determined the volume of expressible water remaining in the cells. Hammel's plot of balance pressure, osmotic potential, and turgor potential as a function of V/V_o is shown in figure 3.9.

Hammel's analysis assumed that all of the cells in the tissue have identical osmotic and turgor potentials. Tyree and Hammel (1972) extended Hammel's analysis and eliminated the need for this assumption by redefining the parameters in the pressure^{-1}-volume model. The

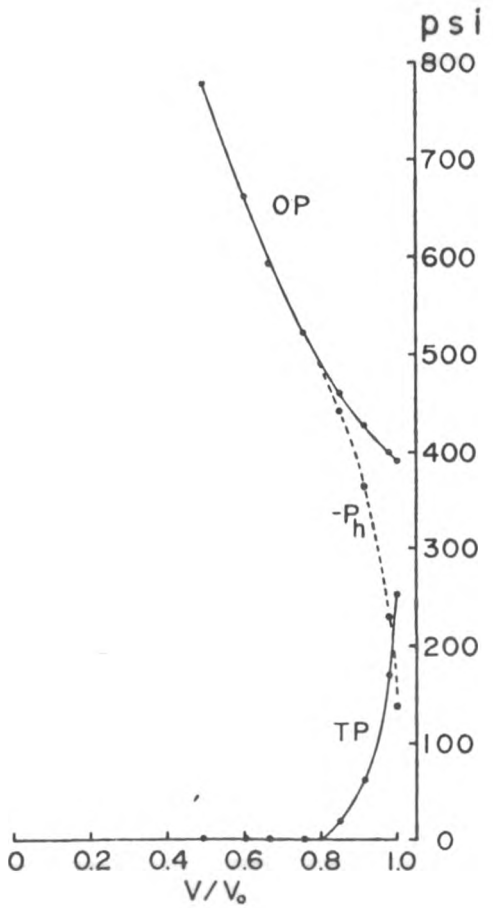

Figure 3.9. A graph of balance pressure ($-P_h$), turgor potential (TP), and osmotic potential (OP), as functions of the relative volume of sap expressed, V/V_o, for the hemlock twig shown in Figure 3.8. This is Figure 5C in the article by Hammel (1967). He assumed the hydrostatic pressure in the xylem, P_h, was negative and was balanced by the pressure of the chamber gases. Therefore, P_h was the negative of the balance pressure.

amount of solutes and the volume of water was defined as the sum of the amounts and volumes of each cell in the leaf. They assumed that the pressure component of potential equalled the sum of the chamber pressure and the turgor pressure, that the expressed sap contained no solutes, and that the surface tension forces in the cell walls were balanced and therefore zero. Using these assumptions they wrote the following equation for balance pressure, P:

$$\frac{1}{P} = \frac{V_o - V_e}{RTN_s - F(V)} \qquad (3.9)$$

V = volume of water remaining in the cells

V_o = the original volume of all the living cells having reasonably pliable walls

V_e = the volume of water expressed from all the cells

N_s = the total number of osmoles of solute in all the living cells

R = the gas constant

T = the absolute temperature

F(V)= the volume of water remaining in the cells multiplied by a turgor pressure function represented as a function of V only

Tyree and Hammel assumed that once the cell reached zero turgor, the turgor potential remained zero. That is, they assumed cells could not develop "negative" turgor. Using F(V) they defined the turgor of the leaf as a volume-averaged value:

$$P_{vat} = \frac{F(V)}{V} = \begin{cases} \dfrac{e(V - V_p)^n}{V_p} & \text{when } V > V_p \\ 0 & \text{when } V \leq V_p \end{cases} \qquad (3.10)$$

$V = V_o - V_e$

P_{vat} = volume averaged turgor pressure

V_p = bulk volume at incipient plasmolysis, equal to the sum of the volumes of each of the cells when the leaf is at incipient plasmolysis

n = the coefficient of nonlinearity

e = the bulk modulus of elasticity of the twig

If the coefficient of nonlinearity in equation 3.10 is set equal to one, their relationship is the same as the one used by Philip (1958). Tyree and Hammel's measured values of "e" for a variety of woody plants were between 190 and 600 bars. The coefficient of nonlinearity, n, was between 1.7 and 3.5. They noted that the linear portion of the curve extended from the zero turgor value of V/V_o to a value of two-thirds. They concluded that F(V) was either zero or much smaller than RTN_s.

Tyree and Hammel mention three assumptions on which their analysis was based. First, since the sap coming from the cut end of the stem was almost pure water, they assumed that the cell did not rupture and no solutes were forced from the cells. Secondly, they assumed that all of the water expressed came from the symplast and that none came from the apoplast. They cited evidence that the amount of the water in the apoplasm was a relatively small proportion of the total. After concluding this error to be small, they noted that it would be difficult to determine its precise magnitude. Finally, they noted that their analysis assumes the balance pressure does not vary

with time. They expressed water from a shoot by increasing the chamber pressure a certain amount (termed the overpressure) above the initial balance pressure. When they determined the new balance pressure, they found that it decreased with time. They hypothesized that the cells varied in permeability and that the initial balance pressure was determined by the more permeable cells. When pressure on the cells was maintained, the more permeable cells released water which could be absorbed by the less permeable cells, increasing their water content. This decreased the pressure required to make water appear at the cut end of the stem. They eliminated this error by observing their balance pressures until they were relatively constant with time. In a test on Pilgerodendron uvifera the balancing pressure became relatively stable within 20 to 40 minutes after release of a 4 bar overpressure.

Helkvist, Richards, and Jarvis (1974) applied the method of Tyree and Hammel to determination of water potential and component potentials in Sitka spruce. They recommended that a large number of data points be taken in the region where the curve becomes linear. This would allow a more precise determination of the value of water potential at which turgor pressure becomes zero. They suggested an alternative relationship for the variation of turgor pressure with water content which gave better agreement with data than Tyree and Hammel's, but which was more complicated.

Tyree, Dainty, and Hunter (1974) reasoned that temperature should affect balance pressure. The Van't Hoff relationship describes the variation in osmotic potential with both changes in the

temperature and the mole fraction of solutes. Since both the cell wall properties and the density of water change with temperature, the turgor pressure should also vary with temperature. They submerged their pressure chamber in a water bath and determined balance pressures on a twig at five temperatures varying between 0 and 36 degrees Celsius. Providing the turgor pressure was zero, they found that the water potential decreased with temperature as predicted by the Van't Hoff relationship. For non-zero turgor potentials, the balance pressure increased with increasing temperature. They concluded that the turgor pressure must decrease with temperature 2 or 3 times more rapidly than the osmotic potential. The results of their experiments help to validate Hammel and Tyree's model.

Cheung, Tyree, and Dainty (1976) developed a mathematical model of turgor pressure, osmotic potential, and cell volume relationships for a hypothetical aggregate of cells. Their objective was to determine possible sources of error in the analysis of pressure^{-1} -volume curves. In the same manner as Philip (1958a) they considered a single cell and used the Van't Hoff relationship to describe changes in osmotic potential with changes in cell volume. They assumed that turgor pressure varied linearly with cell volume and that chamber pressure equalled the sum of the osmotic and turgor components of potential. When they substituted the expressions for osmotic potential and turgor pressure into the equation relating chamber pressure, turgor pressure, and osmotic potential, they had a quadratic equation. They assumed appropriate values of the parameters and solved the equation. For each cell with its particular parameters they

determined the volume of water expressed as a function of chamber pressure. They found the total volume of water expressed by summing the volumes expressed from each cell.

Using their model Cheung, Tyree, and Dainty determined the effect of variations in cell parameters on the shape of the pressure^{-1}-volume curve. They held all but one of the parameters constant for the cells in the tissue. When they assumed six different values of initial osmotic potential for six groups of cells, their pressure^{-1}-volume curve was similar in shape to experimental curves. Varying modulus of elasticity had a similar effect. Because they used a linear relationship between cell volume and turgor potential, using only two sets of any one parameter gave them a curve made up of straight line segments joined at the endpoints. They noted that if Helkvist's relationship was used for the relationship between cell volume and turgor, the curve would have the proper shape.

Cheung, Tyree, and Dainty's analysis led them to several conclusions. First, they found that it was extremely difficult to determine the value of water potential where turgor potential becomes zero. This was the same observation that Helkvist (1975) made when he said that many data points were needed in the region where the pressure^{-1}-volume curve becomes linear. Secondly, they pointed out that the lack of a good relationship between volume and turgor pressure makes it impossible to determine a value of the modulus of elasticity unambiguously.

The papers summarized in this section have demonstrated how the pressure chamber can be used to measure cell properties. They have

also pointed out its limitations. One of the most striking appears to be the lack of understanding of the functional relationship between turgor and cell volume.

3.6 Modeling Efflux Curves

After a leaf or twig is placed in a pressure chamber and brought to its balance pressure, water can be forced from it by increasing the chamber pressure. The magnitude by which the pressure is increased is called the overpressure. If the water forced from the end of the stem is collected for short time intervals and weighed, the volume of water expressed can be plotted as a function of time to give an efflux curve. This section describes work that has been done on water efflux from leaves and discusses its significance to the pressure chamber.

Tyree and Dainty (1973) studied the efflux of water from hemlock shoots using a modification of the method first proposed to them by Dr. H.T. Hammel. They placed a shoot in the pressure chamber and used a rubber fitting to connect a polyethylene capillary tube to the protruding end of the stem. By collecting the expressed water in a beaker placed on an electronic balance, they found efflux curves for overpressures between 0.3 and 1.0 bars.

Tyree and Dainty analyzed the curves using a model which related chamber pressure to volume of water expressed (Tyree, Dainty and Benis, 1973). The model was derived from the following relationship between chamber pressure and cell osmotic and turgor potentials:

$$P = \overline{\pi}_i - {}_iP_t \qquad (3.11)$$

P = chamber pressure

$\overline{\pi}_i$ = osmotic potential of the ith cell

${}_iP_t$ = turgor pressure of the ith cell

They modeled changes in values of osmotic potential and turgor pressure when an overpressure was applied to a shoot initially at balance pressure P^o. They assumed that small amounts of water were expressed. Using the Van't Hoff relation they wrote the following expression for osmotic potential as a function of volume of sap expressed:

$$\overline{\pi}_i \cong \overline{\pi}_i^o + \left(\frac{\overline{\pi}_i^o}{{}_iV_o}\right)_i \cdot {}_iV_e \qquad (3.12)$$

$\overline{\pi}_i^o$ = osmotic potential for the ith cell when the shoot is at its initial balance pressure, P.

${}_iV_o$ = cell volume of the ith cell when it is at its initial balance pressure P.

${}_iV_e$ = volume of sap expressed from the ith cell

They developed the following functional relationship between volume of sap expressed and turgor pressure using a Taylor series expansion about ${}_iP_t$, the turgor pressure at the initial balance pressure P^o:

$${}_iP_t \cong {}_iP_t^o + \frac{\partial({}_iP_t)}{\partial({}_iV_e)} \cdot {}_iV_e \qquad (3.13)$$

They differentiated the relationship between cell volume and turgor developed by Tyree and Hammel (1972) (section 3.5) to get the following:

$$\frac{\partial({}_iP_t)}{\partial({}_iV_e)} \cong \frac{n\varepsilon}{{}_iV_p}\left(\frac{{}_iV_o - {}_iV_p}{{}_iV_p}\right)^{n-1} \qquad (3.14)$$

n = coefficient of nonlinearity

ε = elastic modulus of the ith cell

${}_iV_p$ = the volume of the ith cell at incipient plasmolysis

${}_iP_t$, ${}_iV_e$, ${}_iV_o$ are as defined previously

Substituting equations 3.12, 3.13, and 3.14 into equation 3.11 gave:

$$P = a_i + k_i \cdot {}_iV_e \qquad (3.15)$$

where:

$$a_i = k_i^o - {}_iP_t^o$$

$$k_i = \frac{\pi_i^o}{{}_iV_o} - \frac{\partial({}_iP_t)}{\partial({}_iV_e)}$$

In the above expression they called k_i the cell constant. When they tested the above relationship on hemlock shoots they found it valid for shoots near full turgor, providing less than one half percent of the total water content (fresh weight minus dry weight) had been expressed.

Tyree and Dainty used their model to predict efflux from cells. Assuming a water potential difference across the cell membrane of $\Delta\psi$, they used the relationship for flow of water across a membrane (Slatyer, 1967, equation 6.3) to write:

$$\frac{\partial({}_{i}v_{e})}{\partial t} = (AL_{p})_{i}\,\Delta\psi \qquad (3.16)$$

A = cell wall area across which water flows

L_p = hydraulic conductivity of the semipermeable membrane across which water flows

$\Delta\psi$ = water potential difference across the membrane

Using equation 3.15 they found an expression for $\Delta\psi$ when the chamber pressure is instantanteously increased by an amount ΔP:

$$\Delta\psi = \Delta P - k_i \cdot {}_{i}v_{e} \qquad (3.17)$$

Substituting this expression into their differential equation and integrating they found the efflux from the cell to be:

$${}_{i}v_{e} = \frac{\Delta P}{k_i}\left(1 - e^{-k_i(AL_p)_i t}\right) \qquad (3.18)$$

They assumed the water efflux from a population of cells was the sum of the efflux from individual cells. This gave them equations of the same form but with the values $(AL_p)_i$ and k_i replaced by the following:

$$AL_p = \sum_{\text{cells}} (AL_p)_i \qquad (3.19)$$

$$\frac{1}{K} = \sum_{\text{cells}} \left(\frac{1}{k_i}\right) \qquad (3.20)$$

Differentiating the efflux equation with respect to time gave them the

following expression for rate of water efflux from the leaf:

$$\frac{\partial V_e}{\partial t} = AL_p \Delta P e^{-AL_p Kt} \qquad (3.21)$$

Defining the half time, $T_{\frac{1}{2}}$, for a group of cells with cell constant k_i as the time required for the efflux rate to decrease to one half the value it had at time zero, they used equation 3.21 to find:

$$T_{\frac{1}{2}} = \frac{\log_e 2}{k_i (AL_p)_i} \qquad (3.22)$$

Tyree and Dainty analyzed their efflux curves using the above model. They discovered that a hemlock shoot left in the chamber for extended time periods would absorb water from the beaker at a daily rate equal to 0.2 to 0.5 per cent of the total shoot water content. They explained this influx of water as the result of metabolic activity. After correcting the efflux data for this metabolic water uptake, they plotted efflux on semi-logarithmic co-ordinates as shown in part (a) of figure 3.10. The curve has both linear and nonlinear portions. They extended the linear portion and found the difference between the actual data points and the corresponding values on the ordinate of the straight line. Plotting this residual gave them the curve marked with the circles in part (b) of figure 3.10. They repeated this procedure and found the set of data points marked with dots and shown in part (b) of the figure. Tyree and Dainty concluded that there were three distinct populations of cells each with its own value of AL_p. The half-times for these populations were 1700, 400, and

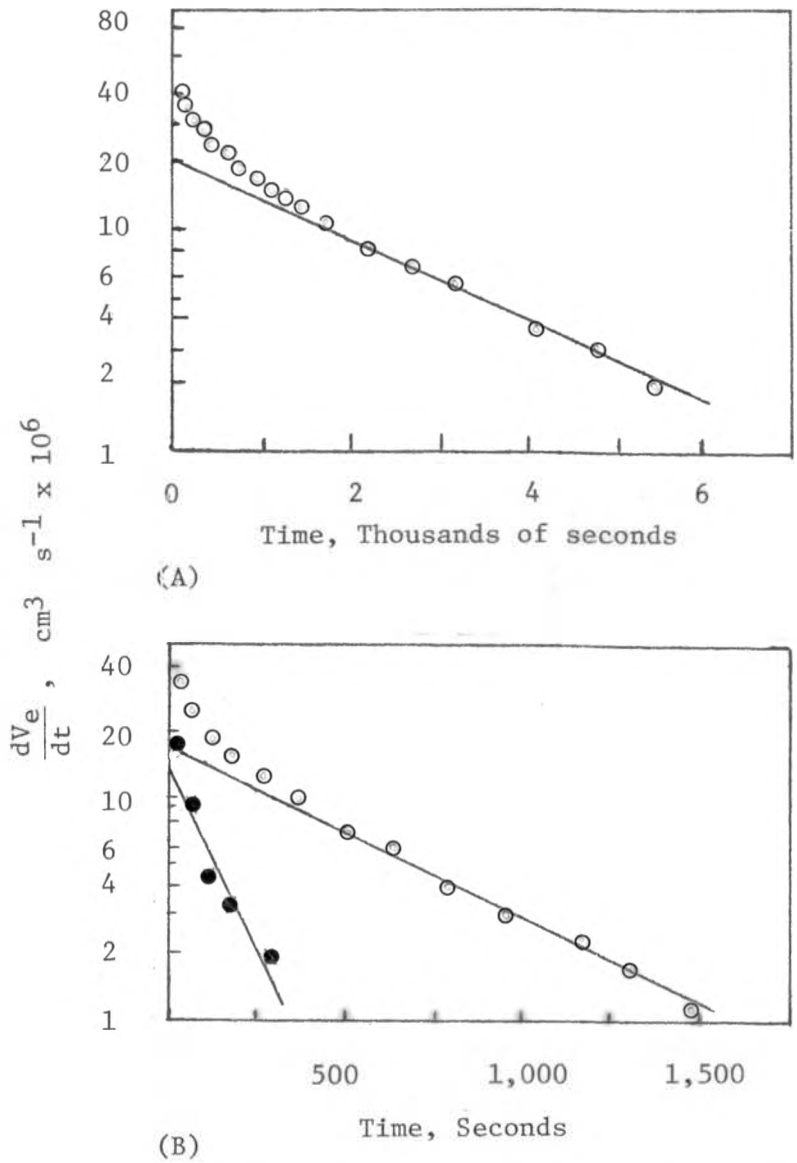

Figure 3.10 Graphs of the logarithm of the instantaneous efflux rate as a function of time after application of a 0.345 bar overpressure on a 27.6 gram hemlock shoot. This is figure 3 in Tyree and Dainty's (1973) article. Part (A) shows the original data. After approximately 2,000 seconds the points fell on a straight line. Tyree and Dainty drew a line through these points and extended it to the y axis. In part (B) the circles represent data taken from the graph in part (A). Tyree and Dainty subtracted the efflux rates in part (A) from the corresponding ordinates of the line. They plotted the logarithm of the difference as a function of time (the circles in part (B)). The dots in part (B) were points determined in the same manner using the data points marked as circles.

96 seconds. By estimating the value of A from leaf surface area and the A_{mes}/A ratio, they estimated values of L_p for the three populations as 5.37, 7.13, and 2.94 x 10^{-5} cm^3/sec-bar. The population cell constants were 136, 12.3, and 5.33 bar/cm^3 respectively.

Tyree, Benis, and Dainty (1973) applied the Arrhenius rate theory and determined the activation energy for the efflux of water from stems. To determine the activation energy they had to find the temperature dependence of the initial efflux rate. For the hemlock shoots they studied, calculated changes in resistance to water flow through xylem were less sensitive to temperature than the measured efflux rate. They estimated that the membrane resistance was at least one fourth the value of the xylem resistance.

Tyree, Caldwell, and Dainty (1975) extended Tyree and Dainty's work by studying the efflux of water from hemlock shoots which had been infiltrated with water. They forced water into the leaves by placing them in the chamber "upside down" with the cut end of the stem inside the chamber and submerged in a beaker of water. Pressurizing the chamber forced water into the shoot. By comparing the efflux from infiltrated and uninfiltrated stems they estimated the upper and lower limits for the resistance to water flow from the intercellular spaces. Their value for total shoot resistance was 3.45 - 6.00 x 10^{-3} bar-sec/cm^3. Their estimates of resistance to flow from the air spaces ranged from 1.13 to 17.5 x 10^{-3} bar sec/cm^3. The values for this resistance were usually about twice the corresponding values for flow across the cell membranes. About two thirds of the resistance to water flow from the shoot appeared to be in the xylem. Their original

model had described the shoot as containing three populations of cells which lost water independently of each other. Since they found that much of the resistance was actually in the xylem, they concluded that the original model was incorrect. They stated that it was inappropriate to develop a more complex model which would take into account shoot geometry, "the complicated coupling between the efflux of individual cells," and the limiting effect of the xylem on the flow of water from the leaf.

In a more recent article, Tyree and Cheung (1977) report efflux experiments on beech (Fagus grandifolia) leaves. They measured the efflux rate from both infiltrated and uninfiltrated leaves for overpressures of 1 to 3 bars and initial balance pressures of 3.0 and 17.8 bars. The initial efflux rates at both initial balance pressures, as reported in figure 1 of their article, appear identical. However, the efflux rate at the 3.0 bar initial balance pressure declined more rapidly than the efflux rate at 17.8 bars initial balance pressure. This was reflected in the values of the half-times for the efflux rates. Tyree and Dainty defined these as the time required for the efflux rate to reach one-half its original value. For a 3.0 bar initial balance pressure the value was 0.90± 0.14 minutes and for the 17.8 bar initial balance pressure it was 2.04 ± 0.32 minutes. The efflux rates in each case declined rapidly at first but then became log-linear. The half times for the log-linear portions of the efflux curves for the 3.0 and 17.8 bar initial balance pressures were, respectively, 14.2 ± 2.0 minutes and 23.0 ± 4.0 minutes. They estimated the initial resistance of leaves by calculating the value of

the overpressure (P) divided by the efflux rate from the leaf. The infiltrated leaves had efflux rates from 2 to 5 times that of uninfiltrated leaves while their resistances were 0.4 times as great. They measured xylem and petiole resistance by forcing water through the stem and petiole after detaching the leaf. This resistance was 0.08 times the resistance of the entire shoot. They noted that this contrasted sharply with the value of 0.66 times shoot resistance which had been measured for hemlock. They measured the resistance of the leaf xylem by removing the margin from a beech leaf, placing the leaf in a beaker of water, placing the leaf and beaker in a pressure chamber, mounting the leaf in the chamber head, and pressurizing the chamber. The measured resistance was nearly identical to the value for the stem and petiole. Tyree and Cheung concluded that the resistance of the xylem vessels in the leaf was therefore negligible.

Using the above information, Tyree and Cheung investigated possible pathways for water movement in leaves. One pathway was flow out of the individual cell walls into the cell wall area and then flow through the cell wall to the nearest vessel element. The second was flow from cell to cell combined with flow through cell walls. The third was flow from cell to cell through the cell membranes. In the first case, the cell wall resistance was assumed negligible. In the second it was assumed to be one tenth to one third the cell membrane resistance. In the third it was assumed to be much larger than the cell membrane resistance. By using each of these models to analyze their results, Tyree and Cheung were able to calculate the resulting values of cell membrane and cell wall permeabilities.

Tyree and Cheung termed the above calculations inconclusive. However, the temperature dependence of water efflux corresponded to changes in membrane permeability, as would be expected if water traveled through the second of the three pathways. They suggested this temperature dependence was evidence that water followed that pathway. In other words, the water driven from living cells or infiltrated air spaces of leaves would "pass in and out of cells and the thinnest part of the cell walls between cells." However, they suggested that the temerature dependence of efflux in other plants would have to be measured before a final conclusion could be drawn. Their estimate of cell membrane conductivity, calculated on the assumption that water followed the second pathway, was 1.5×10^{-6} cm/sec-bar.

Cheung and Tyree's assumption that the xylem resistance is negligible is open to question. The method they describe for testing the resistance of the xylem involved cutting the edge from the leaf. This should have exposed secondary veins and allowed water to pass through the leaf without passing through the tertiary and smaller veins. Since the resistance to water flow varies with the fourth power of the vessel radius, this could mean that a significant resistance was not considered.

The research cited in this section has described the technique for measuring and quantifying the resistances encountered by water being forced from leaves in pressure chambers. In the case of the beech leaf, xylem resistance was assumed negligible. Tyree, Caldwell, and Dainty (1975) suggested that a more accurate model would have to

take into account the geometry of the leaf and the effect of the xylem on limiting water efflux. The model described in chapter 8 takes both of these factors into account and adds insight into water efflux from leaves placed in a pressure chamber.

CHAPTER 4

PRESSURE CHAMBER EXPERIMENTS

In chapter 3 I discussed efflux and pressure^{-1}-volume experiments reported in the literature. In this chapter I describe my own efflux and pressure^{-1}-volume experiments on wheat leaves and compare them to the literature results. I used the efflux experiments to verify the mathematical models developed in chapters 7 and 8 and the pressure^{-1}-volume curves to measure the components of water potential in the leaves. The curves included in this chapter are typical of those obtained from all of the leaves tested. Although I used a winter variety for most of the tests, I performed several tests on a spring variety. Chapter 5 summarizes anatomy data for these leaves.

4.1 Background

Three sets of pressure^{-1}-volume and efflux experiments are reported in this chapter. The experimental techniques were developed by Dr. Jay Cutler and Mr. Kevin Shahan of the Agronomy Department. Dr. Cutler and Mr. Shahan did the March experiments and I adapted their techniques for the July/August and November experiments using their laboratory and equipment. The basic techniques for running pressure^{-1}-volume tests they developed are described in a paper by Cutler, Shahan, and Steponkus (1979). They later applied their techniques to studies of changes in turgor and osmotic potentials in both water-

stressed and well-watered rice plants (Cutler, et al.,1980). Both wheat and rice are in the grass family and have leaves similar in shape. Although wheat leaves are smaller, I applied the technique to them without difficulty.

The pressure chamber technique measures wheat leaf water potential with reasonable accuracy. Frank and Harris (1973) measured the leaf water potential of wheat plants in the late tillering growth stage using both a pressure chamber and a thermocouple psychrometer. Pressure chamber measurements were about 8 per cent less than those made with the thermocouple psychrometer. For wheat in the early heading stage, the measurements were about 16 per cent less. Lawlor (1972) found that pressure chamber and thermocouple psychrometer measurements were nearly identical. Campbell and Campbell (1974) found that pressure chamber measurements were consistently one bar lower (in absolute value) than thermocouple hygrometer measurements.

4.2 Experimental Procedures:

Dr. Cutler, Mr. Shahan, and Mr. Melkonian grew the wheat plants used in the pressure chamber experiments in the Guterman laboratory greenhouses. They used no supplemental lighting. Dr. Cutler and I tested both winter (Triticum durum L. cv. 'Yorkstar') and spring (Triticum aestivum L. em Thell cv. 'Super X') varieties. Before planting the wheat seeds in flats filled with vermiculite, Dr. Cutler and his co-workers aerated them in tap water for 24 hours. They vernalized the winter wheat used in the July/August experiments by storing newly emerged seedlings in a cold room at 2 degrees Celsius

for 6 to 8 weeks. At the appropriate time for each variety, they transplanted 4 seedlings into each of several 10 liter clay pots filled with silt loam soil (a fine, illitic, mesic, Glossoboric Hapludalf, soil series Hudson silt loam). They fertilized them weekly and watered them at least every other day. Daytime greenhouse temperature was 27 degrees Celsius and nighttime temperature was 21 degrees Celsius.

Dr. Cutler developed the following standardized procedure to reduce experimental error and to characterize the leaves tested. To ensure that the leaves of each plant were at a uniform water potential, he put them in a dark, humid incubator room several hours before the test. Incubator room temperature was 23 degrees Celsius. The plants were in the late tillering or early heading stage of growth. Because preliminary tests on flag leaves gave inconsistent results, Dr. Cutler and I measured the water potential of the first or second leaf below the flag leaf using a Soil Moisture Equipment Corporation model 3005 pressure chamber (available from Soil Moisture Equipment Corporation, Santa Barbara, California). To get an estimate of leaf volume, I amended Dr. Cutler's procedure at this point and measured leaf thicknesses at intervals of 2.54 centimeters (1 inch) with a micrometer that could be tightened to a constant compressive force. Dr. Cutler humidified a double-layered plastic bag by breathing into it and placed it over the leaf. This bag prevents moisture evaporation and reduces leaf temperature changes during the test (Wenkert, et al., 1978). Immediately after placing the bag over the leaf, Dr. Cutler cut the leaf from the plant using a razor blade

and placed the bag-enclosed leaf in the chamber with its base protruding through the sealing grommet in the chamber head (see figure 1.1).

I characterized the physiological properties of the wheat leaves used in the July/August experiments by conducting pressure^{-1}-volume tests on several leaves taken from different plants. I pressurized the chamber until water began to appear at the cut end of the stem. The chamber pressure at which this occurs (called the initial balance pressure) represents the absolute value of the leaf water potential. After weighing a 2 dram vial half-filled with cotton, I placed it over the end of the leaf, and increased the chamber pressure 3 bars for two or three minutes. In order to stop the water flow, I reduced the pressure to the previous balance pressure. Then I removed, sealed, and weighed the vial, found the new balance pressure, placed a new vial over the end of the leaf, and increased the pressure three bars. I continued applying three bar overpressures, collecting and weighing expressed sap, and then removing the overpressure until the balance pressure exceeded 20 bars.

Cutler, Shahan, and Steponkus (1979) used leaf water content in their analysis of pressure chamber experiments. I used their procedures in the tests on wheat leaves. When the leaf is fastened in the chamber, a portion between 25 and 50 mm long is outside the chamber (see figure 1.1). I removed this portion of the leaf and sectioned it for anatomical studies. I weighed the remaining portion, dried the sample in an oven at 80 degrees Celsius for at least 48 hours, and then reweighed it. The total weight of water in the leaf

was fresh weight minus dry weight. Fresh weight was the sum of the weight of the leaf after removal from the chamber and the weight of the water expressed from the leaf.

Because the leaf is subjected to high pressures in the chamber, some tissue deformation must occur. I investigated changes in leaf tissue structure by collecting and sectioning samples from portions of leaves 2-G and 1-I after they were removed from the chamber at the completion of an experiment. I compensated for the weight of the section removed as follows. Using the weight of the leaf before and after the sample was removed, I estimated the original dry weight of the leaf. I assumed that the ratio of residual weights before and after removal of the sample was the same as the ratio of the dry weights before and after sample removal.

Dr. Cutler developed the following procedure for measuring efflux from a leaf. After finding the balance pressure, he rapidly (in less than 5 seconds) increased the pressure of the chamber by 3 bars and collected the expressed sap in vials which he changed at half minute intervals during the first portion of the test and 1 to 10 minute intervals during the remaining portion. I modified his procedure slightly when I did the July/August and November experiments. If the leaf I was testing was relatively large, I changed the vials at one minute intervals during the first several minutes of the test. When I tested smaller leaves, I changed the vial at two minute intervals.

Dr. Cutler applied the above procedure at a series of beginning balance pressures and determined a pressure^{-1}-volume curve and several

efflux curves simultaneously. After removing a leaf from a plant and finding the balance pressure, he ran an efflux experiment using the procedure described above. At the completion of the test, he found the new balance pressure and used this as the beginning balance pressure for the next test. In most cases, he continued this procedure until the balance pressure reached 20 bars or more.

When I adapted Dr. Cutler's procedure to the July/August and November experiments, I modified it slightly. Dr. Cutler called my attention to the following. When leaf cells still have turgor, only a small amount of water is expressed from the leaf during an efflux experiment. As the cell looses turgor, a given increment in chamber pressure will force more water from the leaf. When the turgor first becomes zero, the maximum amount of water will be expressed for a given increase in chamber pressure. During subsequent efflux experiments, less and less water will be expressed. For the wheat leaves tested the largest amounts of water were expressed when an efflux experiment was begun at a balance pressure between 10 and 15 bars. When turgor was still present in the leaf, I could express only small amounts of water. These amounts were often of the same order of magnitude as the errors in weighing. Since I could not express enough sap to collect data for an efflux curve, I often began an experiment by first conducting a pressure^{-1}-volume test in the manner which I described in the first portion of this section. When the balance pressure was between 10 and 15 bars, I began conducting a series of efflux experiments on the leaf. I continued the efflux experiments until the balance pressure exceeded 20 bars. At this point, I resumed

using the pressure^{-1}-volume procedure but applied the overpressure for 5 to 10 minutes instead of 3 minutes. I usually continued the pressure^{-1}-volume procedure until the balance pressure exceeded 30 bars. I have summarized the efflux experiments in section 4.4.

4.3 Pressure^{-1}-volume Experiments

A typical pressure^{-1}-volume curve for a wheat leaf is shown in figure 4.1. Results of all the experiments are included in Appendix A. In the calculations described below, I converted from weight to volume by assuming the density of water was 1 mg/mm^3. I analyzed the pressure^{-1}-volume curve shown in figure 4.1 using the techniques of Tyree and Hammel (1972) and Cutler, et al. (1979). By extrapolating the straight line portion of the curve to zero volume of water expressed, I found $-\overline{\pi}_i$, the initial volume-averaged turgor potential of the leaf cells, to be -11.7 bars. (Osmotic potential is less than zero. I wrote it in this manner to make it conform to the convention that all parameters such as $\overline{\pi}$ are positive numbers.) The initial turgor potential, P_i^t was 8.1 bars, and the volume-averaged osmotic potential at zero turgor, $-\overline{\pi}_o$, was 12.7 bars. By extrapolating the straight line portion of the curve to the volume of water expressed at infinite pressure, I found the total osmotic volume in the leaf, V_π, to be 165 mm^3. The total volume of water in the tissue, V_t, was fresh weight minus dry weight, or 259 mm^3. The osmotic fraction of tissue water, V_π/V_t was 0.637. Values of the above parameters for all of the leaves on which pressure^{-1}-volume tests were conducted, are shown in Table 4.1. The leaf designations are explained in detail in Appendix

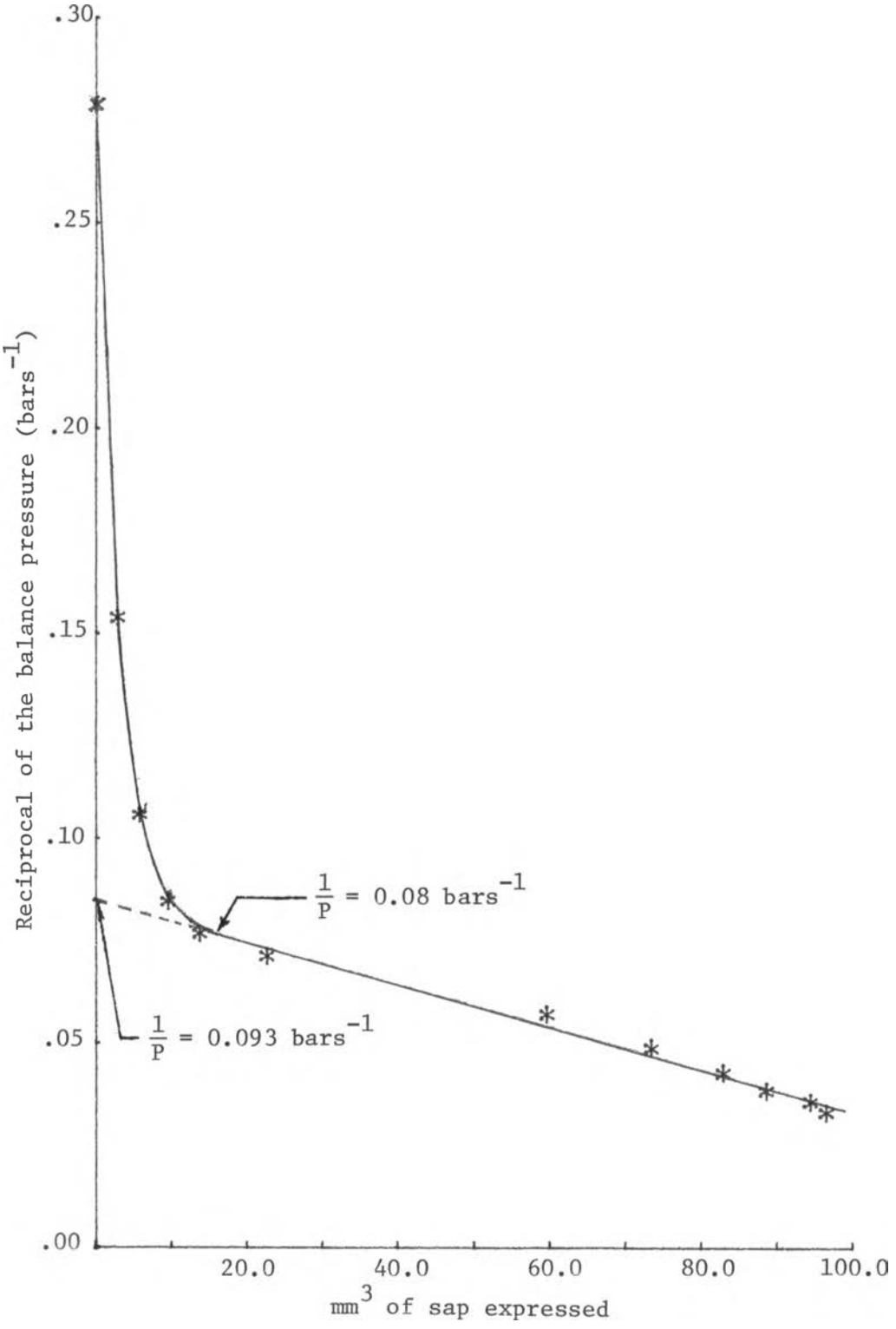

Figure 4.1. Pressure^{-1}-volume curve for wheat leaf 2-G.

Table 4.1. Summary of data from pressure^{-1} - volume tests conducted on wheat leaves.

Leaf[a]	Date Tested	Initial Values			Osmotic Potential at Zero Turgor	Slope of linear portion of curve
		Water Potential (Ψ) bars	Turgor Potential (P_t^i) bars	Osmotic Potential ($-\bar{\pi}_i$) bars	($-\bar{\pi}_o$) bars	bars/mm^3
1-16	3/13/79	-2.8	6.5	-9.3	-10.9	-.000432
2-16	3/13/79	-3.2	6.2	-9.4	-10.6	-.000683
1-C	7/27/79	-5.8	7.5	-13.4	-13.3	-.000375
1-D	7/30/79	-7.2	5.5	-12.7	-13.3	-.000846
2-E	7/31/79	-3.4	8.7	-12.1	-12.5	-.000186
1-F	8/1/79	-6.2	7.5	-13.7	-14.3	-.001190
2-F	8/1/79	-3.4	8.2	-11.6	-12.7	-.000540
1-G	8/2/79	-3.7	8.1	-11.8	-12.5	-.000316
2-G	8/2/79	-3.6	8.1	-11.7	-12.7	-.000517
3-G	8/2/79	-3.5	9.7	-13.2	-13.9	-.000509
1-H	11/20/79	-3.4	5.6	-9.0	-10.0	-.001189
2-H	11/20/79	-3.8	4.7	-8.5	-10.3	-.001475
1-I	11/21/79	-2.8	7.6	-10.4	-12.2	-.000796

[a]See Appendix A for an explanation of the leaf numbering system.

(continued)

Table 4.1. concluded.

Leaf	Date Tested	Osmotically Active Volume of Water (V_π) mm^3	Total Volume of Water in Tissue (V_t) mm^3	Osmotic Fraction of Tissue water $\left(\frac{V_\pi}{V_t}\right)$	Leaf Volume mm^3	Leaf Length mm
1-16	3/13/79	249.	---	---	---	---
2-16	3/13/79	155.	---	---	---	---
1-C	7/27/79	199.	---	---	---	---
1-D	7/30/79	93.4	230.	0.406	428	254
2-E	7/31/79	447.	565.	0.791	865	338
1-F	8/1/79	61.9	135.	0.459	268	178
2-F	8/1/79	160.	228.	0.702	385	225
1-G	8/2/79	268.	309.	0.867	415	237
2-G	8/2/79	165.	259.	0.637	406	238
3-G	8/2/79	148.	191.	0.775	286	202
1-H	11/20/79	93.8	149.	0.630	291	225
2-H	11/20/79	66.7	130.	0.513	272	248
1-I	11/21/79	121.1	168.	0.720	315	246

A. Leaves lettered C through G were winter wheat (cv. 'Yorkstar') and leaves lettered H and I were spring wheat (cv.'Super-X'). The March experiments were designated by numbers only and were conducted by Dr. Cutler and Mr. Shahan on winter wheat plants that had not been vernalized.

The osmotic fraction of tissue water for the leaves shown in Table 4.1 varies widely. This variation is probably caused by a high variability in the osmotically active volume of water, V_{π}. My estimates of this fraction varied because the slopes of the linear portions of the curves varied. The theory discussed in section 3.5 defines the slope of the linear portion of the curve as the reciprocal of RTN_s where R is the gas constant, T is the absolute temperature in degrees Kelvin, and N_s is the total number of osmoles of solute in the leaf cells. This theory predicts that if N_s increases, the slope will decrease. Therefore, the leaves with the larger slopes, such as 1-F and 1-D may have had fewer dissolved solutes in their symplasm. I found no pattern which would explain this variation.

I determined the leaf volumes listed in table 4.1 by applying the prismoidal formula to two inch sections of the leaf. The formula uses the cross sectional area of the solid at the base, top and midsection. I calculated the volume of the two inch sections by assuming that the cross sectional areas of the leaf at the ends of the section were the cross sectional areas of the top and bottom. The cross sectional area of the leaf half way between the ends was the area of the midsection. I assumed the cross sectional area of the leaf was equal to the width of the leaf, as measured from a tracing,

times the thickness of the leaf as measured with the micrometer. Applying the prismoidal formula, the volume of the section is:

$$\text{Volume} = (A1 + 4 \times A2 + A3) \times 8.467 \qquad (4.1)$$

A1, A3= cross sectional areas at opposite ends of the two inch section (mm^2)

A2 = cross sectional area halfway between the two ends of the section (mm^2)

These volume calculations are approximate because leaf dimensions such as thickness and width vary along the length of the leaf. Measurements of leaf width and thickness at one inch intervals along the length of leaves 1-G, 2-G, and 3-G are shown in table 4.2. Figure 4.2 is a plot of the data in table 4.2. It illustrates that the variation in leaf thickness with length is approximately linear. Leaf thickness also varies across the width of the leaf. The midrib is several times thicker than the edge. For example, on December 10, 1978 I sampled the midsection of a leaf from a greenhouse plant similar to those used for the pressure chamber experiments. The thickness at the edge was 0.1 mm and the thickness at two thirds the distance from the edge to the midrib was 0.2 mm. When I calculated the cross sectional areas from the prismoidal formula, I used the micrometer measurement of thickness at one half the distance from the edge to the midrib. This gave me an estimate of the average leaf thickness.

All of the pressure^{-1}-volume curves with the exception of the curve for leaf 2-F remained linear after turgor became zero. The

Table 4.2. Measurements of leaf thickness and width at various distances from the tip of wheat leaves 1-G, 2-G, and 3-G.

Distance From Tip (mm)	Leaf 1-G		Leaf 2-G		Leaf 3-G	
	Thickness (mm)	Width (mm)	Thickness (mm)	Width (mm)	Thickness (mm)	Width (mm)
0	.140	0	.132	0	.132	0
25.4	.140	5.2	.147	5.5	.152	4.9
50.8	.152	7.3	.155	6.2	.165	7.5
76.2	.158	9.7	.158	7.8	.165	9.5
101.6	.178	11.5	.165	9.8	.165	10.8
127.0	.183	12.9	.178	10.9	.165	10.9
152.4	.183	12.9	.183	11.8	.165	10.9
177.8	.178	12.9	.208	11.8	.165	10.2
203.2	.178	12.0	.224	12.2	.173	----
228.6	.216	10.5	.224	11.3	----	----
254.0	.216	10.4	.234	10.9	----	----
279.4	.229	----	.241	----	----	----

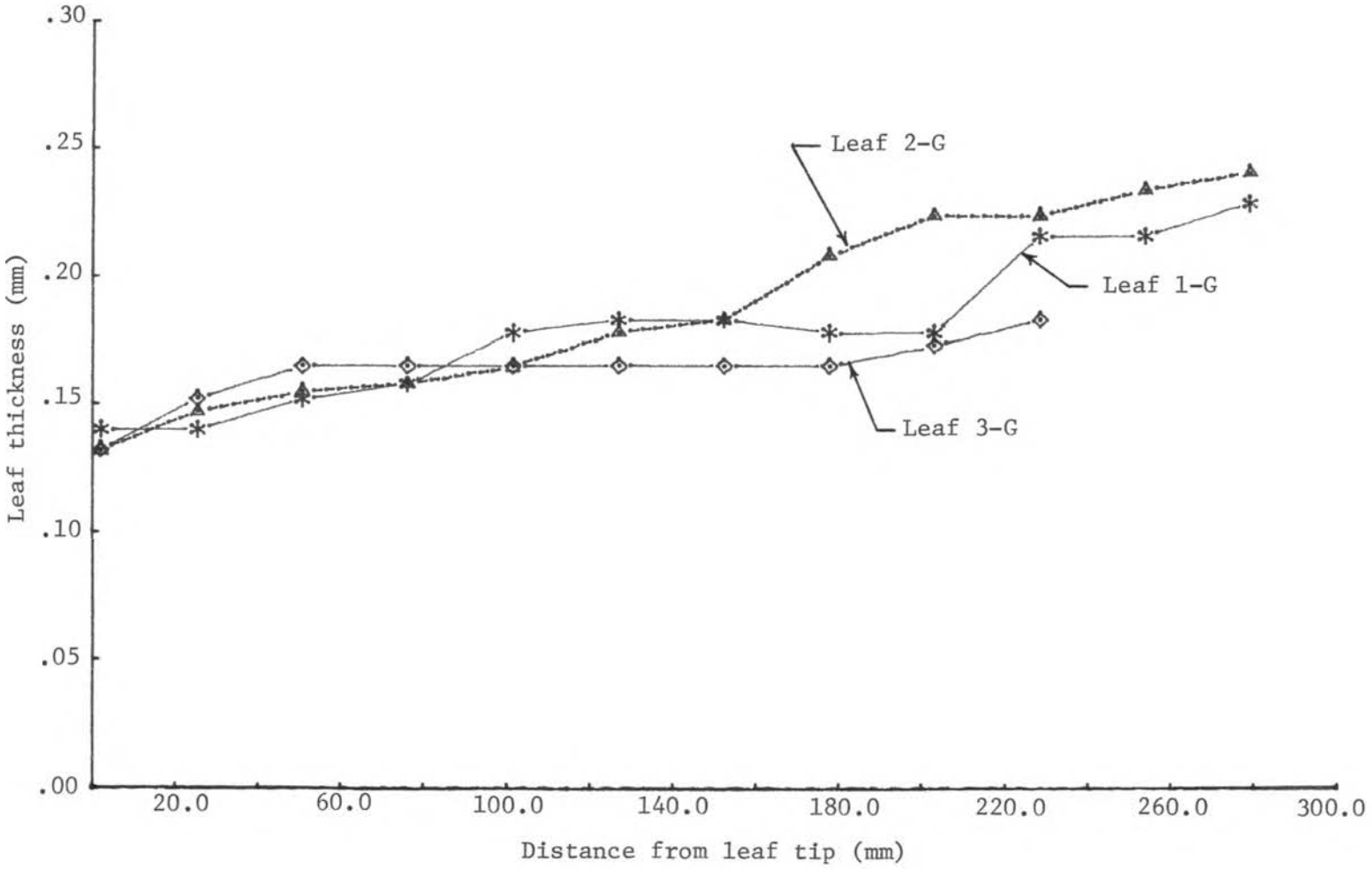

Figure 4.2. Graph of leaf thickness at various distances from the tip of wheat leaves 1-G, 2-G, and 3-G.

highest balance pressure reached was 34.0 bars for leaf 1-G at which point 64 per cent of the osmotically active volume (V_π) had been expressed. The non-linearity of the pressure^{-1}-volume curve of leaf 2-F could have been caused by damage to the leaf. I discuss the possibility of xylem damage in chapter 6.

Hammel (1967) studied the variations in the turgor and osmotic components of leaf water potential as water was expressed from hemlock leaves placed in a pressure chamber. He plotted these potentials against the relative volume of expressible water remaining in the leaf. His plot is shown in figure 3.9. In figure 4.3, I show a similar plot based on my experiments with wheat. His definition of V_o is the same as my definition of V_π. The expressible water remaining in the cell is the total expressible water initially in the cell, V_π minus the volume of water that has been expressed, V_e. Therefore, $1-V_e/V_\pi$ is equal to Hammel's value of V/V_o. Using figure 4.1, I determined V_π, V_e, and the turgor and osmotic potentials for points on the pressure^{-1}-volume curve and plotted the total potential and the osmotic and turgor components of potential. The curves appear similar in shape to those reported by Hammel and shown in figure 3.9. The turgor potential appears to be nearly a linear function of relative cell volume when small amounts of water have been expressed from the leaf. After larger amounts of water have been expressed, the turgor potential approaches zero and the relationship between cell volume and turgor potential appears to be non-linear.

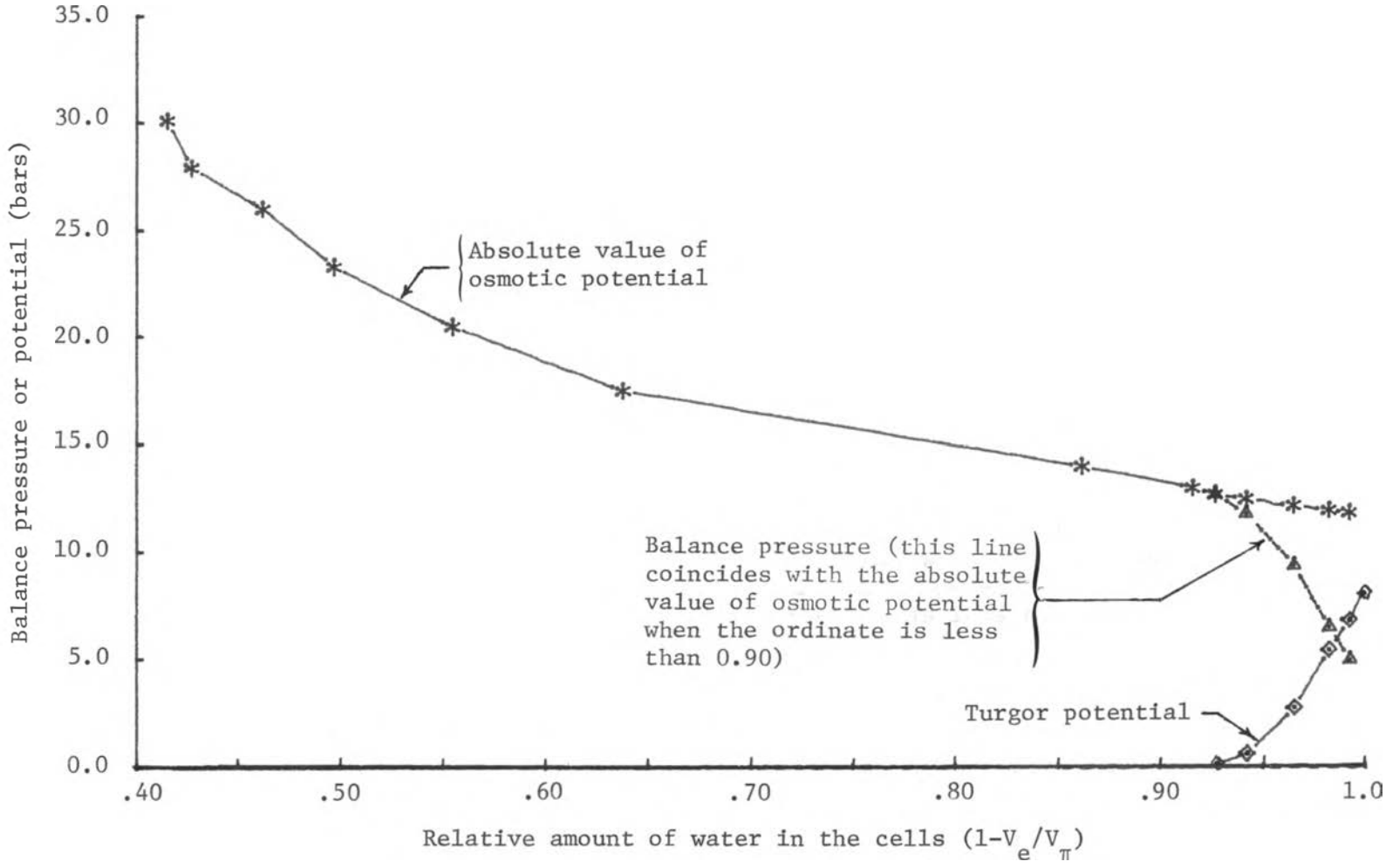

Figure 4.3. Balance pressure, turgor potential, and absolute value of osmotic potential as functions of relative volume of leaf cells (1 - V_e/V_π) for leaf 2-G.

4.4 Efflux Experiments

Typical efflux curves for wheat plants are shown in figures 4.4 and 4.5 and the results of all efflux experiments are included in Appendix B. The curves start at various balance pressures between 2.8 and 18.7 bars. I used three bar overpressures in each experiment. As I mentioned earlier, Dr. Cutler first pointed out to me that the total efflux from the leaf varies with the balance pressure at which the test is begun. When the leaf cell has turgor or when the balance pressure exceeds 10-15 bars the 3 bar overpressure expresses less water than the same overpressure at beginning balance pressures near the value of $-\overline{\pi}_o$, the volume-averaged osmotic potential at zero turgor. This behavior is predicted by the model of Tyree and Hammel (1972) as described in section 3.5. This same general pattern occurred in all of the efflux experiments. This is clearly shown in figure 4.4. Leaf 1-16 had an initial balance pressure of 2.8 bars. When Dr. Cutler applied a 3 bar overpressure, only 9.0 mm^3 of water was expressed (see also Appendix B, table B.4). After water had been driven from the leaf, the balance pressure was 6.4 bars. Dr. Cutler applied the next overpressure without collecting data for an efflux curve. After this overpressure, the balance pressure was 10.8 bars. When he applied another 3 bar overpressure, 54.5 mm^3 of water was expressed. The subsequent balance pressure was 14.0 bars. The next efflux experiment was started at a balance pressure of 14.8 bars and 30.6 mm^3 of water was expressed. The last efflux experiment on the leaf was begun when the balance pressure was 18.7 bars and 16.7 mm^3 of water was expressed.

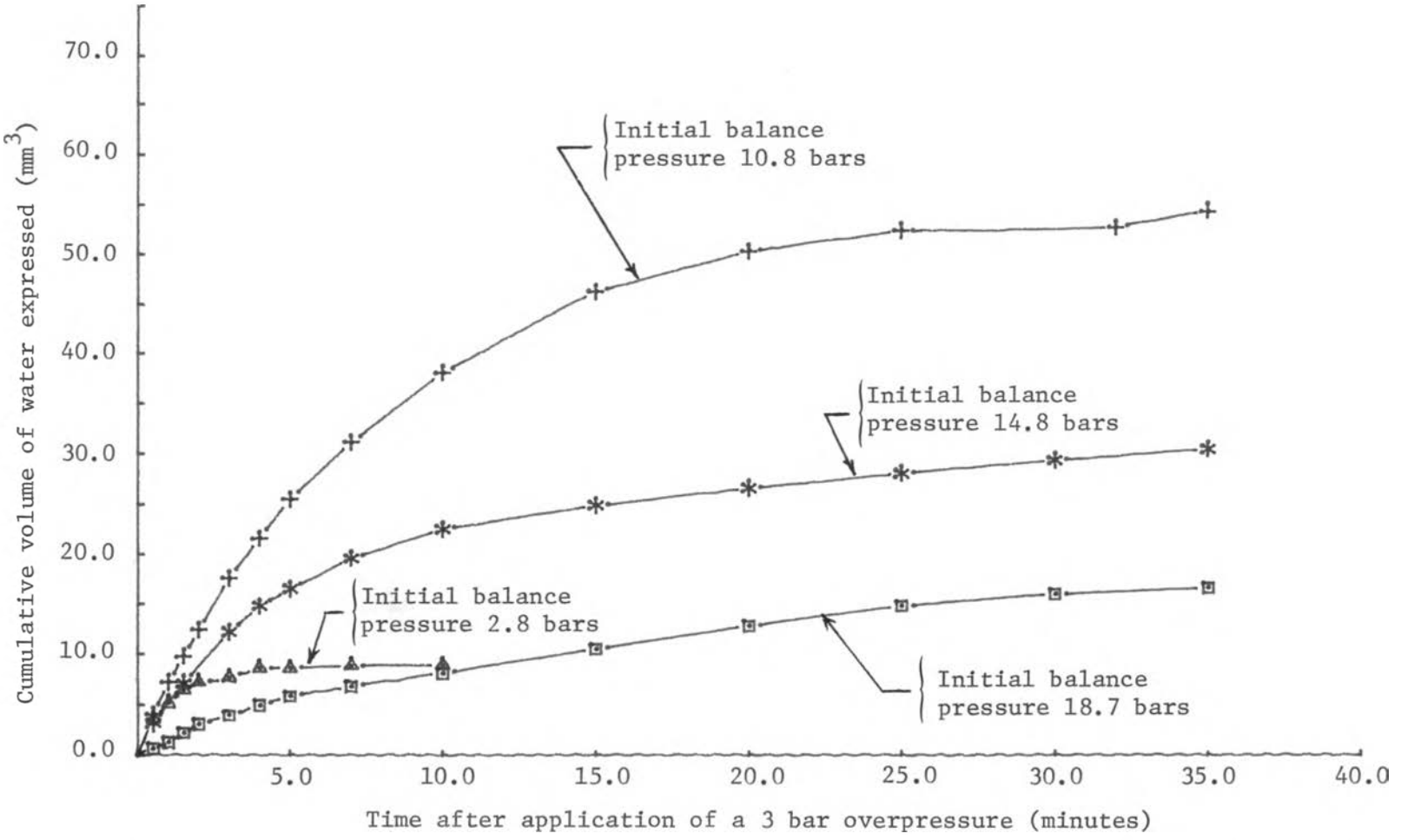

Figure 4.4. Efflux curves for wheat leaf 1-16 showing water expressed from the leaf for various initial balance pressures at various times after application of a 3 bar overpressure. (The experiment was conducted 3/13/79)

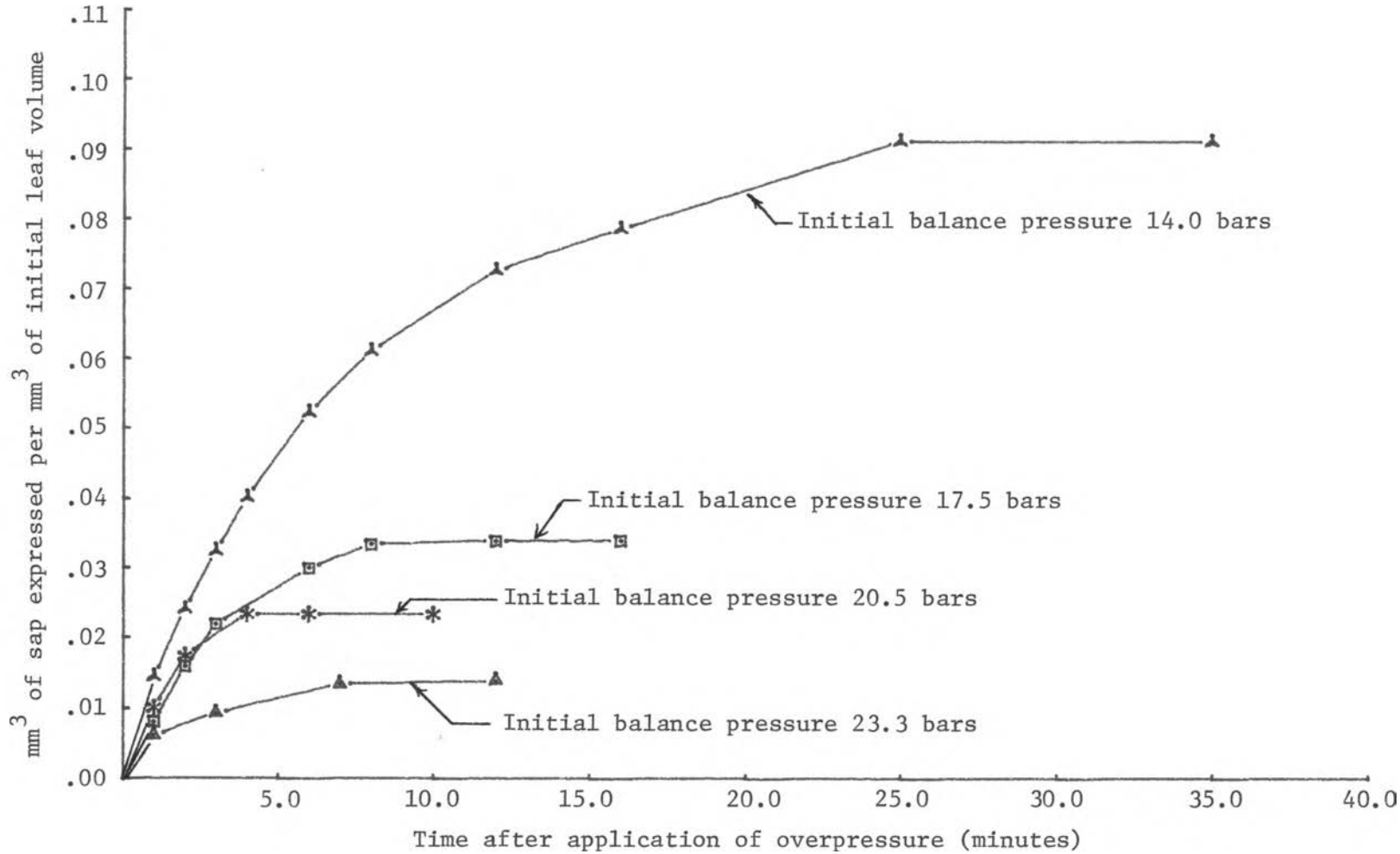

Figure 4.5. Efflux curves for various initial balance pressures when an overpressure of 3.0 bars was applied to leaf 2-G. Leaf length was 238 mm. Leaf volume was 406 mm^3.

The curves in figure 4.5 are similar in shape to those in figure 4.4. However, when I plotted the data, I normalized the efflux by dividing it by leaf volume. This technique allowed me to compare efflux curves from small and large leaves. The turgor potential for leaf 3-G first became zero at a balance pressure of 12.7 bars. Therefore, the largest volume of water was expressed at the pressure of 14.0 bars which was the balance pressure nearest to 12.7 bars.

It was difficult to get good efflux curves when turgor was still present in the leaf cells. Quite often only a few milligrams of water were expressed when the first several overpressures were applied to a leaf. Although the collecting vials could be weighed to the nearest 0.1 milligram, repeated weighings of the vials gave variations of several tenths of a milligram. Therefore, to reduce the experimental error, I needed to collect several milligrams of sap. Consequently, I could seldom get more than two accurate data points when I tried to conduct efflux experiments at these initial balance pressures. Therefore, I began most of the efflux experiments after I had removed most of the turgor from the cells using the pressure^{-1}-volume method.

Tyree and Dainty (1973) did an extensive analysis of the time variation of water efflux from hemlock leaves. I wanted to compare my data with theirs, so I estimated efflux rates for the experiments reported in Appendix B. I calculated the efflux rate at the midpoint of the time intervals in which water was expressed from the leaf. I assumed this rate was equal to the efflux during the time interval divided by the length of the interval. For example, the total efflux from leaf 1-16, 0.5 minutes after application of a 3 bar overpressure

was 3.6 mm and the total efflux 0.5 minutes later was 5.2 mm^3. The efflux during that time interval, 1.6 mm^3, divided by the length of the interval, 0.5 minutes, gave me an efflux rate of 3.2 mm^3/min. I assumed this to be the efflux rate 0.75 minutes after application of the overpressure.

When Tyree and Dainty (1973) plotted the natural log of the efflux rate from a hemlock shoot as a function of time after application of a 0.345 bar overpressure, they found that the data points fell on a straight line after 2000 seconds (see section 3.7, figure 3.10). Figures 4.6 through 4.9 are similar plots for wheat leaves 1-16 and 2-G. For each initial balance pressure I fit a regression line to the points which appeared to fall on a straight line. For example, I drew the regression line for the *'s plotted in figure 4.6 as follows. There are 14 estimates of efflux rate for this experiment plotted in figure 4.7. The 10th through the 14th points appear to fall on a straight line and I fit a regression line through these points.

The non-linearity observed by Tyree and Dainty for hemlock was evident for leaf 1-16 at initial balance pressures of 14.8 and 18.7 bars (see figure 4.7). There was a slight non-linearity for an initial balance pressure of 10.8 bars (see figure 4.6). For leaf 2-G, the non-linearity appeared only in the data for an initial balance pressure of 14.0 bars (see figures 4.8 and 4.9). Even for this case, the non-linearity was indistinct. Similar plots of efflux rates for tests conducted between 3/8/79 and 3/13/79 showed nonlinearities occurring in the curves when initial balance pressures were close to the water

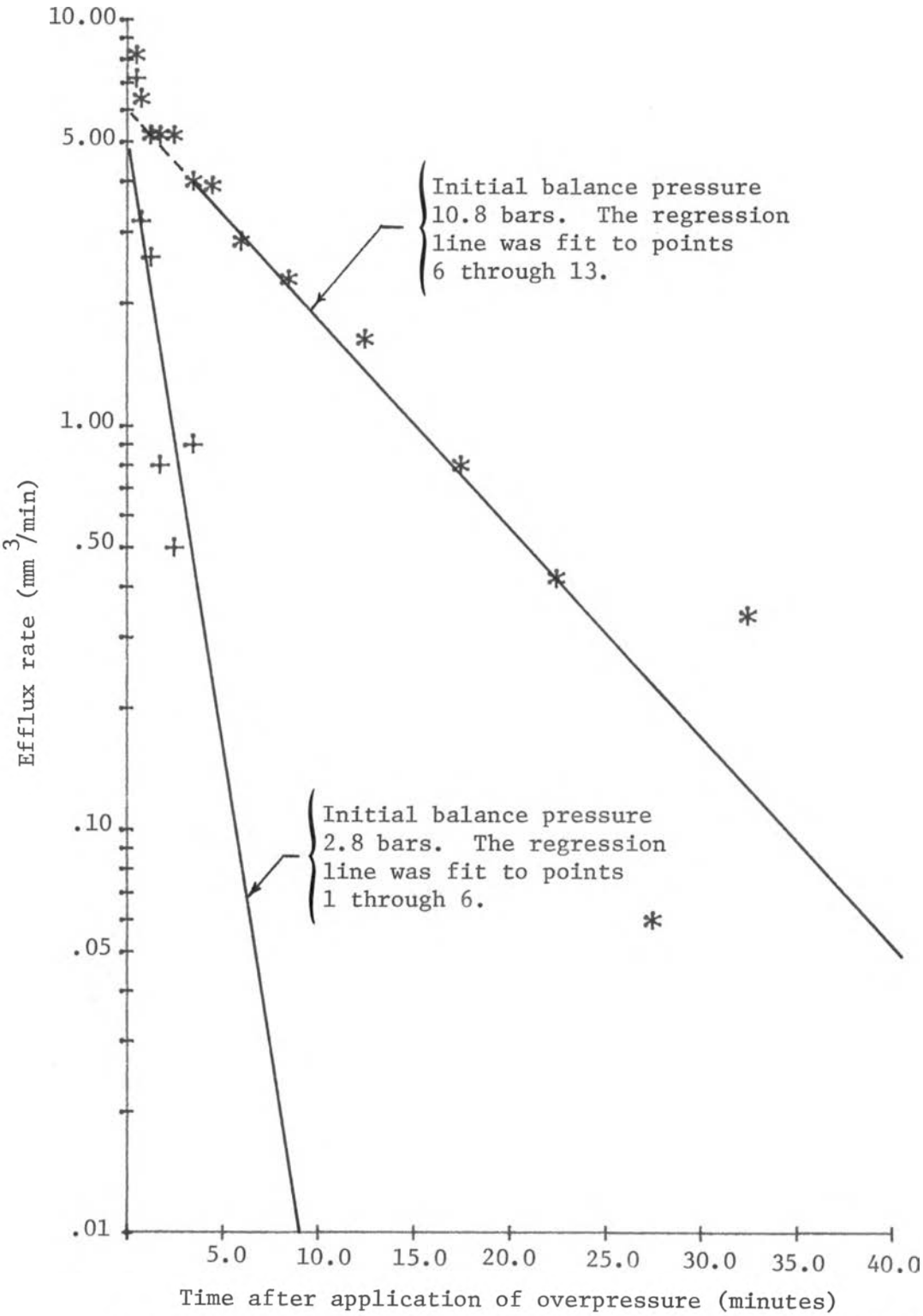

Figure 4.6. Graph of the natural log of the efflux rate from leaf 1-16 as a function of time after application of overpressure. The points are for efflux rates with initial balance pressures of 2.8 bars (+'s) and 10.8 bars (*'s).

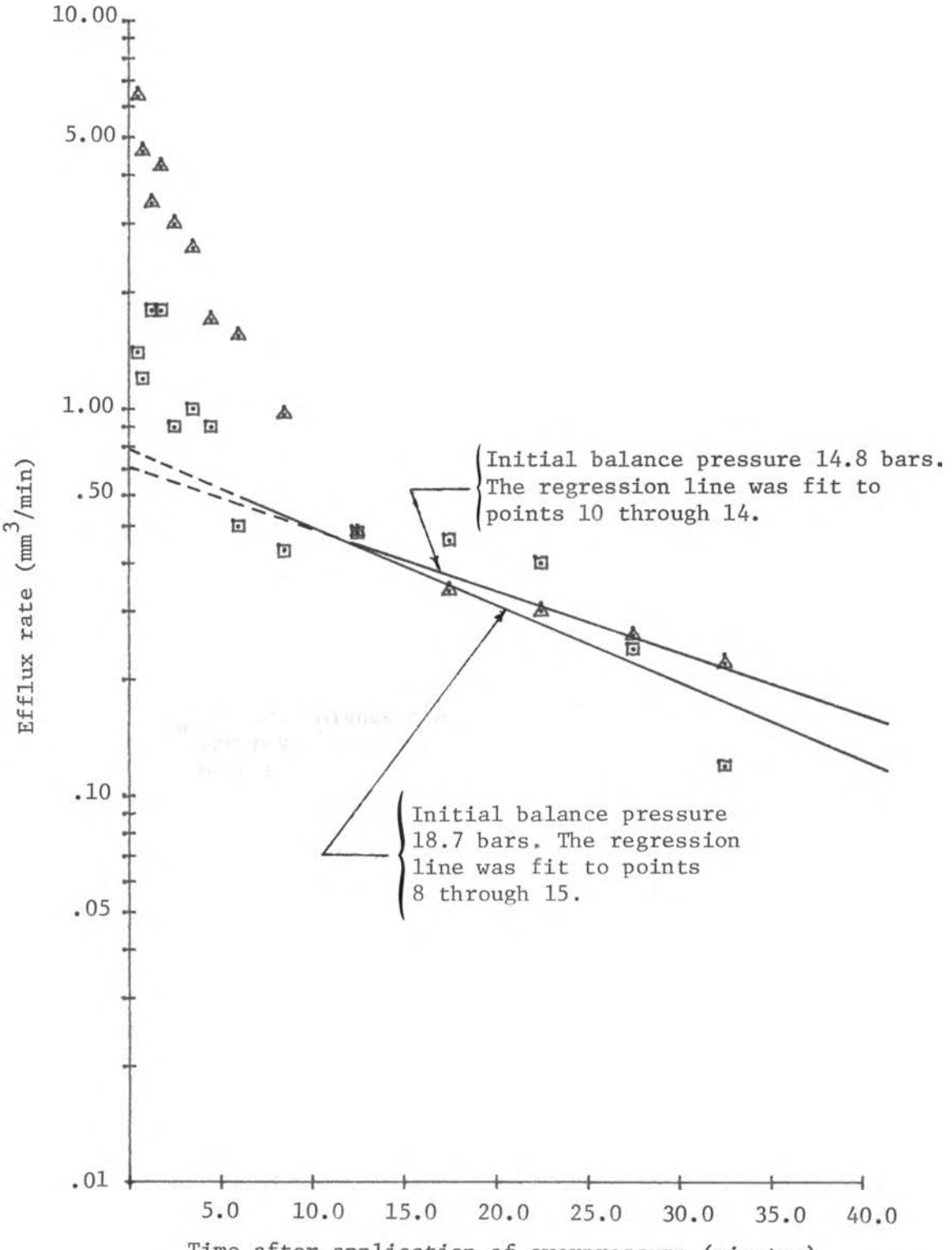

Figure 4.7. Graph of the natural log of the efflux rate from leaf 1-16 as a function of time after application of overpressure. Points are for efflux rates with initial balance pressures of 14.8 bars (△'s) and 18.7 bars (⊡'s).

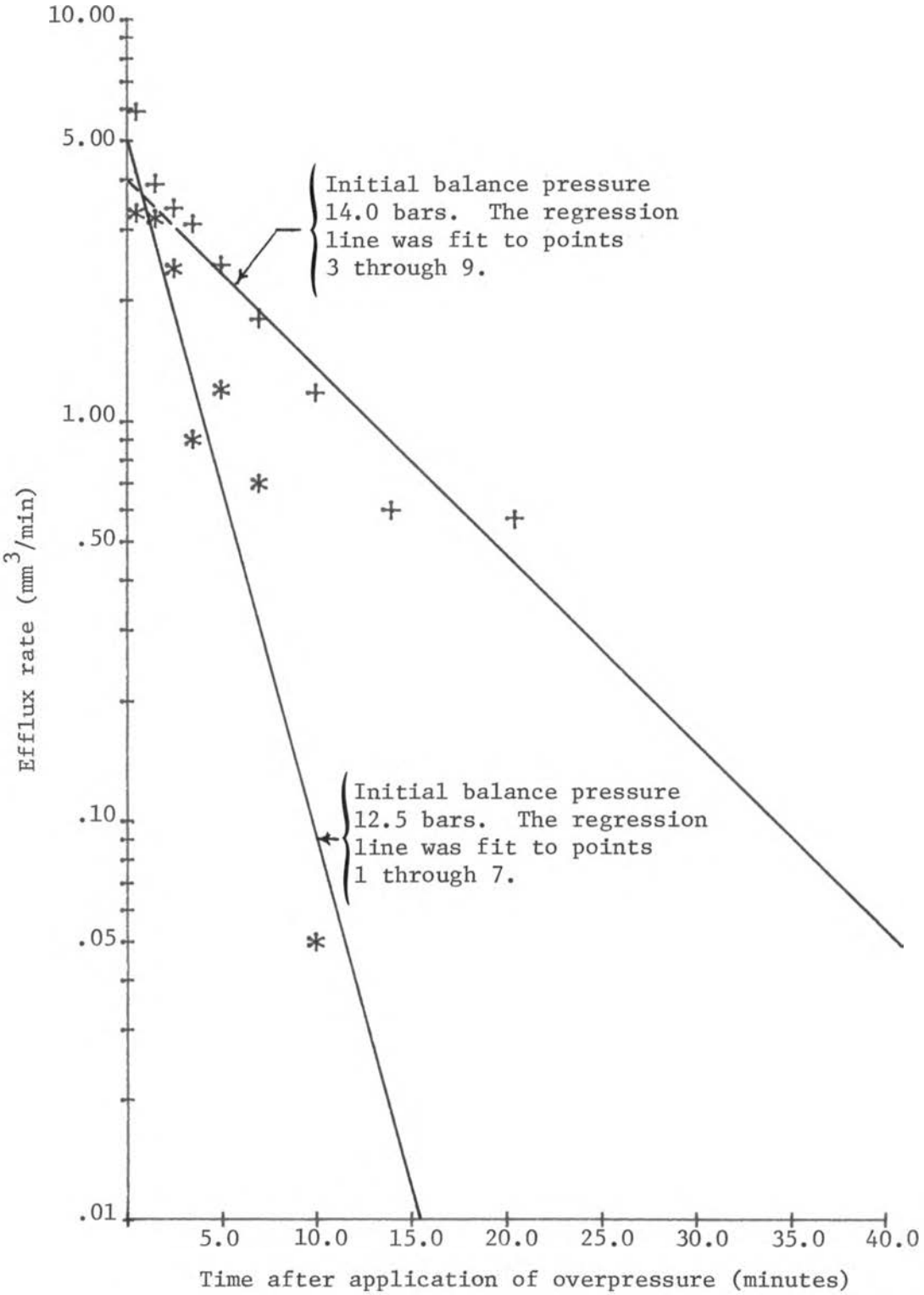

Figure 4.8. Graph of the natural log of the efflux rate from leaf 2-G as a function of time after application of overpressure. Points are for efflux rates with initial balance pressures of 14.0 bars (+'s) and 17.5 bars (*'s).

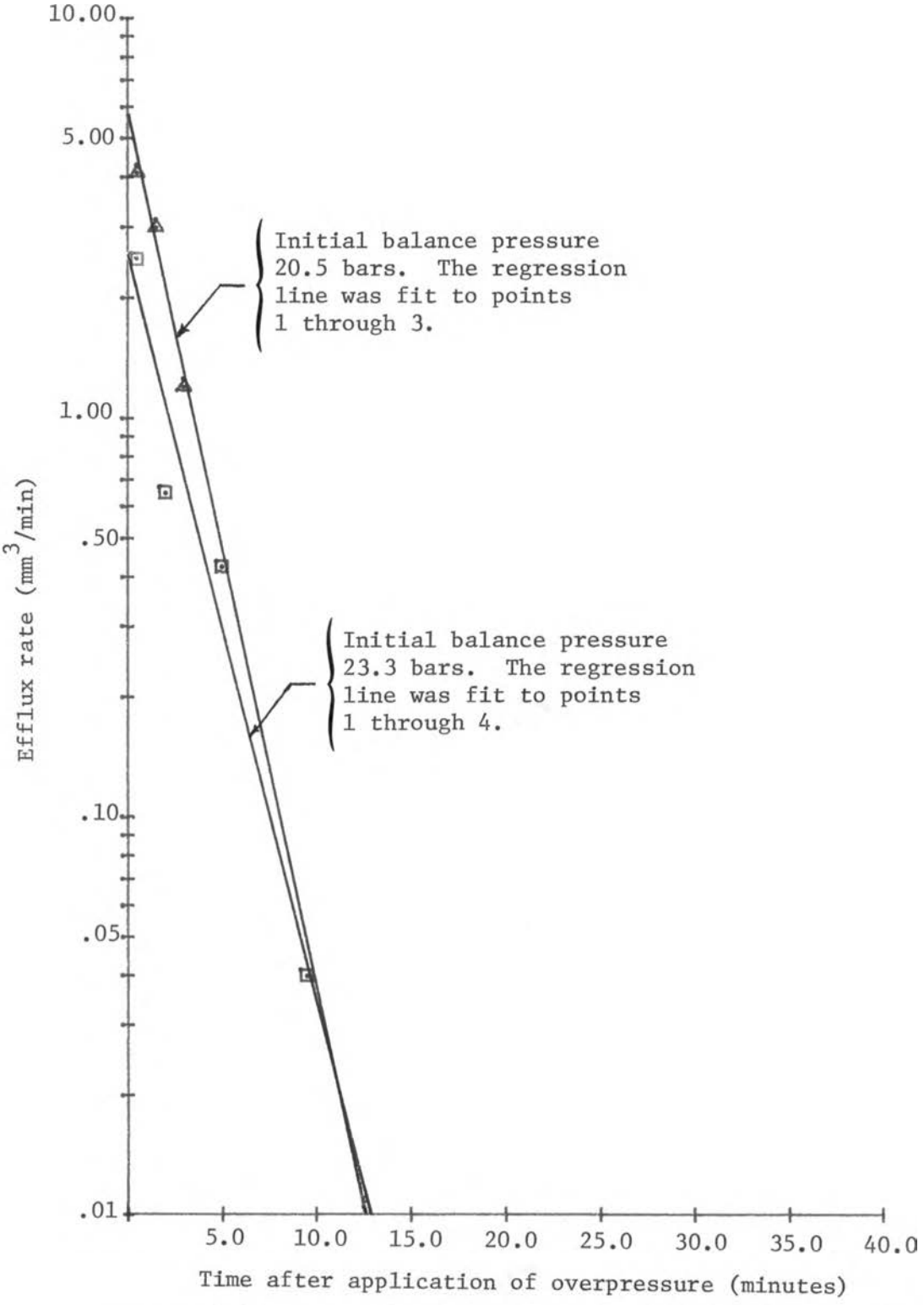

Figure 4.9. Graph of the natural log of the efflux rate from leaf 2-G as a function of time after application of overpressure. Points are for efflux rates with initial balance pressures of 20.5 bars (△'s) and 23.3 bars (⊡'s).

potential where the turgor first became zero, 10.8 bars. None were as pronounced as those shown in figure 4.7. For the tests conducted between 7/30/79 and 8/2/79, the non-linearity was noticeable only in leaf B-6 when the beginning balance pressure was 14.0 bars, in leaf 2-E when the beginning balance pressure was 16.4 bars, and in leaf 1-I when the beginning balance pressure was 13.6 bars.

The non-linearities in efflux rates were most evident in the March experiments. When Dr. Culter performed these experiments, he collected the expressed water for half minute intervals. When I performed the July/August experiments I collected the water at intervals of one to two minutes. Because I used longer time intervals, the efflux rate calculations from my data were less accurate. Since the time intervals were longer, there were also fewer data points. When the initial balance pressures exceeded 20 bars, I could determine only 4 or 5 data points. The plants tested in March had not been vernalized and were in a growth stage where leaves contained more water. In most cases, more water was expressed from them during the efflux experiments (refer to the tables in appendix B). This allowed Dr. Cutler to collect the sap for shorter time intervals.

In general, the slope of the regression line was greater when the turgor potential was greater than zero or when the absolute value of osmotic potential was large. The efflux model developed by Tyree and Dainty (1975) and described in section 3.6 predicts this type of behavior. Equation 3.21, their equation for efflux rate, dV_e/dt (mm^3/min), can be written:

$$\frac{dV_e}{dt} = C\ \Delta P\ e^{-DKt} \qquad (4.2)$$

C,D= constants (see equation 3.20 for units)

t = time after application of overpressure (min)

ΔP = applied overpressure (bars)

K = cell constant (see equation 3.20) (bar/mm^3)

The value of K will determine the slope of the regression line fit through the semilog plot of the efflux rates versus time. The individual cell constants depend on the osmotic potential at the beginning balance pressure and the modulus of elasticity of the cell wall (see equation 3.15). A non-zero value of turgor increases the value of K. As water is expressed from the cell, the ratio of the osmotic potential to cell volume increases. The value of K increases correspondingly. Therefore, for small overpressures, the slope should be a minimum at the point where turgor becomes zero.

I analyzed the efflux from leaf 2-G using equation 4.2. Although the overpressures were large enough to introduce an error into the approximation of k_i, the results still agreed qualitatively with the equation. I assumed that all of the cells in the tissue had identical k_i values, and I limited my consideration to cases where the cells had zero turgor. If turgor is zero, then $1/k_i$ is equal to the cell volume divided by the osmotic potential at the beginning of the efflux experiment (see equation 3.15). Adding the individual cell volumes gives the volume of water in the leaf. I assumed this volume was V_π. The volume of water in the leaf at any time will equal V_π minus the volume of water expressed from the leaf, V_e. Therefore, from the

definitions of K and k_i (see equations 3.15 and 3.20), 1/K will equal $V_\pi - V_e$ divided by $-\overline{\pi}$. Using this approximation, I calculated a K of 0.09838 bar/mm^3 for the efflux experiment which began at a balance pressure of 14.0 bars. The experiment with a beginning balance pressure of 20.5 bars had a K of 0.2240 bar/mm^3. This K value is 2.3 times the K for the 14.0 bar experiment.

If efflux is described by equation 4.2, then a plot of the natural logarithm of efflux rate as a function of time should be a straight line with slope dependent on K. Figures 4.8 and 4.9 show such a plot for leaf 2-G. If the model and approximations are correct, then the slope of the regression line fit to the efflux data from the experiment with a beginning balance pressure of 14.0 bars (the +'s in figure 4.8) should be 2.3 times the slope of the regression line for the efflux with a beginning balance pressure of 20.5 bars (the Δ's in figure 4.9). The slope is 4.6 times larger.

The model described by equation 4.2 could not account for all of the observed changes in the slope of the regression line fit through the efflux data. There are several possible explanations. First, D may not be a constant. D is the product of cell membrane permeability and the area of the cell membrane. If either of these values change significantly as the beginning balance pressure changes, then D, and hence the slope of the regression line, will also change. Secondly, the model may not be complete. The resistance to flow across the cell membranes may not be the only factor which limits efflux from the leaves. Other resistances to flow, such as the resistance to water flow through the xylem, may also be important. Finally, K may have

not been estimated accurately. The assumption that the applied overpressures were small was not fulfilled. However, it would be difficult to repeat the experiments with smaller overpressures, because this would reduce the amount of water expressed from the leaf and increase the experimental error.

I could extend my investigations into efflux rates if I could determine the efflux rate more accurately. Tyree and Dainty were able to monitor efflux continuously. They collected the expressed water in a vial which was resting on an electronic balance. By connecting their balance to a chart recorder, they found an efflux curve. The slope of this curve at any given time was their estimate of the efflux rate at that time. Their technique seems to have given them a better estimation of the efflux rate, because their curves are smoother with less deviation. If a technique similar to Tyree and Dainty's were applied to the wheat efflux experiments, then the efflux rates might be determined more accurately. Application of the above analysis to this more accurate data might give additional information.

Preliminary work with the model described in chapter 8 suggested that leaf length should have an effect on the time required for the water to be expressed from a leaf. To test this I conducted the July/August and November experiments on leaves of varying length. I normalized the efflux curves by dividing water expressed by the volume of each leaf. The results are shown in figure 4.10. The length of each leaf is given on the graph. All of the water was expressed from the shorter leaves much more rapidly than from the longer leaves. For example, the efflux rate from leaf 1-F was nearly zero after 10.0

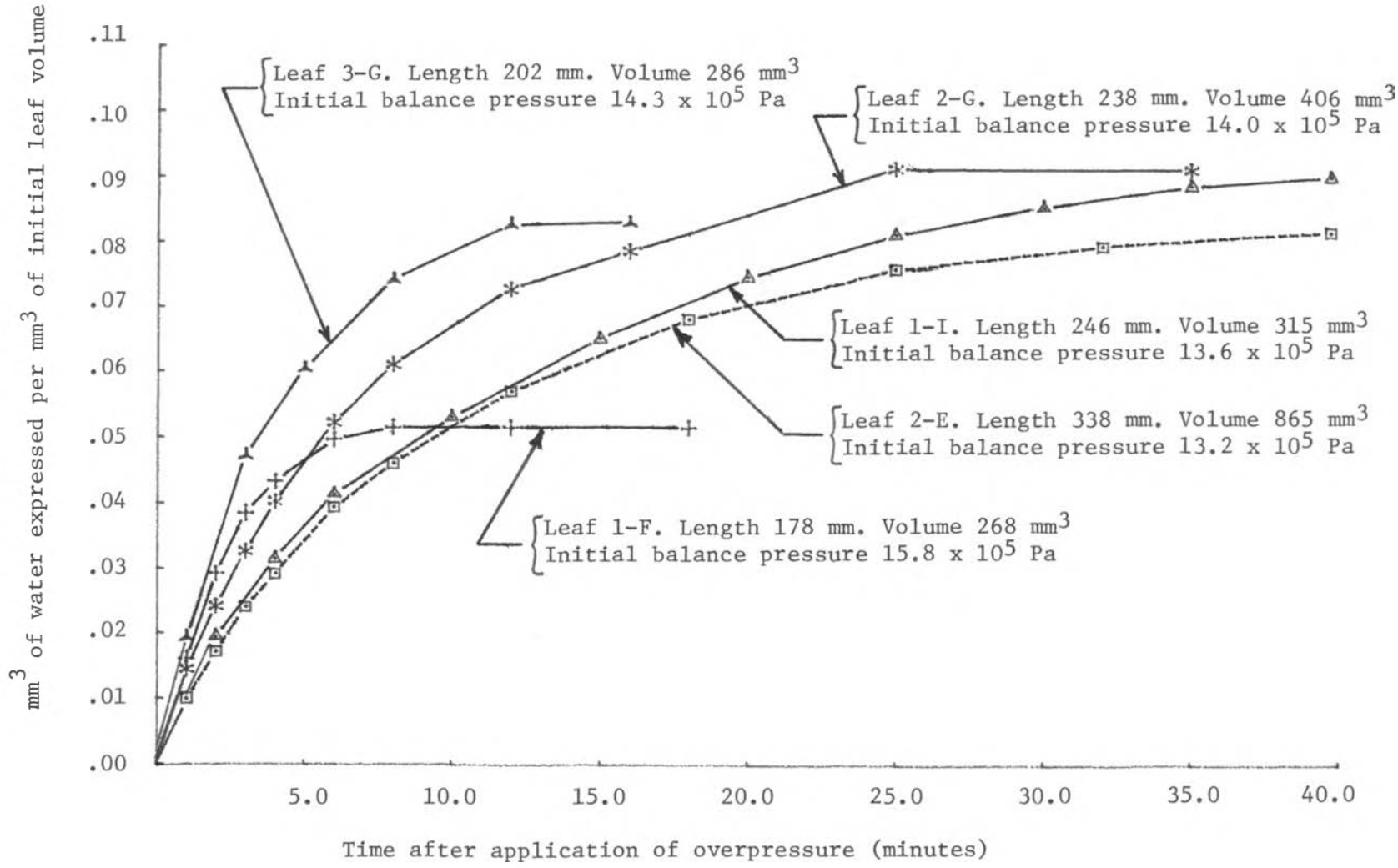

Figure 4.10. Efflux curves for various initial balance pressures when an overpressure of 3.0 bars was applied to leaves of various lengths.

minutes. However, only after 40 minutes did the efflux rate from leaf 2-E approach zero. This suggests that the xylem vessels affect the efflux of water from the leaf.

The pressure chamber experiments described in this chapter provide a basis for comparing the water efflux from wheat plants with the behavior reported in the literature. The shape of the efflux curves and the time variation in efflux rate are similar to that reported by Tyree and Dainty (1973) for hemlock. Furthermore, the experiments suggest that any model of water efflux must include the xylem resistance.

CHAPTER 5

WHEAT LEAF ANATOMY

This chapter describes studies of wheat leaf anatomy which helped me to formulate the models described in chapters 7 and 8. I used leaf cross sections and paradermal sections, scanning electron micrographs, and transmission electron micrographs to study the cell shape and leaf structure. These studies helped me to understand possible pathways of water movement through the leaf. Using leaf cross sections and paradermal sections I gathered information such as the number and size of vessel elements in a bundle, the number of bundles in a leaf, the total volume of cells in a leaf, and the number of cells feeding into each bundle. I used this information to estimate the values of the parameters in the models. My study was not extensive, but it gave me reasonable estimates of the parameters.

5.1 Collection, Preservation, Staining, and Sectioning of Samples:

Dr. Jean Chabot of the Ecology and Systematics Department instructed me on the techniques used in these studies. They are standard techniques used by plant anatomists which Dr. Chabot adapted to studies of wild strawberries (Chabot and Chabot, 1977). With Dr. Chabot's guidance, I applied these techniques to the studies of wheat leaves.

Dr. Chabot and I collected the samples used in this study from the greenhouse grown wheat plants used for pressure chamber

experiments (see section 4.2). Before removing a sample from a leaf we measured leaf length and width. Using a razor blade we cut pieces several millimeters square from the midsection and leaf tip and placed them in a solution of fixative. This solution was prepared by adding 2 per cent by volume gluteraldehyde and 2.5 per cent formaldehyde to a 0.1 molar aqueous phosphate buffer solution. The formaldehyde was made from solid paraformaldehyde. This fixing process preserved the samples indefinitely.

We used the following procedure to prepare samples for microscopic examination. After washing samples three times in 0.1 molar phosphate buffer we post fixed them for 2 to 4 hours in a solution of 1.0 per cent osmium tetroxide in 0.1 molar phosphate buffer. We dehydrated the samples with a series of washes in acetone solutions. Each acetone wash lasted 15 minutes and each successive wash contained a higher proportion of acetone. The first solution was 50 per cent acetone and 50 per cent water. The second was 75 per cent acetone. The third and fourth were 95 per cent acetone and the fifth was 100 per cent acetone. Since acetone absorbs water from the atmosphere, we washed the samples a sixth time with acetone from a recently opened bottle.

We soaked samples in a mixture of propylene oxide and araldite and then placed them in araldite at room temperature for 12 hours. During this period, the araldite infiltrated the samples. After curing the infiltrated samples in an oven at 65 degrees Celsius for several days, we sectioned them at various angles using a Sorvall MT-1 ultramicrotome equipped with glass knives. We mounted the sections on

glass slides, stained them with toluidene blue, and viewed them under a light microscope. Dr. Chabot mounted several sections on copper grids, stained them with uranyl acetate and lead citrate, and photographed them with a Phillips 300 transmission electron microscope.

5.2 Preparation of Scanning Electron Microscope Samples:

Using an AMR-1000A scanning electron microscope I studied some of the preserved and dehydrated samples. I dried several samples in a freeze dryer and used critical point drying on the remainder. Since the critical point drying process caused less damage to the specimens, I used it for most of the samples. Using either double stick tape or aquadag, I mounted the dried samples on aluminum stubs and coated them with a layer of gold using a sputter coater. I viewed the gold-coated samples under the scanning electron microscope (SEM).

The SEM shoots a beam of electrons at the sample. When they strike it, they emit secondary electrons. These secondary electrons are collected and converted to a cathode ray tube image by a photomultiplier.

5.3 Descriptive Anatomy

This section summarizes features of wheat leaf anatomy which affect water movement. There are two photographs of wheat leaf cross sections shown in figure 5.1. Figure 5.1a is a photograph of a cross section near a large vascular bundle and figure 5.1b is a photograph

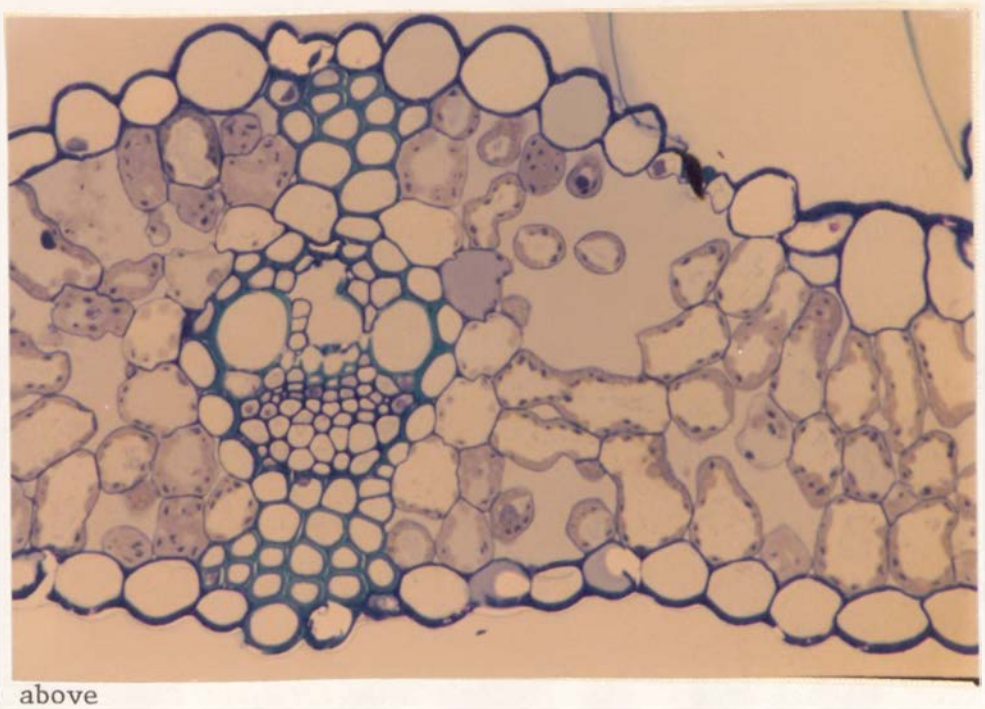

(A) above

(B) below

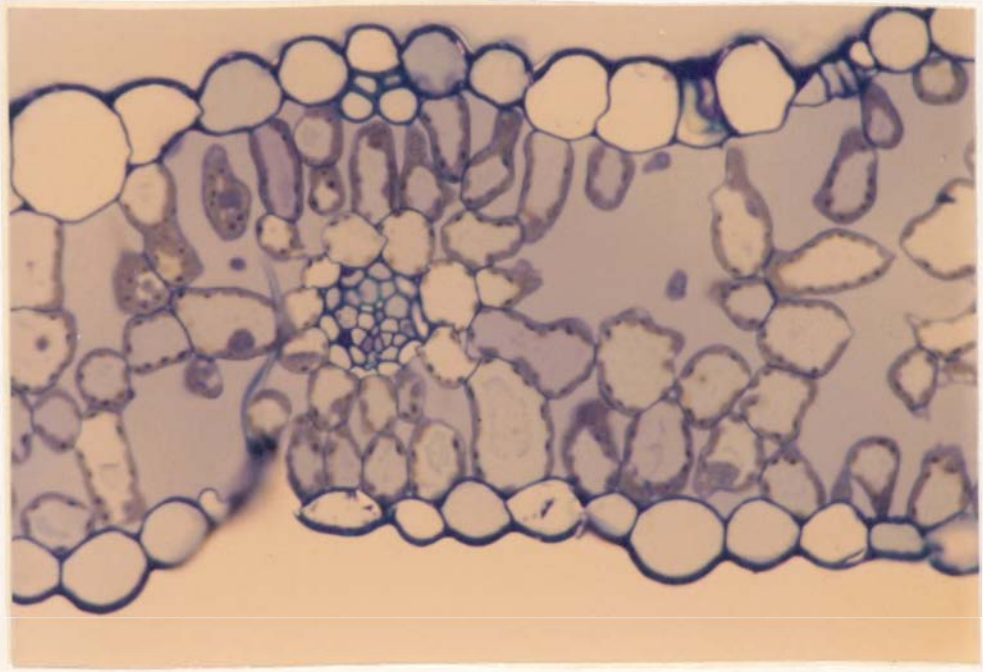

Figure 5.1. Cross sections of wheat leaves in the vicinity of vascular bundles. Part (A) shows a cross section near a large vascular bundle and part (B) a cross section near a small bundle. Magnification 400X.

near a small vascular bundle. Figures 3.2 and 3.3 are tracings of these photographs. The epidermal cells in the cross sections are large and thick-walled and appear to have no cytoplasm. Cytoplasm lines the relatively thin walls of the mesophyll cells. Thick-walled schlerenchyma cells extend from the large vascular bundles to the epidermis but are only found adjacent to the epidermis in the small vascular bundles. Surrounding the vascular bundles are two layers or rings of cells called the inner and outer bundle sheaths. The walls of the inner bundle sheath cells vary in thickness. The portion of their cell walls adjacent to the xylem and phloem is much thicker than the outer portion. This is quite evident in figure 5.2 which is a transmission electron micrograph of an inner bundle sheath cell. Studies by O'Brien and Carr (1970) (see section 3.1) showed that there is a suberized layer in the middle lamellae of the inner bundle sheath cells.

The photographs in figure 5.1 are oriented so that the upper epidermis of each leaf is at the top of the page. Large bundles characteristically have two or more large vessels approximately 2.5 x 10^{-2} mm in diameter. Between these two large vessels is a protoxylem lacuna formed during the leaf development. The protoxylem elements are the first to form and their wall thickens. As the leaf elongates their rigid structure resists growth and they are pulled apart leaving a cavity in the bundle. The xylem elements are always located on the side of the vascular bundle closest to the upper epidermis.

The photograph of a paradermal section shown in figure 5.3 shows several aspects of the leaf structure not apparent in the cross

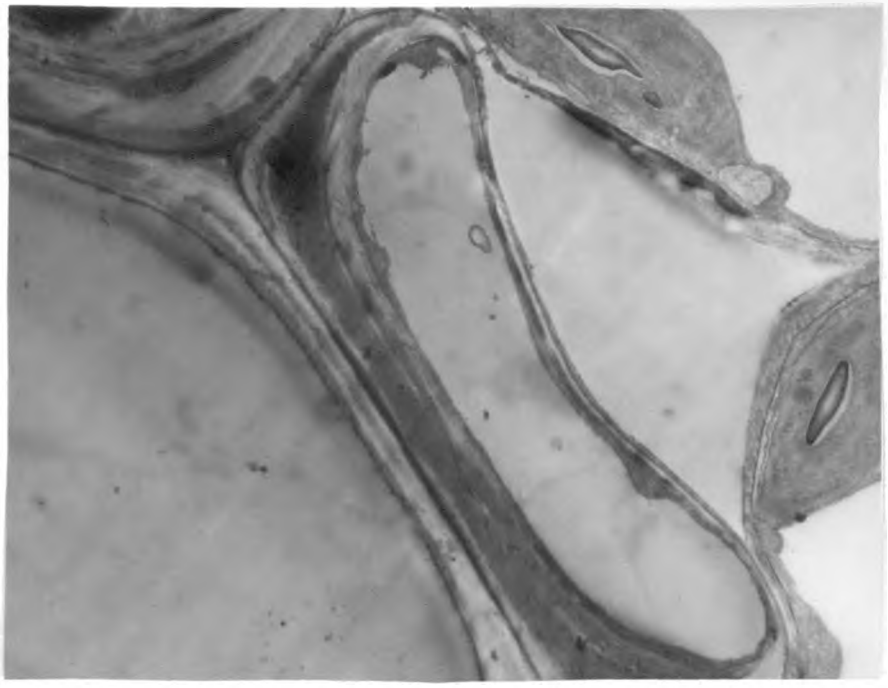

Figure 5.2. Transmission electron micrograph of an inner bundle sheath cell showing thickened portion of the cell wall adjacent to xylem. Magnification 6840X.

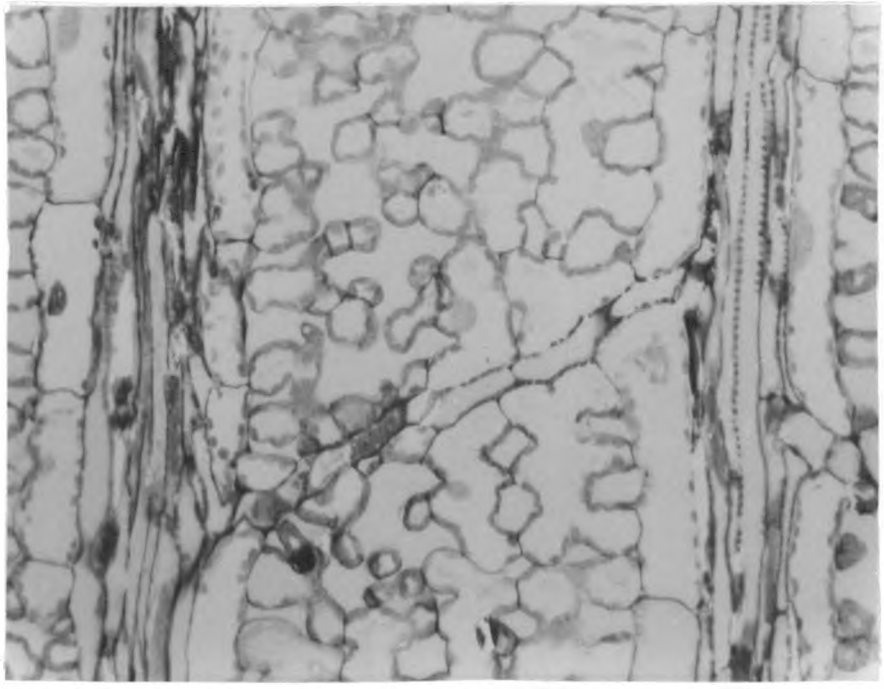

Figure 5.3. Paradermal section of a wheat leaf showing a transverse vein and the irregular shape of the mesophyll cells. Magnification 185X.

sections. The mesophyll cells are quite irregular in shape. One cell may have a number of pockets or "fingers." This is not noticeable in the cross sections shown in figure 5.1. What appears to be two different cells in figure 5.1 may in many cases be part of the same cell. Therefore, water forced from a cell furthest from a vascular bundle would have to travel no more than two or three cell lengths before reaching the vascular element. As shown in figure 5.3, the transverse vein connecting the two bundles contains a single xylem vessel. Kuo, O'Brien,and Zee (1972) observed that the transverse veins consist of one xylem vessel and one phloem sieve tube, and are without bundle sheath cells. The section shows that the bundle sheath cells are long and have no projections. The transverse and paradermal sections show that these cells form a continuous ring around the vascular bundle and apparently seal it off from the intercellular spaces of the mesophyll cells.

The scanning electron micrographs in figure 5.4 and 5.5 confirm the observations made on the leaf sections. Figure 5.4 shows a section through the leaf in the vicinity of the midrib. The midrib provides a relatively thick and structurally rigid framework to which the thin blades of the leaf are attached. It has a number of thick-walled cells which apparently make it resistant to bending. The vascular bundles in the midrib are closer to the lower epidermis and the xylem elements of the bundles are in the portion of the bundle closest to the upper epidermis. The epidermal cells have thick walls and can apparently maintain their shape when the section is cut. The thin-walled mesophyll cells are apparently disrupted by the cutting.

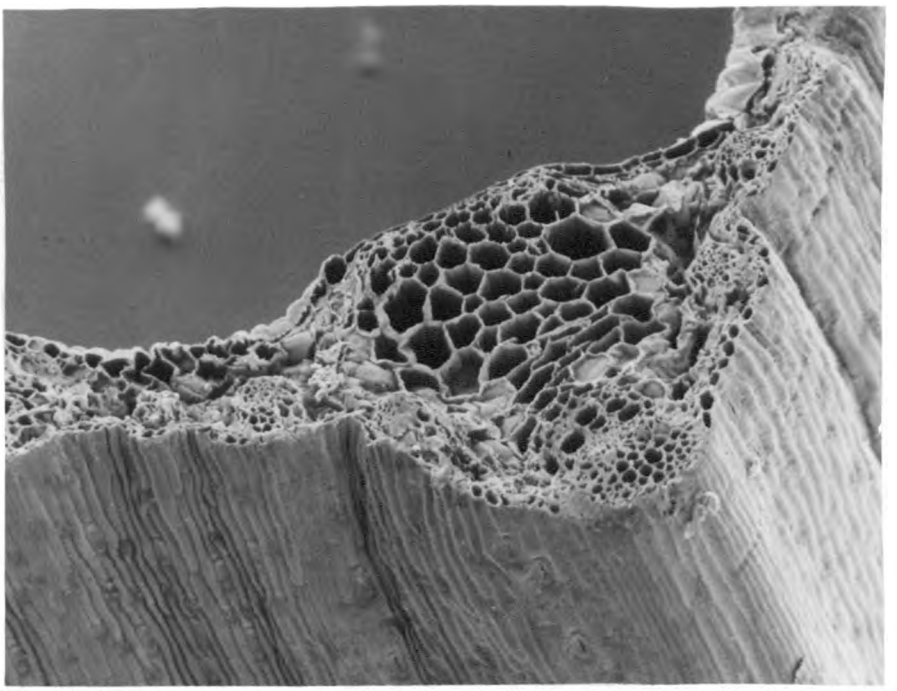

Figure 5.4. Scanning electron micrograph of a wheat leaf cross section showing the midrib structure and the orientation of the vascular bundles. Magnification 108X.

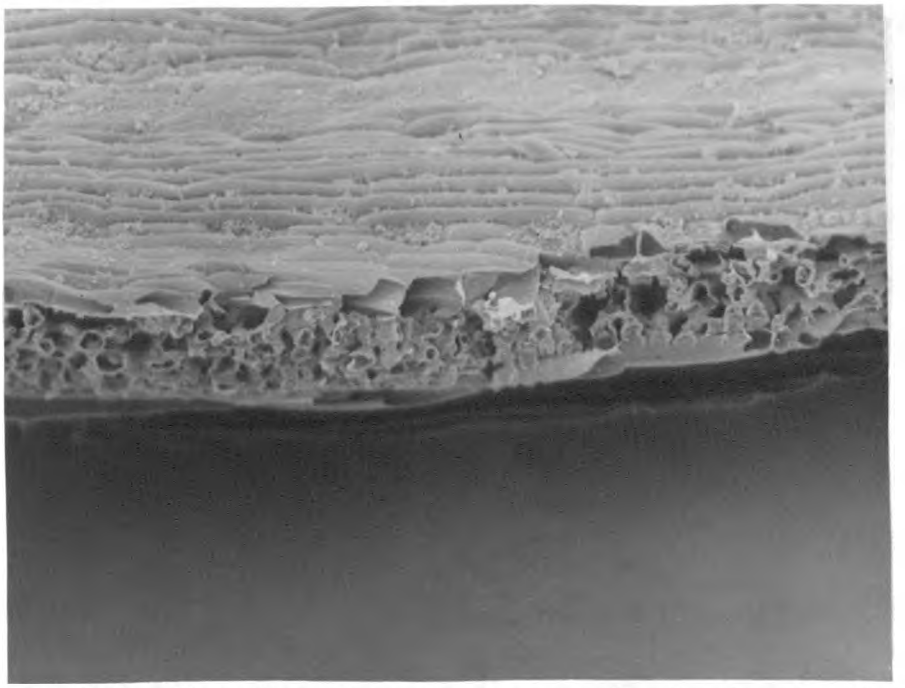

Figure 5.5. Scanning electron micrograph of a longitudinal section through a wheat leaf showing the irregular shape of mesophyll cells and intercellular spaces. Magnification 208X.

In order to gain a better view of the mesophyll cell structure, I cut the specimen shown in figure 5.4 longitudinally at a slight angle to the vascular bundles. A micrograph of this section is shown in figure 5.5. The mesophyll cells are irregularly shaped and mesophyll tissue contains large air pockets.

When water is forced from cells by the high pressures in the chamber, the cell volume decreases. As I mentioned in section 4.2, I investigated physical changes in leaf structure by taking cross sections of leaf 1-I after it was removed from the chamber. When the leaf is fastened in the chamber, a 25-50 mm section remains outside (see figure 1.1). Figure 5.6 is a photograph of a cross section taken from this portion of leaf 1-I at the completion of an experiment. The cells are unharmed and there are many air spaces in the leaf. Figures 5.7 and 5.8 are photographs of cross sections taken from a portion of the same leaf which had been inside the chamber. The mesophyll cells appear undamaged. However, with the exception of the substomatal cavities, there are few air spaces. Apparently the cells were drawn closer together as they lost water. The tissue deformation is apparently inelastic. In section 5.4, I have included quantitative data on the relative volume of the airspaces in cross sections such as those in figures 5.6 through 5.8.

When the leaf is placed in the chamber, the grommet which seals the chamber must be tightened around a portion of the leaf. If the xylem vessels are crushed, water flow through them could be impeded. Figure 5.9 is a picture of one of the transverse sections of the portion of leaf 1-I in contact with the seal. Although the mesophyll

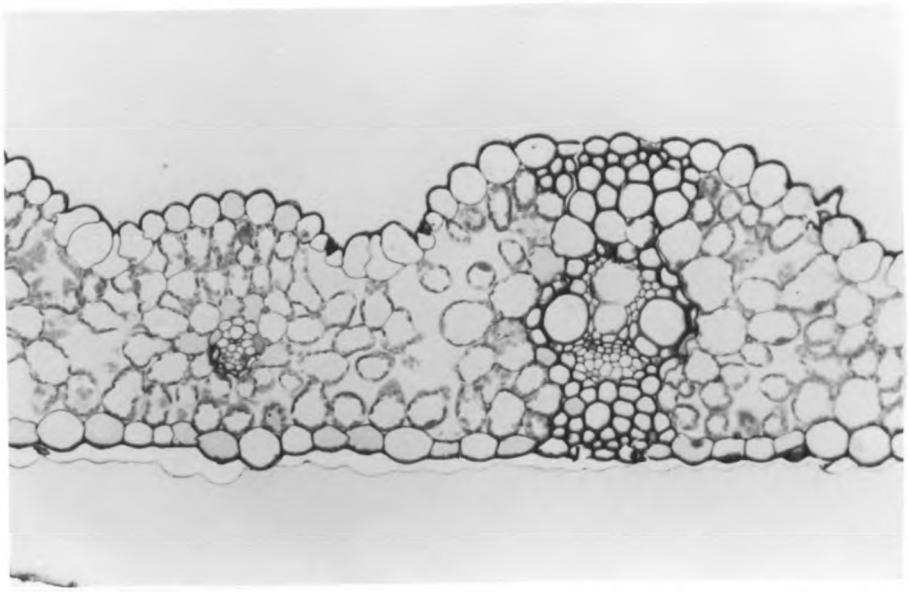

Figure 5.6. Cross section of wheat leaf 1-I taken from the portion of the leaf which was protruding from the chamber after completion of the experiment. Magnification 175X.

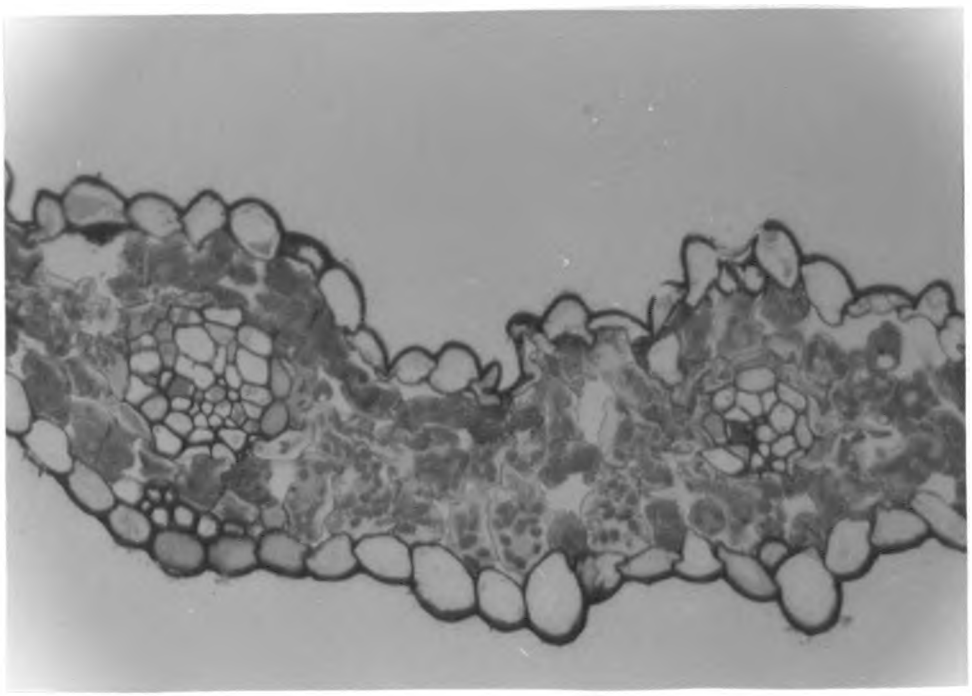

Figure 5.7. Cross section of wheat leaf 1-I taken from a portion of the leaf inside the chamber after completion of the experiment. Magnification 185X.

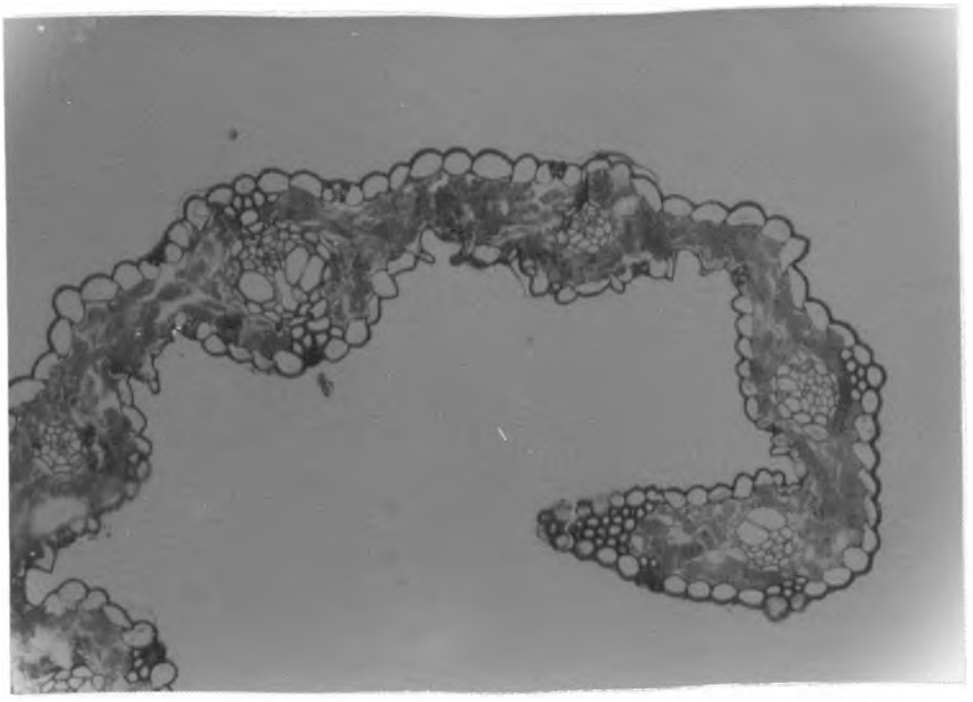

Figure 5.8. Cross section of wheat leaf 1-I taken from a portion of the leaf inside the chamber after completion of an experiment. Magnification 92X.

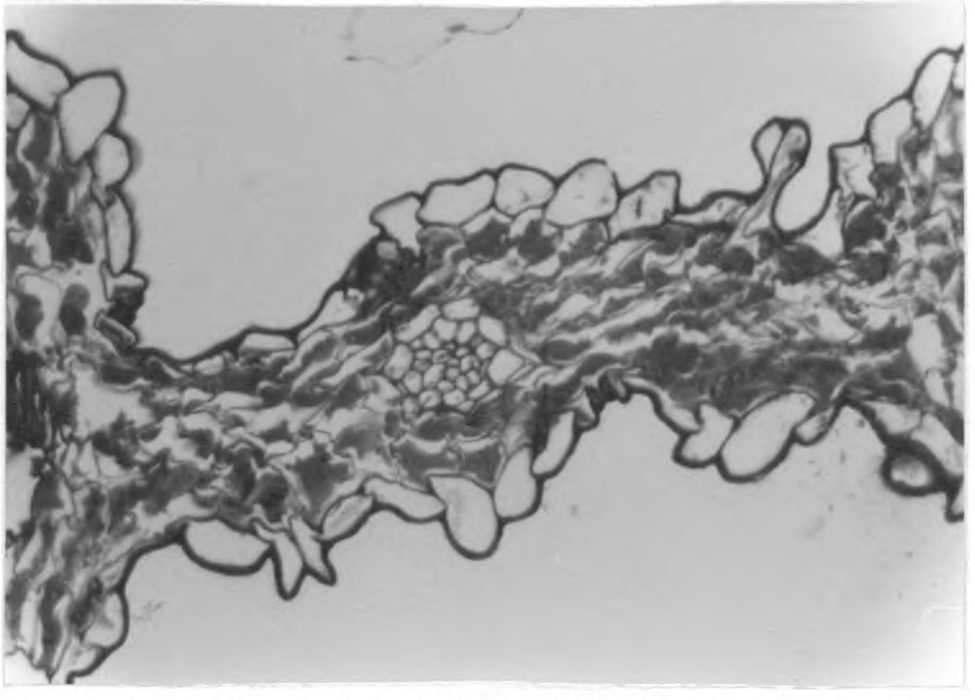

Figure 5.9. Cross section of leaf 1-I taken from a portion of the leaf which was compressed by the chamber seal. Magnification 185X.

cells and most of the epidermal cells have been permanently deformed, the vessel elements in both the large and small vascular bundles are undisturbed. The resistance to water flow through these bundles should not have been changed by the action of the seal.

5.4 Quantitative Anatomy

Modeling of water flow from wheat leaves requires not only an understanding of the overall physical structure of the leaf but also quantitative data on the size of the vessel elements and the volume of water in the cells. I estimated these values by taking measurements on leaf cross sections. This section summarizes the results of those measurements.

Wheat leaves have vascular bundles with varying sizes and numbers of vessel elements. Kuo, et al. (1974) classified vascular bundles into five types: midrib, large and small intermediates, and large and small laterals. They designated as laterals those bundles which develop before extension growth is complete and as intermediates those which develop after extension growth is complete. Using samples of leaves collected on December 10, 1978, I prepared leaf cross sections and photographed them. After printing the pictures, I taped them together to form an enlarged picture. Applying Kuo's classification scheme, I found that the bundles were distributed as diagrammed in figure 5.10. Kuo used this type of diagram to describe his cross sections. In each leaf, two or three large or small intermediate bundles lie between two large or small lateral bundles.

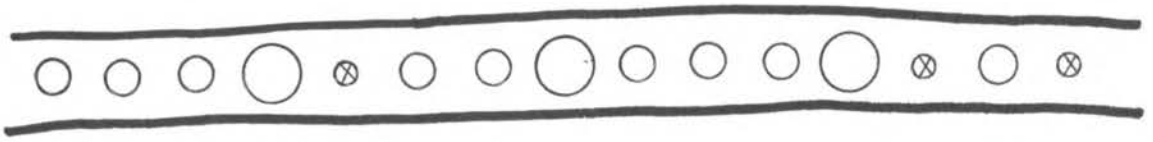

Leaf number one collected 12/10/78

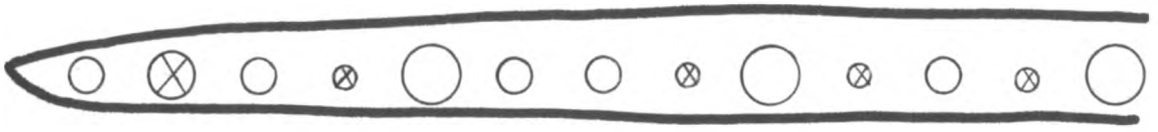

Leaf number two collected 12/10/78

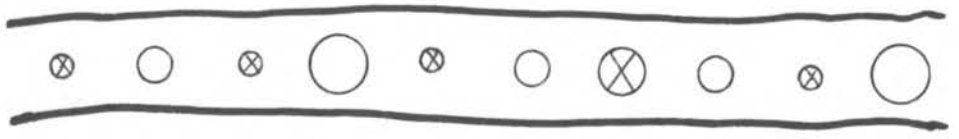

Leaf number three collected 12/10/78

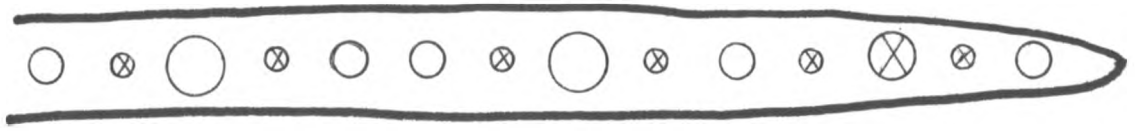

Leaf 2-G collected 8/3/79

Figure 5.10. Diagram of wheat leaves showing the placement of bundle types. Shown at the bottom is a key defining the symbol used to designate each bundle type.

Kuo estimated that the water flow resistance of the large and small intermediates was much greater than that of the large or small laterals (see section 3.1). He speculated that the lateral bundles were specialized for water transport whereas intermediate bundles, which contain a greater proportion of phloem cells, are specialized for solute transport.

I used Kuo's classification scheme but did not take measurements on the midrib bundle. Using a dividers and a picture of a micrometer scale taken at the same time as the picture of the cross section, I measured the radii of the vessel elements in the leaves diagrammed in figure 5.10. Using these values I calculated the sum of the fourth power of the radii of all the vessels in a bundle. The results are summarized in Table 5.1 and compared to Kuo's data. Kuo's values for lateral bundles of Triticum aestivum L. cv. 'Heron' were approximately equal to the values I calculated. The values for the small laterals and large intermediates agree within a factor of 4. The small intermediates in the plants I studied had larger radii, perhaps because my leaves were from more mature plants.

Using leaf cross sections such as the those pictured in figure 5.1, I determined the relative volume of epidermal cells, vascular tissue, mesophyll cells, and air spaces in samples of wheat leaves. I assumed the inner bundle sheath cells were part of the vascular bundle. These measurements along with the values of the ratio of mesophyll cell area to leaf surface area are shown in table 5.2. To determine these values, I used the method of Wiebel (1969) which Chabot and his co-workers (Chabot and Chabot, 1977; Chabot, Jurick,

Table 5.1. Values of the inside radii of the inner bundle sheath and values of the sums of the fourth power of vessel radii for the vascular bundles in wheat leaves. Standard deviations are included for measurements where they could be calculated.

Bundle Type	Number of Bundles Measured			Inside Radius of Inner Bundle Sheath (mm)			Value of Σnr_i^4 (mm^4)		
	Samples collected 12/11/78	Samples from leaf 2-G collected 8/2/79	Data from Kuo, et al., (1974)	Samples collected 12/11/78	Samples from leaf 2-G collected 8/2/79	Data from Kuo, et al., (1974)	Samples collected 12/11/78	Samples from leaf 2-G collected 8/2/79	Data from Kuo, et al., (1974)
Large lateral	8	2	6	$4.54\pm.40 \times 10^{-2}$	4.20×10^{-2}	4.4×10^{-2}	$3.85\pm.15 \times 10^{-8}$	4.94 ± 1.62	4.29×10^{-8}
Small lateral	2	1	4	3.10×10^{-2}	3.10×10^{-2}	3.5×10^{-2}	$9.17\pm1.06 \times 10^{-9}$	3.19×10^{-8}	1.79×10^{-8}
Large inter-mediate	15	4	13	$2.00\pm.23 \times 10^{-2}$	$1.55\pm.13 \times 10^{-2}$	1.4×10^{-2}	$2.56\pm2.20 \times 10^{-10}$	$7.73\pm1.73 \times 10^{-10}$	1.89×10^{-10}
Small inter-mediate	11	5	10	$1.67\pm.18 \times 10^{-2}$	$1.33\pm.20 \times 10^{-2}$	1.05×10^{-2}	$1.97\pm1.26 \times 10^{-10}$	$3.35\pm2.54 \times 10^{-10}$	2.60×10^{-11}

Table 5.2. Summary of measurements of the relative volume of various types of tissue in a wheat leaf and the A_{mes}/A ratio on leaf cross sections.

Leaf Number	Date Sampled	Number of cross sections examined	Per Cent Volume				A_{mes}/A [d] ratio
			Epidermis	Vascular bundle	Mesophyll cells	Air spaces	
(1)	12/22/78	2	21.4±2.0	17.7±1.2	43.3±3.5	17.6±6.8	9.8±.99
(2)	12/22/78	2	20.2±4.2	12.4±3.7	43.6±1.1	23.8±0.5	18.6±1.1
(3)	12/22/78	5	22.3±1.6	6.7±1.7	44.8±3.1	26.1±4.3	15.5±1.9
Average [a]	12/22/78	-	21.3±1.1	12.3±5.5	43.9±0.8	22.5±4.4	14.6±4.5
2-G [b]	8/2/79	4	18.3±1.8	14.4±2.5	47.6±3.4	19.6±0.3	-
2-G [c]	8/2/79	4	27.9±6.0	15.4±2.0	46.2±8.0	10.6±1.3	-

[a] The two samples from leaf (1), the two samples from leaf (2), and the five samples from leaf (3) were averaged to give these values.

[b] After completion of the experiment, this sample was taken from a portion of the leaf which had been outside the chamber.

[c] After completion of the experiment, this sample was taken from a portion of the leaf which had been inside the chamber.

[d] The A_{mes}/A ratio is the ratio of the area of the mesophyll cell walls to the surface area of the leaf.

and Chabot, 1979) adapted to cross sections of plant leaves. Using a microscope with a grided reticule, I counted the number of grid points which were located in parts of the cross section corresponding to air spaces or one of the three types of tissue. The relative volume of each category equaled the percentage of the total number of grid points which fell into that category. Dr. Chabot estimated the thickness of the cross sections as 3.0×10^{-4} mm by using the interference colors produced on a dissecting microscope (Dawes, 1971, p. 105). This is about 0.05 times the average radius of the cylindrically shaped mesophyll cells.

I determined the value of A_{mes}/A using the same method used by Chabot, Jurick, and Chabot (1979). They counted the number of wall intersections along a known length of grid line and applied an appropriate formula.

The relative volume of mesophyll and epidermis in the leaves sampled in December 1978 varied by only two per cent while airspace and vascular bundle volume varied widely. This variation was probably caused by the relatively small length of the cross sections. In future work, we may be able to reduce this variation by taking a series of sections across the entire width of the leaf.

The relative volumes of the tissues in leaves 2-G and 1-I changed during the time when they were in the chamber. As I mentioned in section 4.2, I sectioned portions of the leaves which had been inside the chamber and compared them to sections of the 25-50 mm portion of the leaf that protrudes from the chamber during an experiment (see figure 1.1). Although I only collected data from the

cross sections of leaf 2-G, the cross sections from leaf 1-I were similar in appearance. The relative volume of air spaces in the portion of the leaf that was inside the chamber was 10 per cent less than the volume in the portion of the leaf that had been outside the chamber. On the other hand, the relative volume of the epidermal cells in the portion that had been inside the chamber was 10 per cent greater than the value for the portion that had been outside. Apparently the cells that had been inside the chamber drew closer together as they lost water. The epidermal cells must have been relatively resistant to permanent deformation while the mesophyll cells and vascular tissue must have been compressed proportionately. The bundle sheath cells were counted as part of the vascular tissue. Water loss from the bundle sheath cells may have caused the decrease in vascular tissue volume.

Before I could use the model described in chapter 8, I needed to know the number of mesophyll cells per unit length of vascular bundle. I estimated this number by assuming the volume of the mesophyll tissue was equal to the product of leaf volume and the per cent of leaf volume which is mesophyll tissue. Using a microscope, I counted the number of vascular bundles in the leaves I had tested. I assumed the length of the bundles was equal to the leaf length. By dividing mesophyll cell volume by the number of bundles in the leaf and then dividing again by the leaf length, I found the mesophyll cell volume per unit length of vascular bundle. By estimating the volume of a mesophyll cell and dividing this volume into the mesophyll volume per unit length of vascular bundle, I estimated the number of mesophyll

cells per unit length of vascular bundle. Table 5.3 is a summary of estimates of these values for leaves 1-E, 2-E, 2-G, and 3-G. The magnitude of the standard deviation of these values is about equal to the magnitude of the standard deviation of similar values for strawberry leaves (Chabot and Chabot, 1977).

I used the plant anatomy studies summarized in this chapter to gain an understanding of the structure of the leaf. This understanding helped me to formulate models to describe water efflux from wheat leaves in pressure chambers. In general, the aspects of leaf anatomy which I compared to literature values agreed with data reported in the literature. For example, the radii of the vessel elements in the greenhouse plants I used for my experiments were similar to the radii of the vessels in the plants which Kuo grew in Australia. The quantitative data gave me the information I needed to evaluate model parameters.

Table 5.3. Data used to estimate the number of mesophyll cells per unit length of vascular bundle. Leaves were from experiments conducted between 7/29/79 and 8/2/79.

Leaf	Leaf Volume (mm^3)	Mesophyll[a] Cell Volume (mm^3)	Number of Bundles			Vessel Length (mm)	Mesophyll Cell Volume per millimeter of bundle length (mm^3/mm^{-1})		Number of[c] mesophyll cells per unit length (mm^{-1})	
			Laterals	Intermediates	Total		Volume per mm of lateral bundle	Volume per mm of bundle	Number per mm of lateral bundle	Number per mm of bundle
1-E	600	282	13	34	47	254	.0854	.0236	12,376	3,420
2-E	865	407	12	36	48	338	.1003	.0251	14,536	3,637
2-G	406	191	10	25	35	238	.0802	.0229	11,623	3,319
3-G	286	134	14	35	49	202	.0957	.0135	13,870	1,956
Average			12.3 ±1.7	32.5 ±5.1	44.8 ±66		.0904 ±.0042	.0212 ±.0053	13,101 ±1,336	3,082 ±763

[a] Calculated by assuming that mesophyll cell volume is .47 times the total leaf volume.

[b] This was calculated for two different cases. In the first case the number of vessels equalled the number of lateral bundles. In the second case, the number of vessels equalled the sum of the number of laterals and intermediates.

[c] To calculate this value the volume of a mesophyll cell was assumed to be 6.9×10^{-6} mm^3.

CHAPTER 6

MODEL OF XYLEM DEFORMATION

When pressure is applied to a leaf in a pressure chamber, tissue deformation occurs. Of particular importance is the effect of the pressure on the xylem vessels. If the pressure deforms the vessels so that they collapse or their diameter greatly decreases, then the resistance to water flow out of the leaf through the vascular bundles will also increase. In this chapter I describe the modeling which I used to investigate xylem deformation and collapse.

6.1 Modeling Xylem Deformation

In the wheat leaf cross sections in figure 5.1 the xylem elements appear as thick-walled cylinders. Figure 6.1 is a transmission electron micrograph of a longitudinal section of a portion of the xylem vessel wall. The protrusions are highly lignified and are part of the secondary wall which are formed before the cell contents disappear from the cell. The primary wall is relatively thin and contains simple pits through which water can travel between vessels. The secondary thickenings form rings along the length of the vessels. The vessel radii, measured from leaf cross sections, varied between 1×10^{-3} and 12×10^{-3} millimeters. Wall thickness, measured from transmission electron micrographs, varied between 4 and 12 per cent of the inside vessel radius for vessels with radii greater than 3×10^{-3} millimeters. From figure 6.1 it is apparent that the wall thickness measured on a cross section will vary considerably depending

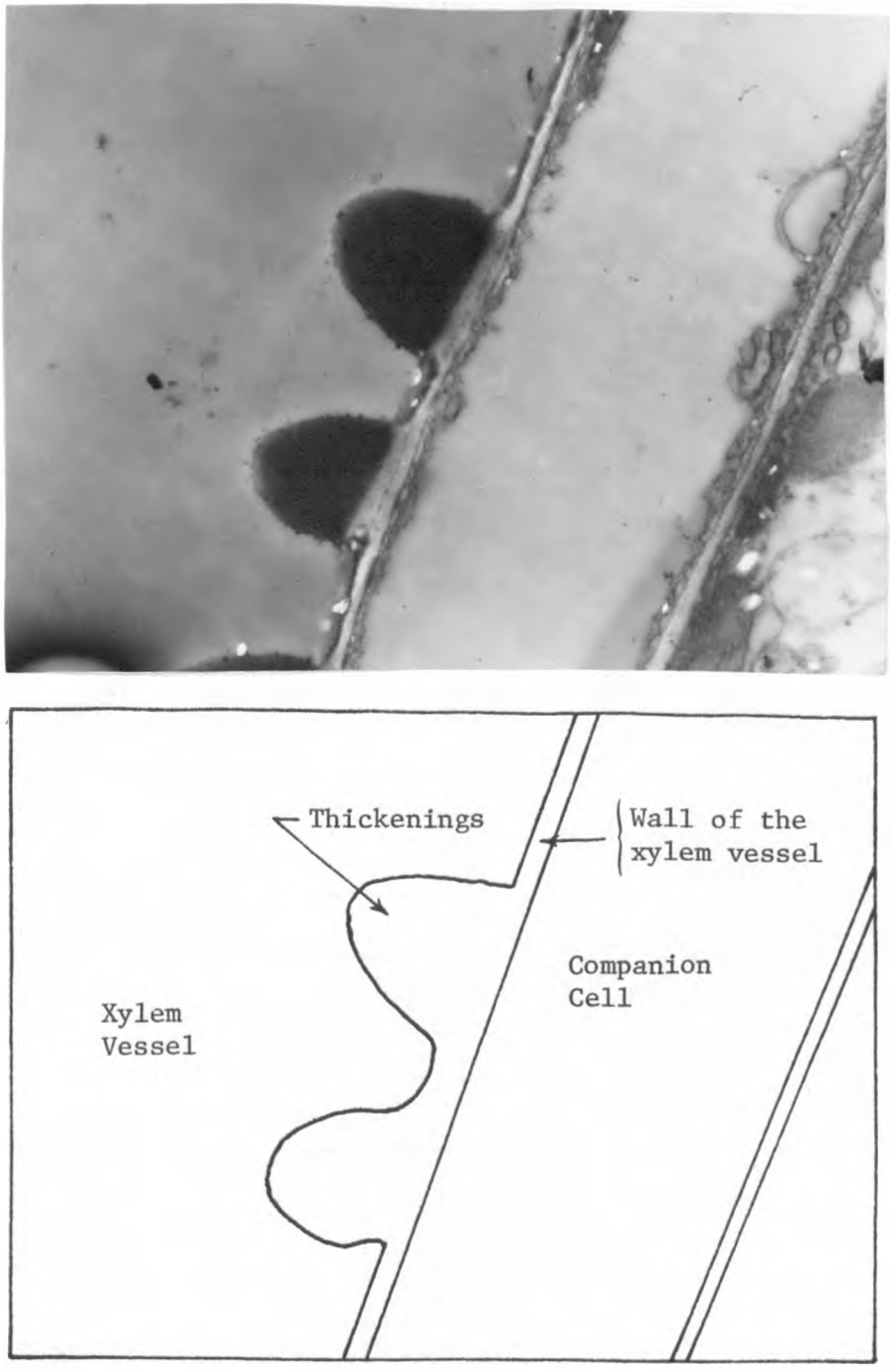

Figure 6.1. Transmission electron micrograph of a portion of the wheat xylem wall showing the thickenings which are part of the secondary wall. These thickenings appear darker than the rest of the wall because they contain tissue which is highly lignified. The vessel, thickenings, wall, and companion cell are identified on the schematic beneath the picture. Magnification 7250X.

on where the section cuts through the secondary wall. The maximum thickness of the xylem wall in figure 6.1 is 1.6×10^{-3} millimeters. This is almost identical to the thickness shown in transmission electron micrographs of palm xylem (Parthasarathy and Klotz, 1976). The ratio of xylem length to radius, measured on a paradermal section of a leaf similar to the one shown in figure 5.3, was greater than 60.

The xylem geometry suggests that they can be modeled as cylinders. In mechanics of materials and theory of elasticity, formulas are available which describe the deformation of both thin-walled and thick-walled cylinders. I modeled xylem deformation using both of these formulas and found their results agreed to within 5 per cent providing the wall thickness did not exceed 10 per cent of the inside radius of the vessel. Estimates of the wall thickness and modulus of elasticity of vessel cell walls are less accurate than 5 per cent. Therefore, I used the thin-wall approximation to estimate xylem deformation.

Figure 6.2 illustrates the model of the xylem vessel as a cylinder. I did not attempt to analyze the bundles as thin-walled cylinders with spiral thickenings, but assumed that the vessels had a wall of uniform thickness either 5 or 10 per cent of the vessel radius. This rough approximation was applied as follows. Since the xylem vessels connect with the atmosphere outside the chamber, I assumed that the pressure in them must be atmospheric. The maximum pressure which is exerted on the outer walls of the xylem is the gauge pressure of the chamber. The bundle sheath cell forms a continuous collar around the xylem vessels (see section 5.3) and O'Brien and Carr

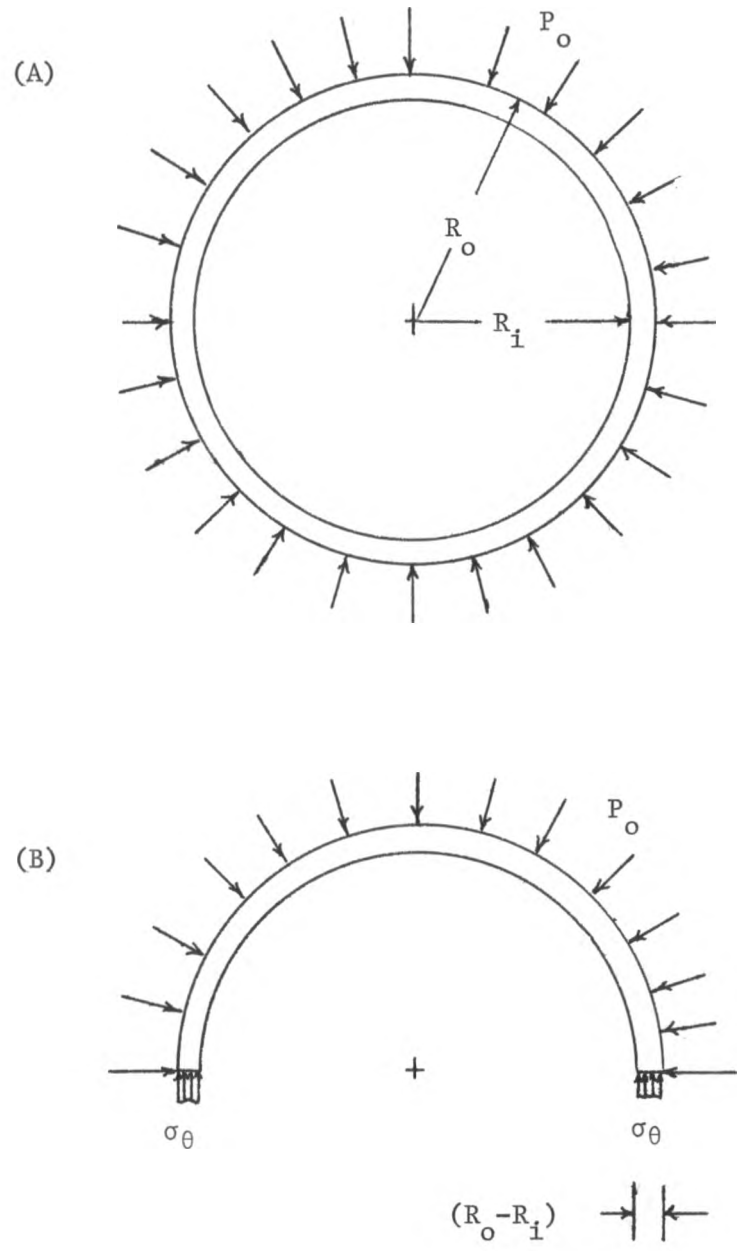

Figure 6.2. Xylem deformation model. Part (A) shows a model of the vessel as a cylinder with inside radius R_i and outside radius R_o. Part (B) shows a free body diagram for the model in part (A) with the compressive stress, σ_θ, balancing P_o, the pressure applied to the outside of the cylinder.

(1970) showed that there is a suberized layer in the inner bundle sheath cells which envelopes the vascular elements. Therefore, it is unlikely that the gas in the chamber presses on the xylem vessels directly. Since the pressure must be transmitted through the tissue surrounding the vessel elements, the actual pressure exerted on the xylem may be less than chamber pressure.

A force balance on the section shown in figure 6.2b gives the stress in the xylem wall:

$$\sigma_\theta = \frac{-P_o R_o}{R_o - R_i} \qquad (6.1)$$

σ_θ = tangential stress in the xylem wall (assumed to be constant throughout the thickness) (micronewtons/micron^2)

P_o = pressure on the outside of the wall (micronewtons)

R_o = outer radius of the xylem vessel (microns)

R_i = inner radius of the xylem vessel (microns)

The decrease in the radius of the xylem can be calculated from the following equation given in Timoshenko (1970,pg 70):

$$\varepsilon_\theta = \frac{u}{R} \qquad (6.2)$$

ε_θ = radial strain at radius R (dimensionless)

u = decrease in radius R (microns)

Assuming that the radial stress is zero, the relationship between σ_θ

and the tangential strain ε_θ is:

$$\varepsilon_\theta = \frac{\sigma_\theta}{E} \qquad (6.3)$$

E = modulus of elasticity of the cylinder

(micronewtons/micron)

Solving equation 6.2 for u, substituting for ε_θ from equation 6.3, and then substituting the right hand side of equation 6.1 for σ_θ, the value of u (the decrease in radius for a balance pressure P_o) is:

$$u = \frac{-P_o R_o R_i}{E(R_o - R_i)} \qquad (6.4)$$

Using this equation I calculated the per cent decrease in volume per unit length of xylem for a given chamber pressure.

I solved equation 6.4 for two values of xylem wall thickness and estimated the modulus of elasticity of the xylem wall. The two values for wall thickness were 5 and 10 per cent of the inside radius. These were the lower and upper limits for most thicknesses measured on leaf sections. Hammel (1967) assumed the wall thickness was 10 per cent of the inside radius when he studied the freezing of hemlock xylem. Estimates of the values of the modulus of elasticity of cell wall materials vary widely. Hammel used a value of 36,000 micronewtons per square micron for the modulus of elasticity of hemlock xylem while Cooke, et al. (1976) used a value of 500 micronewtons per square micron for the modulus of elasticity of guard cells. The modulus of elasticity of wheat xylem walls should fall somewhere between these

values and is probably closer to the value for hemlock xylem. In order to find the upper and lower limits of deformation, I used both values.

The model gave the following predictions. For an elastic modulus of 36,000 micronewtons per square micron and an applied pressure of 30 bars, the radius decreased by less than 0.2 per cent and the relative volume per unit length of vessel decreased less than 1.0 per cent. For a constant wall thickness, the decrease in radius is linearly related to the applied pressure. By contrast to the above results, an elastic modulus of 500 micronewtons per square micron gave a decrease of 12 per cent in the radius and a decrease in volume per unit length of 24 per cent.

6.2 Modeling Xylem Collapse

The above modeling approximates how much deformation occurs in the xylem elements but it does not tell whether they collapse when the chamber is pressurized. Failure of thin-walled cylinders is by buckling. The following formula, taken from Mark's Mechanical Engineer's Handbook (Baumeister, 1967, p 5-65) predicts the external collapsing pressure, W , in pounds per square inch for a thin-walled cylinder of finite length:

$$W_c = KE\left(\frac{t}{D}\right)^3 \text{ psi} \qquad (6.5)$$

K= a numerical coefficient which is dependent on the length to diameter ratio and the diameter to thickness ratio of the cylinder (it is

dimensionless)

E= modulus of elasticity of the material in the cylinder (lbs/in^2)

t= thickness of the cylinder wall (in)

D= inside diameter of the cylinder (in)

This formula assumes that the cylindrical shell is perfectly round with a uniform thickness. It must be made of material which obeys Hooke's law. The radial stresses in the shell must be negligible and the normal stress distribution linear. Since the xylem is relatively thin-walled, the last set of requirements are fulfilled. Although the xylem are not perfectly round and their thickness is not uniform, the formula should still give a rough approximation of the actual behavior.

I evaluated the parameters on the right hand side of equation 6.5 as follows. The value of the diameter to thickness ratio is less than 40 when the wall thickness is 5 per cent or more of the radius. For this ratio and values of length to diameter ratio in excess of 20 the value of K is approximately equal to twice the reciprocal of one minus Poisson's ratio squared. A value of 0.39 for Poisson's ratio (the value used by Cooke, et al., 1976) gives a K value of 2.36. Substitution of the appropriate values into equation 6.5 and conversion from pounds per square inch (psi) to bars gives a collapsing pressure of 3.72×10^{-4} times the modulus of elasticity for a wall thickness 5 per cent of the vessel inside radius. For a wall thickness of 10 per cent, the collapsing pressure is 2.98×10^{-3} times the modulus of elasticity. If the modulus of elasticity of the xylem

wall is 36,000 micronewtons per square micron, collapsing pressures for wall thicknesses of 5 and 10 per cent are 13.3 and 107 bars respectively. Collapsing pressures for these wall thicknesses are 0.2 and 1.5 bars for an elastic modulus of 500 micronewtons per square micron.

6.3 Discussion and Conclusions

The xylem deformation predicted by equation 6.4 is highly dependent on the choice of the modulus of elasticity as is the vessel collapse predicted in section 6.2. The analysis suggests that the vessels would collapse before very large changes in volume per unit length occur.

Experimental evidence reported in the literature and in chapter 5 suggests that the vessels do not collapse. Molz and Klepper (1973) removed xylem tissue from cotton stems and placed them in a pressure chamber under ten bars of pressure. They measured a change in diameter of a 5.07 millimeter cylinder of xylem tissue with an accuracy of 0.068 millimeter and found no deformation. Tyree and Hammel (1972, pg. 274) concluded that compression of vessels in woody tissue was insignificant. The anatomy studies described in chapter 5 agree with these results. The large vesels in the vascular bundle are the most susceptible to collapse. If such a collapse occurred, it would distort the vascular bundles. In the samples taken from leaf 2-G

which had been subjected to pressures up to 30 bars, no distortion of the bundles was apparent.

Raven (1977) pointed out another argument which suggests that the vessels do not collapse. He reasoned that the tension developed in the water in the xylem during transpiration would have the same effect as compression of the xylem. Collapse of the vessels therefore might be prevented by the lignification which occurs as the secondary walls are formed. If Raven's conclusion is correct, then the xylem should be able to withstand compression of at least 15 bars since tensions of this magnitude develop in the xylem of drought-stressed plants.

A collapse of bundles under some circumstances would help to explain results observed by Dr. Jay Cutler while he was a member of the Agronomy Department at Cornell. The initial slopes of all the efflux curves in figure 4.4 are equal with the exception of the slope of the curve for an initial balance pressure of 18.7 bars. Dr. Cutler hypothesized that the initial slope of the curve is an indicator of the resistance to water flow. A decrease in slope means an increase in resistance. Therefore, the curves in figure 4.4 suggest that the pathway of water flow changes or the resistance of the pathway increases at high chamber pressures. A collapse of the larger vessels in the stem could account for an increase in resistance. Such a change occurred in two of the five efflux experiments conducted by Dr. Cutler in March of 1979 but did not occur in the July/August or November experiments. Since Dr. Cutler was working with younger plants, the properties of their xylem may have been different. As reported in

chapter 5, no collapsed vessels were found in the leaves examined. However, since the modeling in this chapter suggests it can occur under certain conditions, examination of leaves after removal from the chamber seems advisable, especially when changes in initial efflux rate are observed above a certain balance pressure.

CHAPTER 7

MODEL OF WATER FLOW THROUGH LEAF TISSUE

The xylem tissue in a leaf is specialized for water conduction. In other words, resistance to water flow through a given length of xylem should be substantially less than the resistance to flow through an equal length of mesophyll tissue. Water expressed from a mesophyll cell will take the path of least resistance through the leaf to the outside of the pressure chamber. Therefore, water should travel from the mesophyll cells to the nearest xylem vessel and then flow out of the leaf through the xylem pathway. The modeling in this chapter neglects the xylem resistance and concentrates on describing flow from mesophyll cells to the xylem. The model in chapter 8 describes flow through the xylem in addition to flow from individual mesophyll cells.

7.1 Background

Philip (1958a,b,c,d) developed one of the simplest models of water flow through plant tissues by assuming that water travels by flowing out of one cell and into the next. He wrote differential equations describing water flow by assuming that the tissue was made up of a large number of cells. However, in a wheat leaf water need only travel a maximum of three or four cell lengths before it reaches a vascular bundle (see chapter 5). Therefore, when I modeled the flow in a leaf, I wrote a system of simultaneous equations which describe water flow between a series of two to six cells. Philip mentioned this approach in his article, but rejected it because he wanted to

model tissue in which water had to flow through large numbers of cells.

When Tyree, Dainty and Benis (1973) modeled pressure chamber efflux curves they assumed that the pressure of the cell contents increased by an amount equal to the gauge pressure of the chamber (see equation 3.11). I applied their assumption to this model. There are numerous stomata in the leaf through which the chamber gases could enter the leaf interior. Once the gases enter the leaf they can press against individual cells. Assuming that the pressure in the leaf is transmitted to the cell contents undiminished by deformation of the cell wall, an increase in chamber pressure would cause an identical increase in the pressure of the cell contents.

The following additional assumption explains how a water potential gradient develops in the leaf. If the vascular bundles are contiguous with the atmosphere, then the water in them will initially be at atmospheric pressure. When the chamber is pressurized and the pressure of the mesophyll cell contents increases, a gradient in pressure (and therefore a gradient in water potential) will develop across the membrane separating the bundle sheath cells from the xylem. In response to this gradient, water will flow from the bundle sheath cells into the xylem vessels. As water flows from the bundle sheath cells, their water potential will decrease and water will flow into them from the surrounding cells.

Using the above assumptions I developed the model shown in figure 7.1. Cell A represents the bundle sheath cell. As water flows from it into the xylem, its potential decreases and water flows into

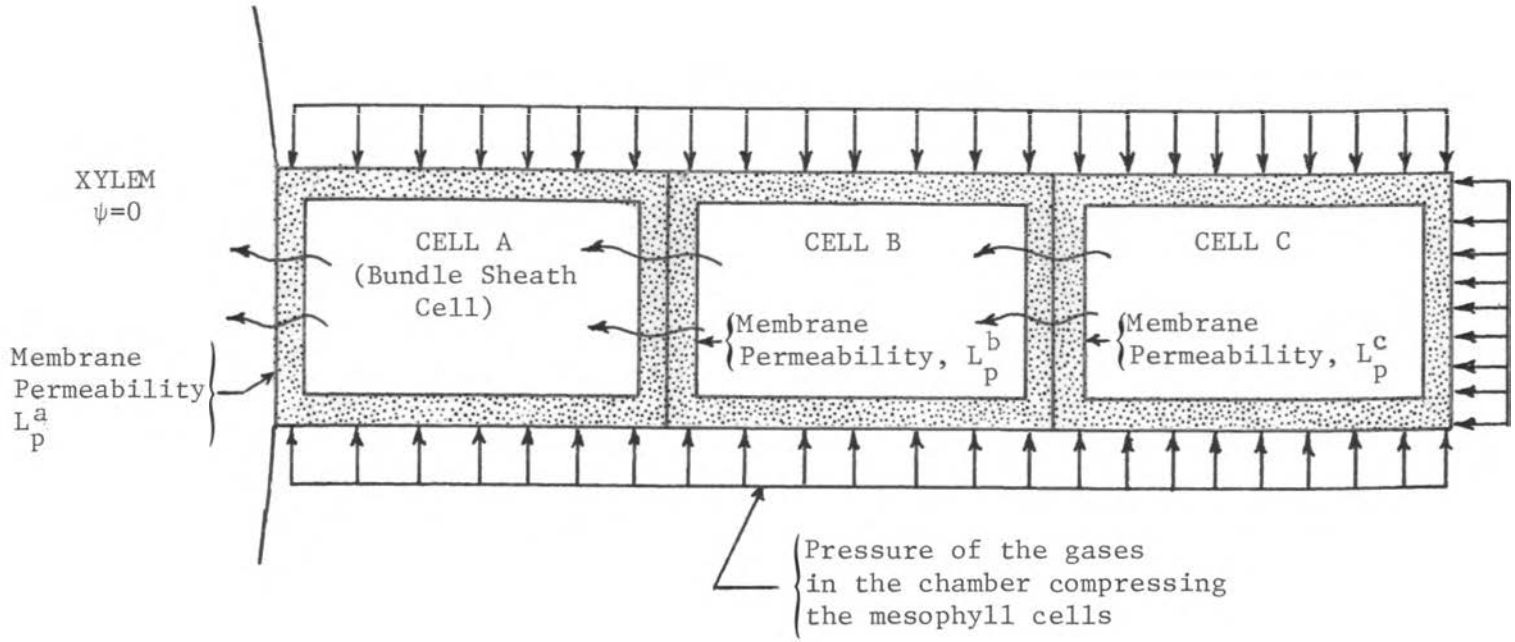

Figure 7.1. Diagram of the model for movement of water from cell to cell as it flows to the xylem vessel. The wavy arrows indicate water flow through cell membranes. The straight arrows represent application of pressure on the cell walls by the chamber gases which have penetrated the leaf interior.

it from cell B. Likewise, as water flows from cell B, its potential decreases and water flows into it from cell C. I assumed that the water potential varies only with distance from a vascular bundle and not with position along the length of the leaf. Therefore, cell A represents a typical bundle sheath cell that would be found adjacent to a typical vascular bundle.

When I developed this model, I neglected flow through the cell walls and assumed that water flows from cell vacuole to cell vacuole. Tyree and Cheung's (1977) pressure chamber efflux experiments with beech leaves gave evidence that "...water driven out of living cells (or infiltrated airspaces) will travel in and out of cells passing through several membranes and the thinnest part of the cell walls between the cells (i.e.,the series cell walls)." They defined the series cell wall as "...the 0.6 micron-thick sheet of cell wall separating adjacent cell membranes." The flow pathway they proposed is shown in figure 7.2, which is redrawn from their paper. Assuming this type of flow occurs in the model of figure 7.1, water would flow from cell B to cell C by first moving into the cell wall area which separates cells C and B. Then it would flow through this cell wall and enter cell B through the cell membrane.

The effect of neglecting cell wall flow can be tested by comparing the model developed by Philip with the one developed by Molz and Ikenberry. Philip modeled flow from cell vacuole to cell vacuole while Molz and Ikenberry also included flow through the cell wall. Zimmerman and Steudle (1978,pg 98) pointed out that the two models "...represent extremes in the present concepts of water transport in

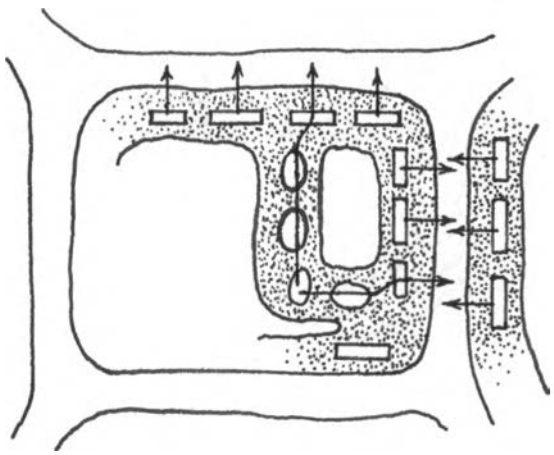

Figure 7.2. A diagram of the area between the veins of a hemlock leaf showing a possible pattern for water movement through the tissue to the veins. The cell walls are exaggerated in size for clarity and are indicated by the stippled areas. Ovals represent mesophyll cell membranes. The small rectangles represent the bundle sheath cells, and the large rectangle represents an intercellular space. (Redrawn from Tyree and Cheung, 1977).

tissue of higher plants." Both models are based on the assumption that the tissues contain large numbers of cells. By making appropriate assumptions Philip, and Molz and Ikenberry wrote single differential equations to describe water flow. Both have the form of equation 3.1 but have different values for diffusivity. A comparison of these diffusivities illustrates the factors which make cell wall flow important.

Philip's model for one-dimensional water flow is described in section 3.3. Substituting water potential, ψ , for η in equation 3.1 gives an equation identical in form to Molz and Ikenberry's. Philip's expression for diffusivity, D, can be written as follows (see also Zimmermann and Steudle, 1978):

$$D = \frac{AL_p \ell^2 (\varepsilon - \overline{\pi}_o)}{2V_o} \qquad (7.1)$$

A = the area of contact between two adjacent cells (mm^2)

L_p = the hydraulic conductivity of the cell membrane (mm/sec-bar)

ℓ = the length of the cell in the direction of water flow (mm)

ε = the elastic modulus of the cell (bars)

$-\overline{\pi}_o$ = the osmotic potential of the cell at zero turgor (bars)

V_o = the cell volume at zero turgor (mm^3)

Molz and Ikenberry (1974) specified that, providing that the

water potential of the cell is equal to the water potential of its surrounding wall, the diffusion coefficient, D can be defined as:

$$D = \frac{2a\ell L_{pw} + \ell^2 A L_p}{2(C_w + C_c)} \qquad (7.2)$$

a,A= cross sectional areas of the cell wall and the cell, respectively (mm^2)

L_p, L_{pw} = hydraulic conductivities of the cell membrane and cell walls, respectively (mm/sec-bar and mm^2/sec-bar, respectively)

C_w = the water storage capacity of the cell wall, approximately equal to $1.5a\ell$ times the storage coefficient, S (mm^3/bar)

$C_c = V_o/(\varepsilon - \bar{\pi}_o)$ = the storage capacity of the cell (mm^3/bar). V_o, ε , and $-\bar{\pi}_o$ have the same definitions used by Philip.

ℓ = the length of the cell in the direction of water flow (mm)

S = the storage coefficient of the cell wall. It is equal to the number of cubic millimeters of water removed from a cubic millimeter of cell wall when it encounters an osmotic gradient of one bar in the surrounding media (bar^{-1})

Molz and Ikenberry estimated the storage capacity of a cell wall to be 0.01 times that of the cell. Neglecting C_w in the denominator of the above equation will make little difference in the result.

Approximating the denominator of equation 7.2 as twice C and substituting the relationship for C_c in terms of V_o, ε, and $\overline{\pi}$ gives a definition of diffusivity in terms of the parameters in Philip's definition. The difference, ΔD, between the diffusivities predicted by equations 7.2 and 7.1 is:

$$\Delta D = \frac{2a\ell L_{pw} (\varepsilon - \overline{\pi}_i)}{V_o} \qquad (7.3)$$

Cell wall flow will be important when ΔD is large. In general, ΔD will increase as cell length, modulus of elasticity, osmotic potential, volume of the cell wall, and cell wall permeability increase. It will decrease as cell volume increases.

Using equations 7.1 and 7.2, I calculated the values of D for data reported in the literature. The results are summarized in table 7.1. The values of D, calculated from equations 7.1 and 7.2 are shown in the last two lines of the table. When the values used by Molz and Ikenberry were substituted into the equations, the diffusivity calculated for flow through both cell wall and cell vacuole was 600 per cent larger than the value for flow through only the vacuoles. Since an increase in diffusivity reflects a decrease in resistance to water flow, the effect of the cell wall pathway was significant. The cell wall affected the value of D because Molz and Ikenberry chose a relatively large cell wall conductivity and a low cell membrane conductivity. The other extreme is represented by Tyree and Cheung's (1977) data. They assigned a relatively low hydraulic conductivity to the cell wall and a moderate value of conductivity to the cell

Table 7.1. Value of diffusivity calculated from Phillip's definition (equation 7.1) and Molz's definition (equation 7.3) for various assumed values of parameters reported in the literature.

Parameter	Definition	Data of Molz and Ikenberry (1974)[a]	Data of Philip (1966)[b]	Data of Molz (1976)	Data of Tyree and Cheung (1977)[c]
A	Area of contact between adjacent cells	9.75×10^{-3} mm^2	2.25×10^{-3} mm^2	2.38×10^{-3} mm^2	9.0×10^{-5} mm^2
a	Cross sectional area of cell walls	2.5×10^{-4} mm^2	2.5×10^{-4} mm^2	1.25×10^{-4} mm^2	1.0×10^{-5} mm^2
$\varepsilon - \overline{\pi}$	Sum of cell elastic modulus and the zero turgor osmotic potential	100 bars	100 bars	100 bars	100 bars
V_o	Cell volume at	1×10^{-3} mm^3	1.25×10^{-4} mm^3	1.25×10^{-4} mm^3	1.0×10^{-6} mm^3
S	Storage coefficient	6.67×10^{-4} bar^{-1}	6.67×10^{-4} bar^{-1}	3.0×10^{-2} bar^{-1}	3.0×10^{-2} bar^{-1}
	Cell length	1.0×10^{-1} mm	5.0×10^{-2} mm	5.0×10^{-2} mm	1.0×10^{-1} mm
L_p	Hydraulic conductivity of the cell wall	1.4×10^{-6} mm/sec bar	2.0×10^{-4} mm/sec bar	3.0×10^{-4} mm/sec bar	1.5×10^{-5} mm/sec bar

(continued)

Table 7.1. Continued.

Parameter	Definition	Data of Molz and Ikenberry (1974)[a]	Data of Philip (1966)[b]	Data of Molz (1976b)	Data of Tyree and Cheung (1977)[c]
L_{pw}	Hydraulic conductivity of the cell wall	1.4×10^{-5} $mm^2/sec\ bar$	5.0×10^{-5} $mm^2/sec\ bar$	2.1×10^{-5} $mm^2/sec\ bar$	5.0×10^{-8} $mm^2/sec\ bar$
D_p	Diffusivity calculated from Philip's definition (see equation 7.1)	6.8×10^{-6} mm^2/sec	5.0×10^{-4} mm^2/sec	7.1×10^{-4} mm^2/sec	6.8×10^{-6} mm^2/sec
D_m	Diffusivity calculated from Molz's definition	4.2×10^{-5} mm^2/sec	9.9×10^{-4} mm^2/sec	1.25×10^{-5} mm^2/sec	7.2×10^{-6} mm^2/sec

[a] They assumed the cells were cubical with sides 0.1 mm long.

[b] These were the values reported in Molz and Ikenberry (1974). Philip assumed only a cell length and Molz and Ikenberry assumed that the cells were cubical.

[c] Tyree and Cheung did not report a value for ℓ. Since they were working with beech leaves, I used their primary reference on anatomy which was Dengler and MacKay (1975) to find the dimensions of a beech mesophyll cell. When I calculated cell area and volume I assumed, as did Tyree and Cheung in the calculations they made, that the cell wall occuppied 10 per cent of the cell volume.

membrane. Their D value changed by only 7 per cent when cell wall flow was considered. The estimates of hydraulic conductivity for the cell membrane and cell wall given in table 7.1 vary widely. Therefore, the values of these parameters will determine the significance of neglecting cell wall flow in any given species of plant or in any given type of tissue. The values which I chose for my model were those of Tyree and Cheung (1977). If these values apply to wheat leaves, then cell wall flow will be relatively insignificant.

Most of the water in a cell is stored in the vacuole. Water passing from one cell vacuole to the next must traverse the tonoplast, the cell cytoplasm, the plasmalemma, and the cell wall of each cell. When I developed the model described in this chapter, I assumed the cell membrane permeability was the combined permeability of all three. I also assumed, as did Tyree and Cheung, that the resistance of the wall separating two adjacent cells (the series cell wall) can be neglected.

When the chamber is pressurized, gas must penetrate the leaf interior. If this happens, gas will penetrate into the intercellular spaces and force out any free water. Nobel (1974, p 50) gives an equation which can be used to calculate the pressure needed to force water from pores of a given diameter. The surface tension of the water in the pores of a leaf will resist the pressure of the chamber gases. Equating the force of the gases acting on a pore of radius r to the surface tension of the water in the pores predicted by Nobel's equation gives the following:

$$P = \frac{2\sigma \cos \alpha}{r} \qquad (7.4)$$

P = the pressure applied to the pore (bars)

r = the radius of the pore (mm)

σ = the surface tension of water at 20 degrees centigrade (7.28×10^{-4} bar-mm)

α = the angle which the meniscus makes with the pore wall. It can be taken as zero degrees when the water is supporting maximum allowable tension.

Using equation 7.4, I found that a pore with a diameter of 5.8×10^{-4} millimeters would resist a pressure of 5 bars. Since most intercellular spaces are larger than this, the water should be pushed from them. On the other hand, the pores in the outer layer of the cell walls have a radius of approximately 5.0×10^{-6} millimeters (Helkvist, et al.,1974, p 661). Equation 7.4 predicts that these pores can withstand a pressure of up to 145 bars. When Tyree (1976) did this calculation, he concluded that no water is forced from the cell wall at the normal pressures encountered in the chamber, and therefore the water content of the cell wall remains relatively constant. In the context of this modeling, the results of equation 7.4 suggest that the gases in the chamber will be unable to penetrate the cell wall. When the chamber pressure is increased, the gases will press upon the cell wall and pressurize the cell contents.

7.2 Development of the Model:

I developed a model of flow through leaf tissues as follows. Figure 7.3 is a schematic of a single cell attached to a xylem element. I estimated the rate of water loss from the cell to the xylem using the following equation adapted from Slatyer (1967, equation 6.3):

$$\frac{dV}{dt} = - L_p A (\psi_{cell} - \psi_{xyl}) \qquad (7.5)$$

V = the volume of the cell (mm^3)

L_p = the permeability of the membrane separating the cell from the xylem (mm/sec-bar)

A = the area of the cell in contact with the xylem (mm^2)

ψ_{cell} = the water potential of the cell (bars)

ψ_{xyl} = the water potential of the xylem (bars)

The water potential in the xylem can be taken as zero, which is the potential of pure water in an open beaker at atmospheric pressure. Assuming the matrix component of potential is negligible, the water potential of the cell is:

$$\psi_{cell} = P_{chamber} + P_{turgor} - \overline{\pi} \qquad (7.6)$$

$P_{chamber}$ = pressure on the water in the cell due to application of chamber pressure (Pa)

P_{turgor} = pressure on the water in the cell due to

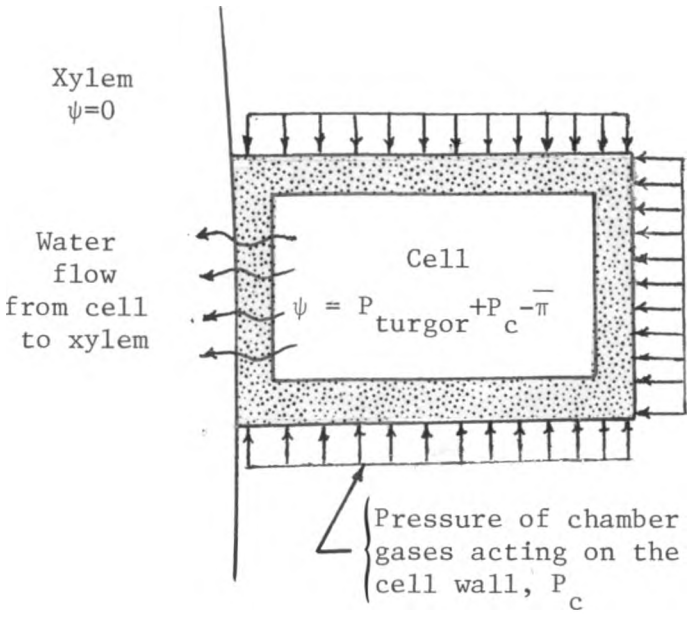

Figure 7.3. Model of a single cell in contact with the xylem. Application of pressure to the cell wall by the pressurized gases in the leaf interior is represented by the straight arrows. Water flow from the cell to the xylem is represented by the wavy arrows. The stippled area represents the cell wall and plasmalemma.

turgor. (Pa) (It is zero in this case since enough water has been expressed from the leaf to decrease the turgor to zero)

$-\overline{\pi}$ = osmotic pressure of the contents of the cell (bars) (Osmotic potential is less than zero. It is written in this manner to make it conform to the convention that all parameters such as $\overline{\pi}$ are positive numbers.)

Tyree and Hammel (1972) also assumed that matrix potential was negligible when they modeled pressure^{-1}-volume curves. Tyree (1976) concluded that it was important in the water relations of the apoplast (the cell wall), but not in the water relations of the symplast.

According to Philip (1958a) the turgor and osmotic potentials can be written:

$$P_{turgor} = \varepsilon\left(\frac{V-V_o}{V_o}\right) \qquad (7.7)$$

$$\overline{\pi} = \frac{\overline{\pi}_o V_o}{V} \qquad (7.8)$$

ε = the modulus of elasticity of the cell wall (Pa)

V_o = volume of the cell at zero turgor (mm^3)

V = volume of the cell (mm^3)

$-\overline{\pi}_o$ = osmotic potential of the cell contents at zero turgor (Pa)

In the same manner as Philip (1958a), I simplified equations 7.7 and 7.8 by defining η as the nondimensional measure of relative volume change, $(V-V_o)/V_o$. Substituting equations 7.6, 7.7, and 7.8 into equation 7.5 and using the change in variable gives an expression for the time derivative of η:

$$\frac{d\eta}{dt} = \frac{-L_p A}{V_o}\left(P_{chamber} + \varepsilon\eta - \frac{\overline{\pi}_o}{1+\eta} - P_{xyl}\right) \qquad (7.9)$$

For $\eta << 1$, this equation can be linearized by taking the first two terms of the binomial expansion of $1/(1+\eta)$. The linearized equation is:

$$\frac{d\eta}{dt} = \frac{-L_p A}{V_o}\left(P_{chamber} + (\varepsilon + \overline{\pi}_o)\eta - \overline{\pi}_o - P_{xyl}\right) \qquad (7.10)$$

This linearization is valid for η near zero. The steady state value of η, calculated by setting $d\eta/dt$ equal to zero in equation 7.9 is -0.22. The steady state value of η calculated from the nonlinear equation is 0.28. This is 1.27 times the steady state value predicted by the linearized equation. Therefore, the linearization introduces a significant error.

The above procedure can be repeated for models with more than one cell. Applying conservation of mass to the model in figure 7.1, I found the following equations which describe the time rate of change in the volumes of cells C, B, and A:

$$\frac{dV^c}{dt} = -L_p^c A^c (\psi_{cell}^c - \psi_{cell}^b) \qquad (7.11)$$

$$\frac{dV^b}{dt} = -\frac{dV^c}{dt} - L_p^b A^b (\psi_{cell}^b - \psi_{cell}^a) \quad (7.12)$$

$$\frac{dV^a}{dt} = -\frac{dV^b}{dt} - L_p^a A^a (\psi_{cell}^a - \psi_{xyl}) \quad (7.13)$$

The superscripts a,b, and c denote variables associated with cells A, B, and C, respectively. By substituting the appropriate values of ψ and changing the variable to η, the system of equations can be described as:

$$\begin{bmatrix} \dot{\eta}^c \\ \dot{\eta}^b \\ \dot{\eta}^c \end{bmatrix} = \begin{bmatrix} a_{11} & a_{12} & 0 \\ a_{21} & a_{22} & a_{23} \\ 0 & a_{32} & a_{33} \end{bmatrix} \begin{bmatrix} \eta^c \\ \eta^b \\ \eta^a \end{bmatrix} + \begin{bmatrix} c_1 \\ c_2 \\ c_3 \end{bmatrix} \quad (7.14)$$

In equation 7.14 the dots denote differentiation with respect to time. The values of the coefficients a_{ij} and c_i are given in table 7.2. By finding the eigenvalues and eigenvectors of the matrix $[a_{ij}]$, I uncoupled the equations and found an exact solution (see Block, et al., 1965,pages 6.47-6.69).

The solution of equation 7.14 gives the following expression for η^a (the value of η for cell A) as a function of time:

$$\dot{\eta}^a = k_1^a e^{\lambda_1 t} + k_2^a e^{\lambda_2 t} + k_3^a e^{\lambda_3 t} + k_4^a \quad (7.15)$$

k_4^a = a constant determined from the particular solution of the matrix equation. The solution was

Table 7.2. Values of a_{ij} and c_i in Equations. (7.14).

$$a_{11} = \frac{-L^c A^c}{\frac{p}{V_o^c}} (\varepsilon^c + \bar{\pi}_o^c)$$

$$a_{12} = \frac{L^c A^c}{\frac{p}{V_o^c}} (\varepsilon^b + \bar{\pi}_o^b)$$

$$a_{21} = \frac{L^c A^c}{\frac{p}{V_o^b}} (\varepsilon^c + \bar{\pi}_o^c)$$

$$a_{22} = -\frac{L^c A^c \frac{p}{o} + L^b A^b \frac{p}{o}}{V_o^b} (\bar{\pi}_o^b + \varepsilon^b)$$

$$a_{23} = \frac{L^b A^b \frac{p}{o}}{V_o^b} (\varepsilon^a + \bar{\pi}_o^a)$$

$$a_{32} = \frac{L^b A^b \frac{p}{o}}{V_o^a} (\varepsilon^b + \bar{\pi}_o^b)$$

$$a_{33} = -\left(\frac{L^b A^b \frac{p}{o} + L^a A^a \frac{p}{o}}{V_o^a}\right) (\varepsilon^a + \bar{\pi}_o^a)$$

$$c_1 = \frac{-L^c A^c \frac{p}{o}}{V_o^c} (P^c_{bomb} - P^b_{bomb} - \bar{\pi}_o^c + \bar{\pi}_o^b)$$

$$c_2 = \frac{-L^b A^b \frac{p}{o}}{V_o^b} (P^b_{bomb} - P^a_{bomb} - \bar{\pi}_o^b + \bar{\pi}_o^a) + \frac{L^c A^c \frac{p}{o}}{V_o^b} (P^c_{bomb} - P^b_{bomb} - \bar{\pi}_o^c + \bar{\pi}_o^b)$$

Table 7.2. Continued.

$$c_3 = \frac{-L^a A^a}{V_o^a} \frac{p^a_o}{RT} (P^a_{bomb} - P_{xyl} - \bar{\pi}^a_o) + \frac{L^b A^b}{V_o^a} \frac{p^b_o}{RT} (P^b_{bomb} - P^a_{bomb} - \bar{\pi}^b_o + \bar{\pi}^a_o)$$

found by assuming the values of η were constants, and then solving equation 7.14 for c_i.

$k^a_{1,2,3}$ = constants which are determined by substituting the eigenvalues and associated eigenvectors of matrix $[a_{ij}]$ into equation 7.14, setting η equal to its value at t=0, and solving for appropriate constants.

λ_i = the eigenvalues of the matrix

Once the value of η^a is known, the rate of flow into the xylem across the cell wall, dQ/dt, can be calculated using an equation similar to equation 7.5:

$$\frac{dQ}{dt} = L_p A \, (\psi^a_{cells} - \psi_{xyl}) \qquad (7.16)$$

Setting ψ_{xyl} equal to zero and ψ^a equal to $P_{chamber} - \overline{\pi}_o(1-\eta^a)$ in equation 7.16, substituting the value of η^a, and integrating with respect to time gives:

$$Q = C - L_p A \overline{\pi}_o \left(\frac{k_1}{\lambda_1} e^{\lambda_1 t} + \frac{k_2}{\lambda_2} e^{\lambda_2 t} + \frac{k_3}{\lambda_3} e^{\lambda_3 t} \right) \qquad (7.17)$$

C is the constant of integration of equation 7.16. The value of the constant of integration can be determined by setting Q equal to zero at time zero.

The above equation gives the amount of flow from three cells. To get an equation for the flow from an entire leaf, I multiplied the flow from three cells by the total number of sets of three cells in a

leaf. Since the λ_i are negative, the value of Q after infinite time will be C. This is the model prediction of the total amount of water which can be forced from a leaf.

7.3 Determination of Parameters

Before I could use the model developed in section 7.2, I had to determine the number of cells in a leaf and evaluate the coefficients in table 7.2. Table 7.3 shows the numerical values of the parameters I used to calculate the coefficients defined in table 7.1. In this section, I explain why I chose these particular values.

As I noted in section 7.1, estimates of cell membrane permeability vary widely. I chose the value reported by Tyree and Cheung (1977) for my first set of calculations. They estimated this value for beech mesophyll cells based on pressure chamber experiments. Since it was the only value available for mesophyll cells of a higher plant, I used it in preference to the other values reported in table 7.2. The values are between 1.0×10^{-10} and 1.0×10^{-11} mm/sec-Pa. Tyree and Cheung's value is at the lower end of this range. In section 7.4, I discuss how changing the cell permeability affects the model's predictions of efflux.

For the models with two or more cells, I adjusted the membrane permeabilities of the cells adjacent to the bundle sheath cell. L_p represents the permeability of a single cell membrane. As shown in figure 7.1, when water flows from cell B to cell A it must pass through two membranes. Therefore, when I evaluated the coefficients for cells B and A, I halved the permeability of the membrane

Table 7.3. Numerical values assigned to the parameters which define the coefficients a_{ij} and c_i. Since leaf 2-G was modeled, experimentally determined values for leaf 2-G were used where appropriate.

Parameter	Meaning	Value	Source
V_o	Volume of a mesophyll cell at zero turgor (mm^2)	6.9×10^{-6}	Calculated by assuming the cell was a cylinder of length 3.0×10^{-2} mm and radius 8.5×10^{-3} mm. These values of length and radius were measured from cross sections such as those in figure 5.1
A	Area of cell to cell contact (mm^2)	2.3×10^{-4}	Calculated by assuming the area is equal to the area of the end of a cylinder with radius 8.5×10^{-3}
$-\bar{\pi}_o$	Osmotic potential of mesophyll cells at zero turgor (Pa)	12.5×10^{5}	Determined from the pressure^{-1}-volume curve for leaf 2-G
P_c	Chamber pressure after the overpressure is applied (Pa)	17.0×10^{5}	Determined by the experimental conditions being modeled
N	The number of mesophyll cells in a leaf	2.8×10^{7}	Estimated for leaf 2-G from total leaf volume, the per cent of total volume which is mesophyll cells, and the value of V_o for a single cell.

Table 7.3. Continued

Parameter	Meaning	Value	Source
L_p	Permeability of the cell membrane (mm/sec Pa)	$1.1\text{-}1.9 \times 10^{-11}$	Measured on onion epidermis (Palta and Stadelman, 1977)
		$2\text{-}5 \times 10^{-10}$	Measured on onion epidermis (Ferrier and Dainty, 1977)
		5×10^{-11}	Measured on pepper fruits (Husken, et al., et al., 1978)
		2.0×10^{-10}	Measured on bladder cells of Mesembryanthemum crystallinum (Steudle, et al., 1977)
		1.5×10^{-10}	Estimated for mesophyll cells of breech leaves by Tyree and Cheung (1977) using pressure chamber experiments

separating the adjacent cells. Thus I assumed that the two membranes in series act like one membrane with a permeability half as large. If I had assumed that the water flowed between adjacent cells and from the bundle sheath cells to the xylem through plasmodesmata I would have used an L_p appropriate to plasmodesmatal flow. In that case, the L_p would have had the same value for all the membranes.

I used the following method to estimate the number of mesophyll cells in leaf 2-G. The mesophyll cells comprise approximately 47.6 per cent of the leaf volume (see table 5.2). The volume of leaf 2-G is approximately 406 mm^3 (see table 4.1). Therefore, the volume of mesophyll cells in leaf 2-G is 0.476 times 406 or 193 mm^3. Assuming the cell volume to be 6.9×10^{-6} mm^3 and dividing this into 193 mm^3 gives 2.80×10^7 for an estimate of the number of mesophyll cells in the leaf and 9.33×10^6 for the number of sets of three cells. The actual value may be smaller. As I noted in chapter 5, the leaf cells are irregular in shape. I determined V_o by assuming that the measurements in the cross section gave the length and diameter of the cell. In fact, these were the the dimensions of one of the "fingers" of the cell. Since one cell may have more than one "finger," my estimate of the number of cells may be too large. However, the cross sections also show that the ends of the fingers often touch. Therefore, each of the individual fingers may act like a cell.

I assumed the value of the modulus of elasticity of the cells was zero. The balance pressures used in this test were in excess of those at which the turgor of the cells first reached zero. Therefore, taking ε as zero was equivalent to assuming that no negative turgor

developed. Tyree (1976) pointed out that, if it did develop, there would be no linear region in the pressure^{-1}-volume curve. The pressure^{-1}-volume curves of all the wheat leaves tested (see chapter 4) had linear regions. Therefore, it seems unlikely that negative turgor developed.

Wheat leaf mesophyll cells are irregular in shape with many "fingers " (see chapter 5). I calculated V_o and A by assuming that each "finger" was a cell and by assuming the "fingers" were shaped like cylinders. I assumed the length and radius of the cylinder were equal to the maximum length and radius measured from cross sections such as those shown in figure 5.1, and I equated V_o to the volume of the cylinder. Since each of the "fingers" in the cross section appear to be touching, I assumed that water flowed from the cells across the ends of the fingers. I used the value of the area of one end of the cylinder for the cross sectional area of flow, A.

The remaining parameters depend on the experiment being modeled and the physiological properties of the leaf. I used the osmotic potential measured for leaf 2-G as shown in table 4.1. Since I was modeling the efflux experiment on leaf 2-G which had an initial balance pressure of 14.0 bars and an overpressure of 3.0 bars, $P_{chamber}$ was 17.0 bars.

7.4 Model Predictions:

The values of a_{ij} and c_i from table 7.2 evaluated using the parameter estimates from table 7.3 are shown in table 7.4 for models with two and three cells. The matrices are symmetric and have

Table 7.4. Matrices $[a_{ij}]$ and vectors $\{c_i\}$ for the two-cell and three-cell models.

I. Two-cell model:

$$[a_{ij}] = \begin{bmatrix} -.003125 & .003125 \\ .003125 & -.009375 \end{bmatrix} \qquad \{c_i\} = \begin{Bmatrix} 0 \\ -.00225 \end{Bmatrix}$$

II. Three-cell model:

$$[a_{ij}] = \begin{bmatrix} -.003125 & .003125 & 0 \\ .003125 & -.006250 & .003125 \\ 0 & .003125 & -.009375 \end{bmatrix}$$

$$\{c_i\} = \begin{Bmatrix} 0 \\ 0 \\ -.00225 \end{Bmatrix}$$

eigenvalues less than zero. The matrix equations for η and the equations for Q predicted by the two models are shown in table 7.5.

I used the procedure described in section 7.2 to develop models containing between 2 and 5 cells. The results for one, three, and five cell models are shown in figure 7.4. In each model I assumed the value of L_p to be 1.5×10^{-10} mm/sec Pa. As the number of cells in the model increases, the total time required to force all of the water out of the leaf increases. For a given time after application of the overpressure, the rate at which water flows from the leaf (the slope of the curve) decreases as the number of cells increases. Decreasing the permeability of the cell membrane has a similar effect on efflux. Figure 7.5 shows efflux curves from a single cell for permeabilities of 1.5×10^{-10} and 1.5×10^{-11} mm/sec-Pa. The efflux curve for a single cell with permeability 1.5×10^{-11} mm/ sec-Pa (figure 7.5) is similar to the efflux curve for a five cell model with a cell wall permeability of 1.5×10^{-10} mm/sec-Pa (figure 7.4). Figure 7.6 shows efflux curves for a single cell model with membrane permeability of 5.0×10^{-11} mm/sec-Pa and a two cell model with cell membrane permeability of 1.5×10^{-10} mm/sec-Pa. The two curves would fit a given set of experimental data equally well.

The two and three cell models fit the experimental data best. The asympotic value of the efflux curves is 0.1142 mm^3 of water expressed per mm^3 of initial leaf volume. The asymptotic value of the efflux curve for leaf 2-G (see figure 4.10) is 0.09113 mm^3 of water expressed per mm^3 of initial leaf volume. In order to compare the efflux curves of the models with the efflux curves of the experiment,

Table 7.5. Values of η and Q for the two-cell and three-cell models. η is dimensionless and Q has units of cubic millimeters of water expressed per cubic millimeter of leaf volume.

I. Two-cell model:

$$\begin{bmatrix} \eta^b \\ \eta^a \end{bmatrix} = \begin{bmatrix} 0.2896 \\ 0.1200 \end{bmatrix} e^{-.00183t} + \begin{bmatrix} -0.0497 \\ +0.1200 \end{bmatrix} e^{-.01067} + \begin{bmatrix} -0.3600 \\ -0.3600 \end{bmatrix}$$

$$Q = .1142 - .0975e^{-.00183t} - .0167e^{-.01067t}$$

II. Three-cell model:

$$\begin{bmatrix} \eta^c \\ \eta^b \\ \eta^a \end{bmatrix} = \begin{bmatrix} .0214 \\ -.0585 \\ .08000 \end{bmatrix} e^{-.0117t} + \begin{bmatrix} -.08000 \\ .08000 \\ .08000 \end{bmatrix} e^{-.00625t}$$

$$+ \begin{bmatrix} .2985 \\ .2186 \\ .0800 \end{bmatrix} e^{-.000837t} + \begin{bmatrix} -0.3600 \\ -0.3600 \\ -0.3600 \end{bmatrix}$$

$$Q = .1142 - .00680e^{-.0117t} - .0127e^{-.00625t} - .0947e^{-.000837t}$$

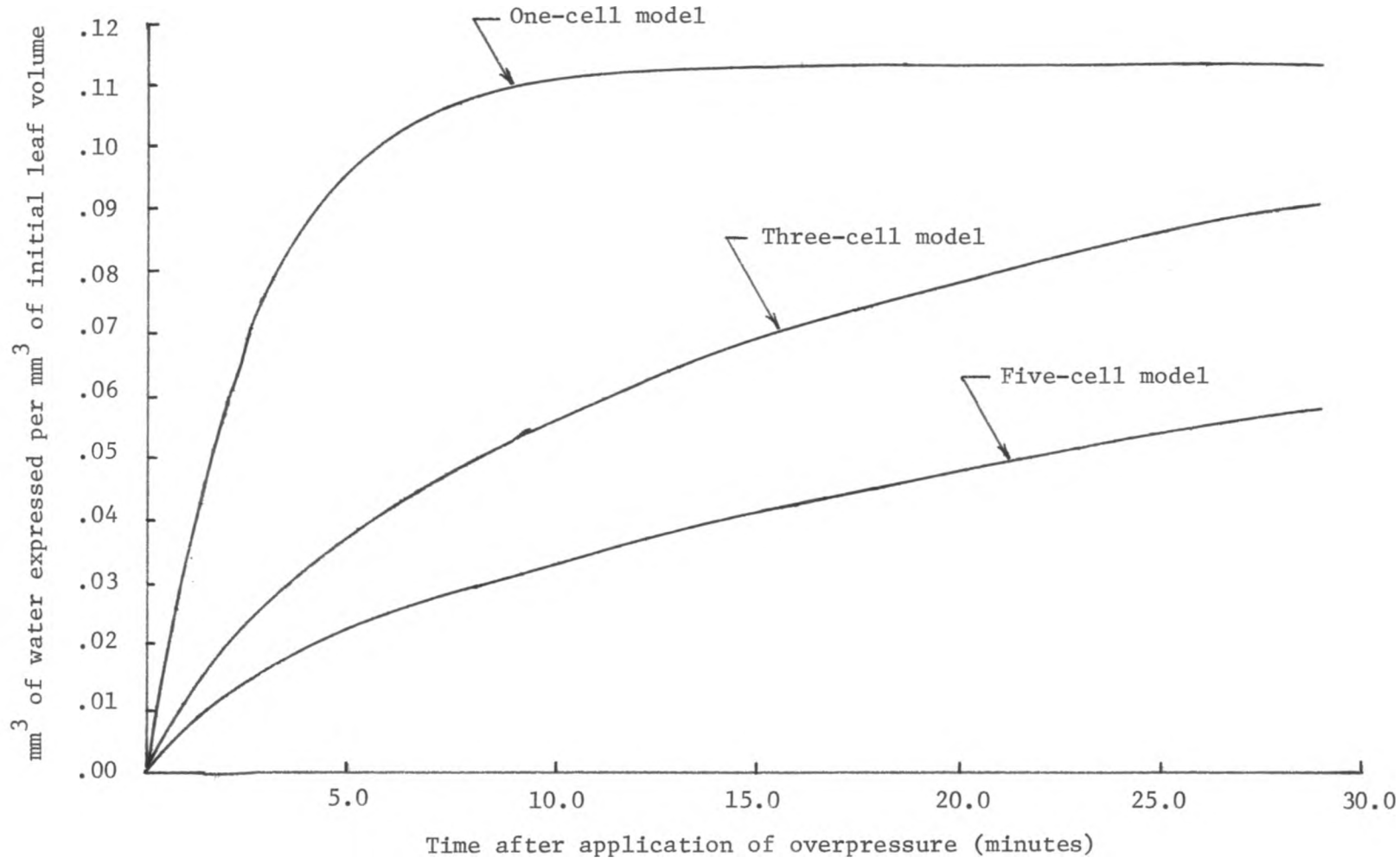

Figure 7.4. Efflux curves for models with one, three, and five cells.

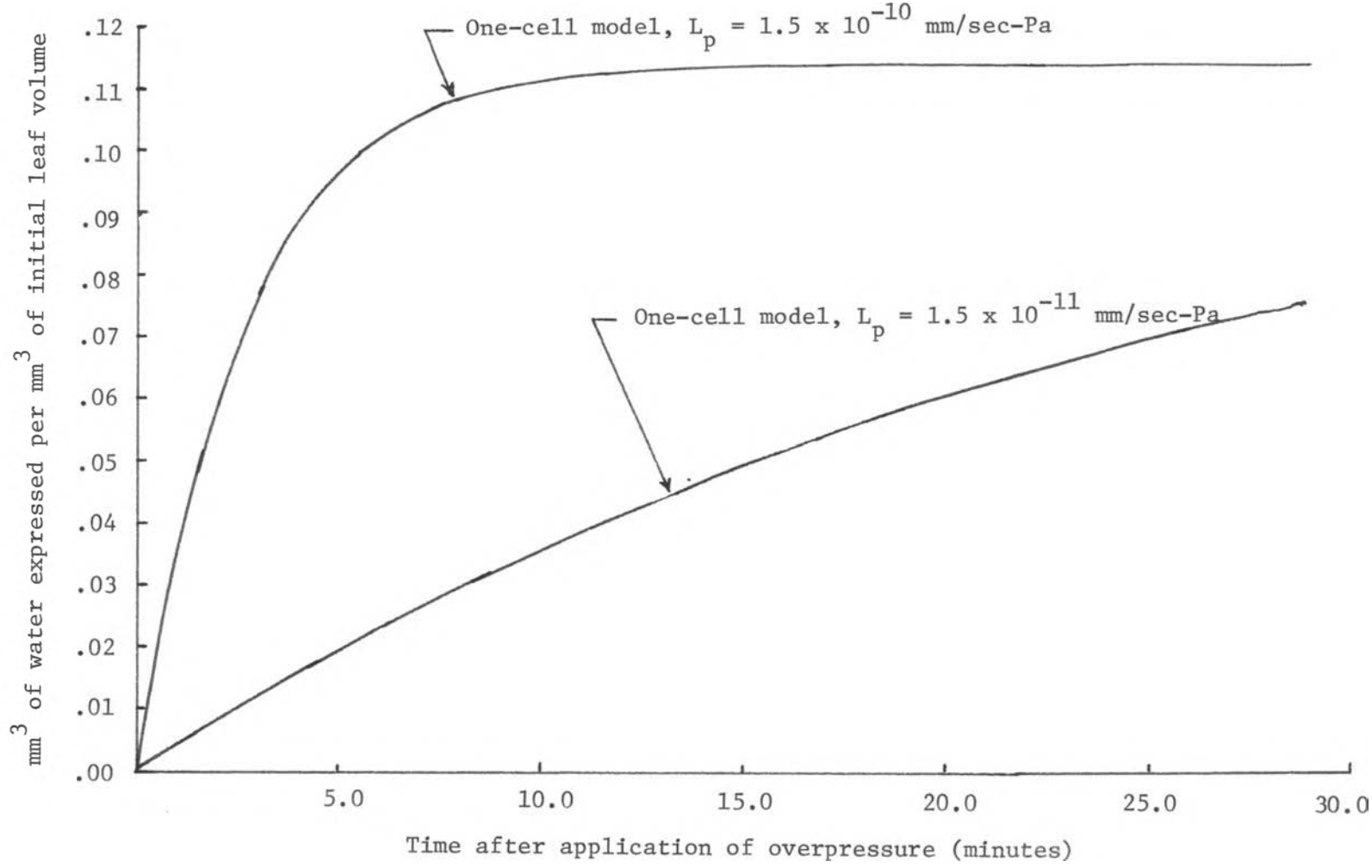

Figure 7.5. Effect of changing the cell membrane permeability on the efflux curves for a one cell model.

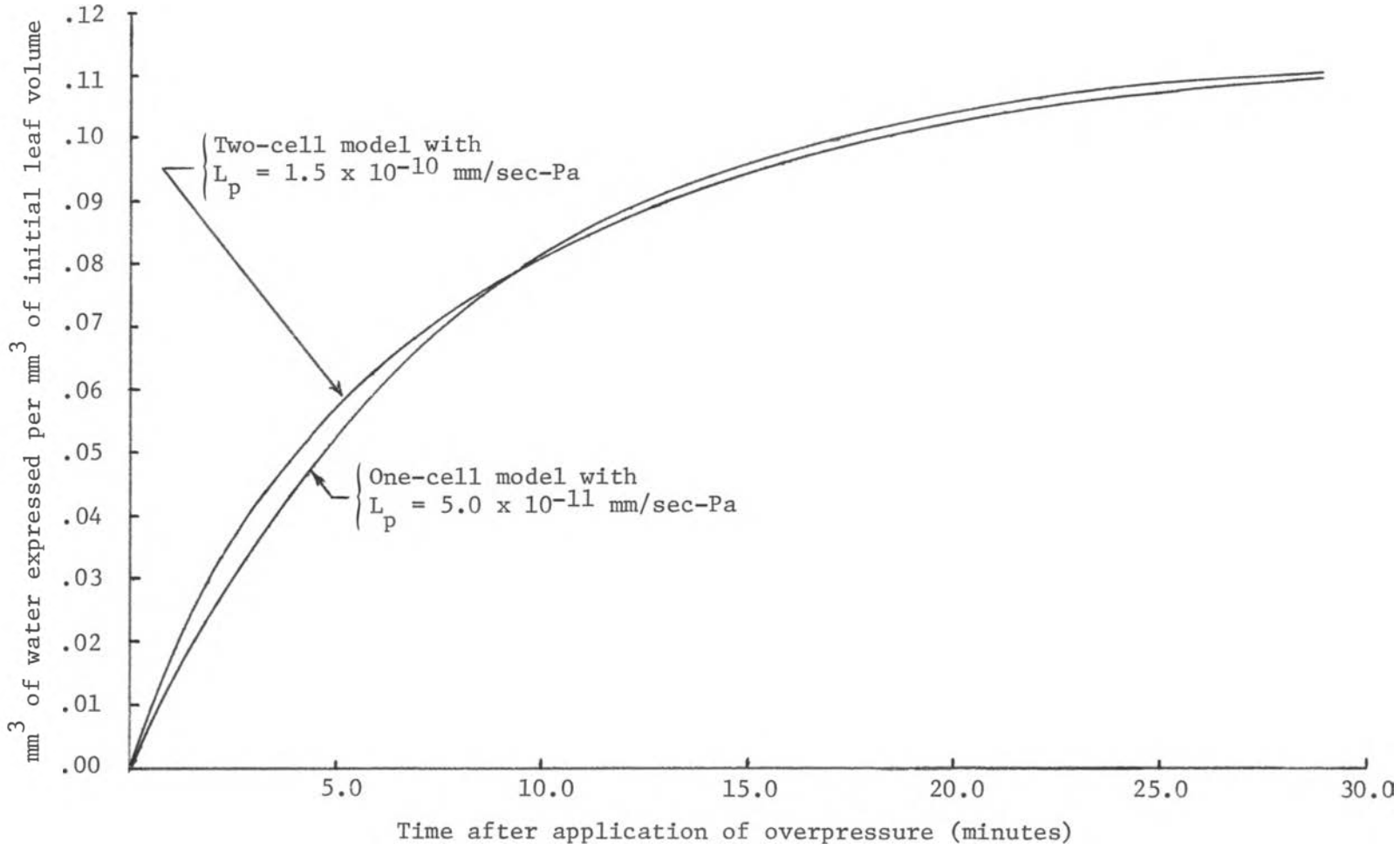

Figure 7.6. Efflux curves for a one cell model with cell membrane permeability of 5.0×10^{-11} mm/sec-Pa and a two cell model with permeability of 1.5×10^{-10} mm/sec-Pa.

I multiplied the equation for efflux by .09113/.1142. This gave me the efflux curves shown in figure 7.7. The two cell model appears to fit the experimental values well.

In order to get analytic solutions for the models, I linearized each equation. Such a linearization is only valid when η is small. In order to better determine the effect of this linearization, I solved the non-linear equations numerically using a fourth order Runge-Kutta method. I used the IMSL (International Mathematical and Statistical Libraries, Inc., Houston, Texas) program DVERK. The results are shown in figure 7.8. The asymptotic value of the non-linear solution is 0.0750 mm^3/mm^3. The efflux curve for the non-linear equation has nearly reached its asymptotic value after 20 minutes. However, the efflux curve for the linearized equation does not approach its asymptotic value until 30 minutes has passed. I could adjust the model to fit the experimental data by increasing the number of cells or by decreasing the permeability of the cell membrane. However, changes in the values of the parameters would not affect the conclusions discussed in section 7.5.

7.5 Discussion and Conclusions:

The parameters which I chose for the modeling described in this chapter were ones which enabled me to neglect cell wall flow. The analytic solution of the two-cell model with L_p of 1.5×10^{-10} mm/sec Pa gave good agreement with experiment. Therefore, the model is consistent with the observations of Tyree and Cheung (1977).

The model is also consistent with the hypothesis that the bundle

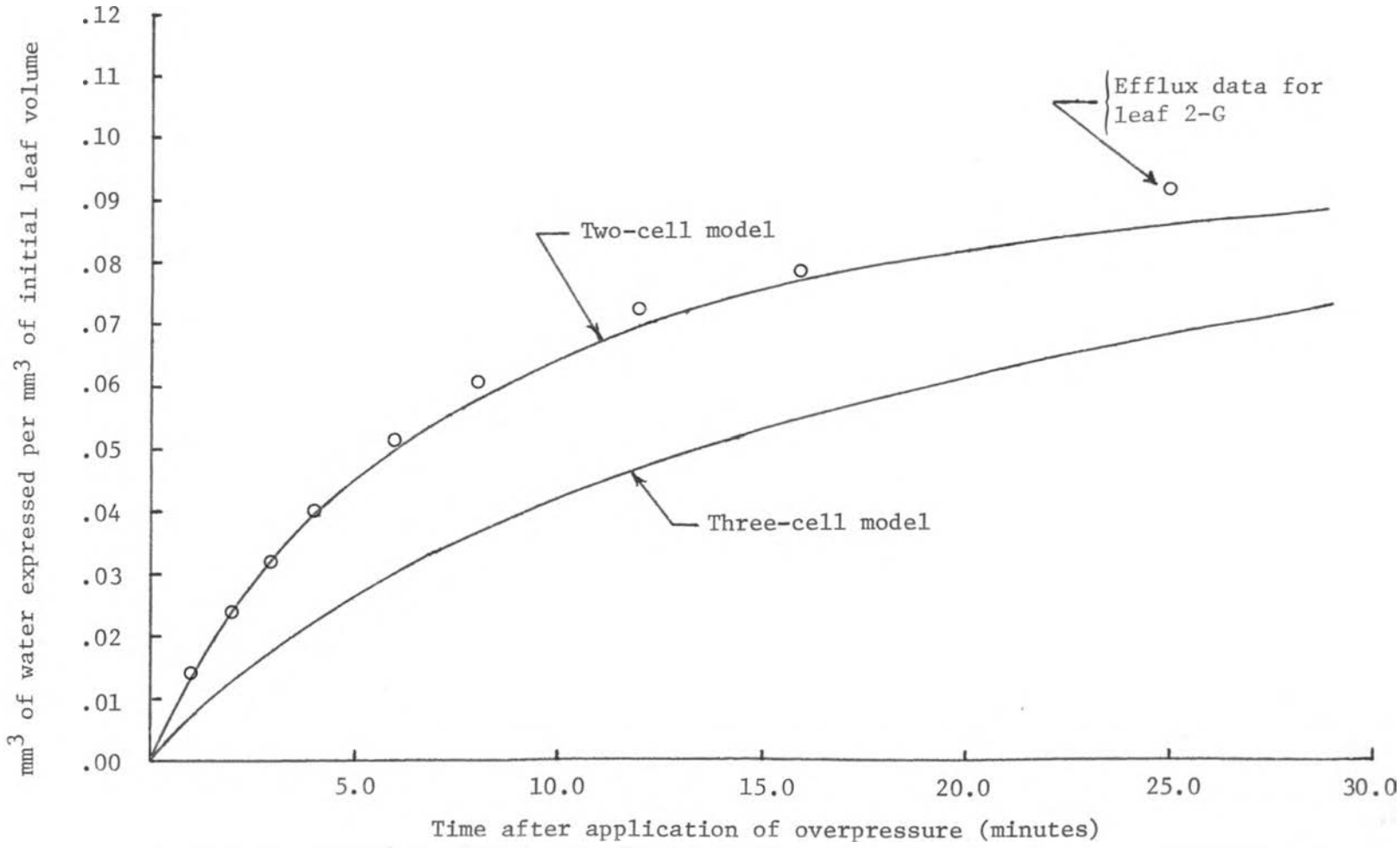

Figure 7.7. Efflux curves for two cell and three cell models compared to experimentally measured efflux from leaf 2-G. The asymptotic values of the models have been adjusted to the asymptotic value of the experimental data, 0.09113 mm^3 of water expressed per mm^3 of initial leaf volume.

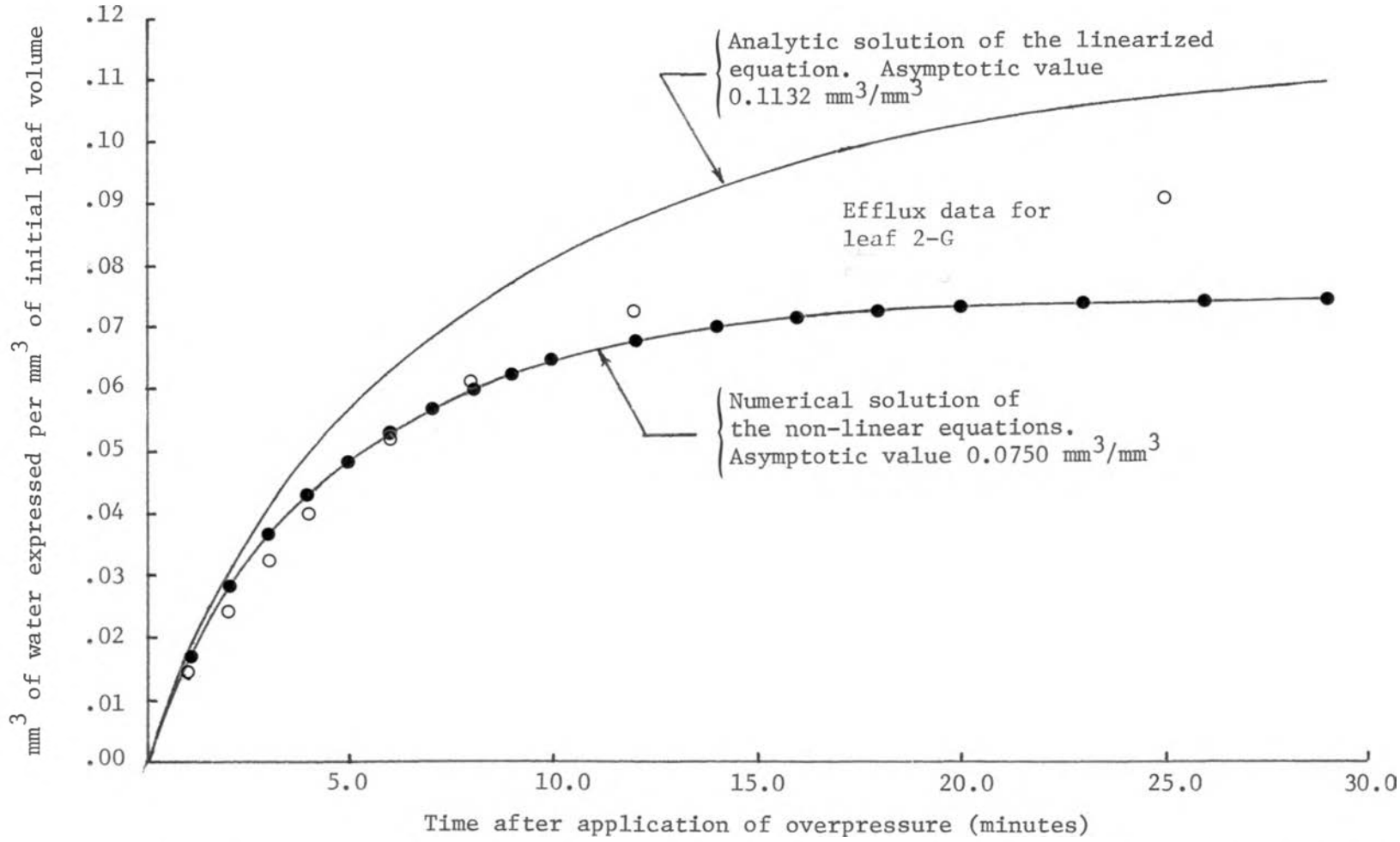

Figure 7.8. Efflux curves predicted by the linear and non-linear cell to cell flow models. The models both had two cells. The linear equations were solved analytically while the non-linear equations were solved numerically. The dots are solution points for the numerical solution and the o's are points from an efflux experiment on leaf 2-G.

sheath cells regulate water flow between the mesophyll and the vascular bundle. O'Brien and Carr (1970) found suberized lamellae in the areas of the cell wall where adjacent bundle sheath cells touched. inner bundle sheath cells. They observed that "... if suberized lamellae should prove to be relatively impermeable to water, one would have to face the possibility that, at least in leaves of some Graminae, Cyperaceae, and Juncaceae, water loss is regulated at the vascular bundle as well as by the stomata." If this suberized layer forces the water entering the vascular bundle to flow in one side of the bundle sheath cell and out the other, then the two or three cell model would best describe the efflux of water from the leaf.

If the permeability of the mesophyll cells is 1.5×10^{-11} mm/sec-Pa or lower, then the one-cell model would give the best agreement with experiment. If the value of L_p were known more precisely, then this model could be used to estimate the number of membranes through which water must flow as it travels from the mesophyll cells to the vascular bundle.

The modeling described in this chapter illustrates that water efflux through a series of cells with a relatively high permeability is quite similar to water efflux from a single cell which has a relatively low permeability. This fact will be used to interpret the results of the model described in chapter 8.

CHAPTER 8

MODEL OF WATER FLOW THROUGH TISSUE AND XYLEM

The model of water flow through tissue described in chapter 7 assumed the xylem offered negligible resistance to water flow. However, gradients of several bars have been measured along the length of transpiring leaves (see section 8.1). Such gradients may be necessary to maintain water flow through the xylem. The model developed in this chapter describes both resistance to water flow across a semipermeable membrane and resistance to water flow through xylem vessels. I used it to investigate the effect of xylem resistance on efflux, and to interpret some of the experimental results described in chapter 4.

8.1 Background

The xylem elements in the leaf may offer a significant resistance to water movement. Rawlins (1963) reported gradients of several bars along the length of a rapidly transpiring tobacco leaf. Hanson, et al. (1977) measured gradients of 30 bars or more in severely stressed barley leaves undergoing rapid transpiration. Denmead and Millar (1976) measured unit length resistances of 0.44×10^4 Pa-sec/mm^4 for sections of wheat leaf and calculated a resistance to water flow of 0.33×10^4 Pa-sec/mm^4 using Poiseuille's equation. These measurements suggest that xylem resistance can be significant

and that it should be taken into account when modeling efflux from the pressure chamber.

The effect of the xylem resistance can be quantified by treating the xylem as pipes to which Poiseuille's law applies. Dimond (1966) modeled flow through a tomato stem using this approach and found reasonable agreement between model predictions and experimental results (see chapter 3, section 3.3). His assumption that water could pass freely between vessels in a bundle meant there was parallel flow through the vessels within a bundle. In this type of flow, the reciprocal of the total resistance of the bundle is equal to the sum of the resistances of the individual vessels. Dimond applied this assumption and wrote an equation for the unit length resistance of the bundle as a function of its vessel radii (see equation 3.7).

Poiseuille's formula can only be applied to flow through the xylem if flow is incompressible, laminar, and steady. The pressure in the xylem never exceeds the overpressure applied during the efflux experiment. Assuming the osmotic potential of the xylem water is zero, its water potential will be equal to its pressure. If the pressure of this water exceeded the overpressure, water would flow from the bundle into the cells rather than from the cells into the bundle. Therefore, for the experiments modeled in this thesis, the pressure in the xylem never exceeds 3 bars and the flow can be considered incompressible.

The nature of the flow in the vessels can only be determined after the velocity of the flow is known. I estimated this for leaf 2-G as follows. I assumed that all of the water flowed through the 10 lateral bundles in the leaf. The flow rate is approximately equal to

one sixtieth the amount of water expressed from the leaf during the first minute of the efflux experiment. Dividing this flow rate by 10 gave me an estimate of the per bundle flow rate. To estimate the velocity of flow through the vessels in the bundle I assumed that all of the water flowed through the 4 vessels with the largest radii and I divided the cross sectional area of these vessels into the flow rate. This gave me a velocity estimate of 6.85 mm/sec. I found the Reynolds number for flow through xylem to be 0.068 . This value is well within the range of laminar flow.

The final assumption to be justified is that of steady flow. Applying an analysis of unsteady state "start-up" flow in a long circular tube (Bird, Stewart, and Lightfoot, 1960, p 126), I found that, if the pressure in the xylem reaches 3 bars as soon as the overpressure is applied, the velocity at the center of the tube reaches 90 per cent of its steady state (Poiseuille flow) value within 10^{-4} seconds. Since the flow rates do not decrease rapidly with time, I feel that the flow of water through the xylem is quasi-steady and therefore Poiseuille's law is applicable.

8.2 Development of the Model:

In the development of the model I assumed, as did Tyree and Cheung (1977), that water forced from the mesophyll cells travels to the nearest longitudinal vascular bundle through which it flows out of the leaf. Figure 8.1 is an idealized paradermal view of a portion of a leaf in a pressure chamber. The leaf is in the chamber at its balance pressure with one end exposed to the atmosphere. I have shown three

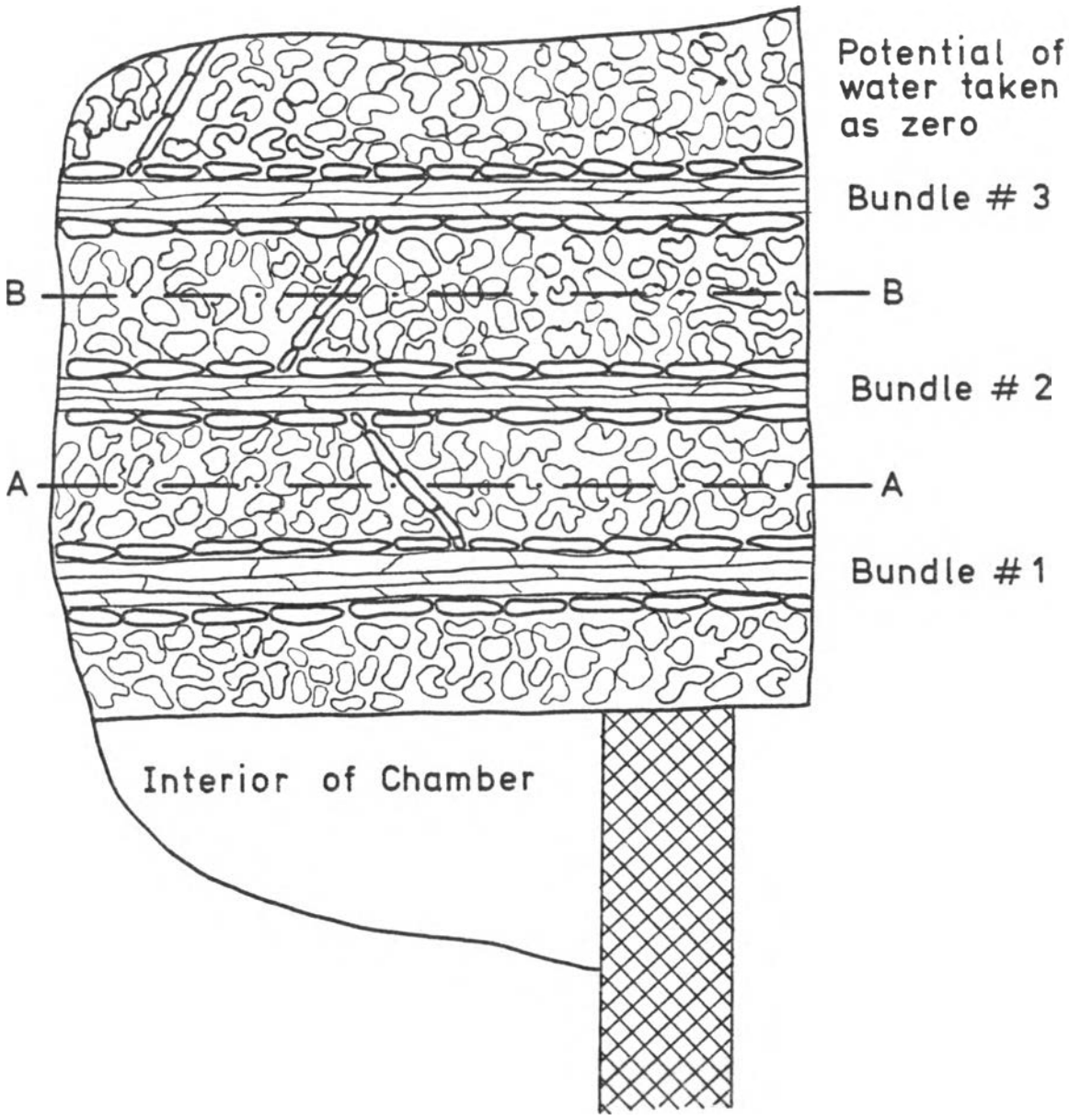

Figure 8.1. Idealized paradermal view of a wheat leaf in the pressure chamber.

vascular bundles surrounded by cells. Assume the contents of the xylem vessels contain no solutes. If one end of the vascular bundle is exposed to the atmosphere, the potential of the water in it will be the same as that of free water. Following the convention of Nobel and others (Nobel, 1975, pg 59) I assumed it was zero. If the pressure in the chamber increases above the balance pressure, the gases in the chamber which have penetrated the leaf will further compress the individual cells. I assumed this pressure is transmitted undiminished to the contents of the cell. As the pressure increases, so does the potential of the water in the cells. This water now has a higher water potential than the water in the xylem, and water flows from the cells to the xylem. Since the vessels are contiguous with the atmosphere, the water flowing into them travels to the cut end of the leaf. The vessels in the bundle have small diameters and resistance to water flow though them will be large. The further water must travel through the bundle, and the smaller the diameter of the vessels in the bundle, the greater will be the pressure gradient needed to maintain a given flow rate.

The water movement through the idealized leaf in figure 8.1 can be quantified as follows. If there is no variation in initial cell water potential across the width of the leaf, then water from cells between lines A-A and B-B will flow into bundle number 2. Now consider a section of bundle number 2 of length dx as shown in figure 8.2. All of the cells between A-A and the bundle and between B-B and the bundle have been lumped into one large idealized cell which forms a collar around the vascular bundle. I treated these cells as a

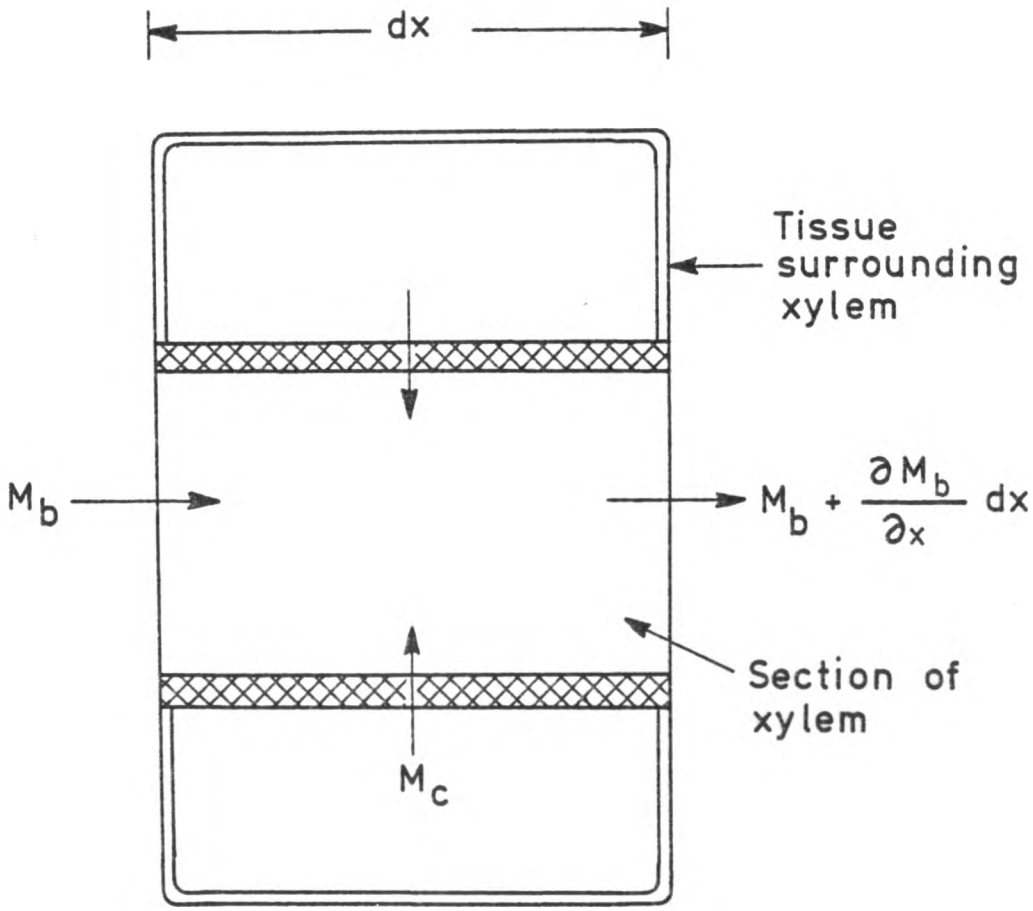

Figure 8.2. A model of a section of a vascular bundle of a wheat leaf showing the volumetric flow of water through the xylem, M_b, and the volumetric flow of water into the xylem from the surrounding cells, M_c. The bundle consists of many vessel elements but has been represented as one large "tube." There are many cells surrounding the bundle but they have been represented as one large cell forming a "collar" around the bundle.

tissue by describing their characteristics in terms of volume averaged tissue parameters. I assumed that all of the water must pass from the collar of cells to the vascular element through a single semi-permeable membrane. In chapter 7, I showed that the resistance to water flow through several cells is equivalent to the resistance to flow through one cell with a low permeability. Therefore, by adjusting the resistance of the membrane used in the model in this chapter, I can account for all of the resistance to water flow presented by the tissue. I ignored water flow through phloem and sclerenchyma cells and used Dimond's approach to lump the resistances of the individual vessel elements in a bundle. Assuming the water to be incompressible and equating flow into the section of bundle to flow out of the section gives:

$$\frac{\partial M_b}{\partial x} = M_c \qquad (8.1)$$

M_b = the volumetric flow rate through the vein (mm^3/sec)

M_c = the volumetric flow of water into a millimeter length of bundle from the surrounding cells (mm^3/sec per mm of bundle length)

The value for M_c can be predicted from Poiseuille's formula by assuming, as did Dimond (1956), that water can pass freely between xylem vessels so that the flow in the vessels is in parallel. As shown by Dimond, the equivalent resistance of a bundle of vessels can be determined by summing the reciprocals of the individual vessel

resistances. Applying his technique:

$$M_b = \frac{-\pi \sum_{i=1}^{j} nr_i^4}{8v} \frac{\partial P}{\partial x} \qquad (8.2)$$

r_i = the radius of the ith element in the bundle (mm)

n = the number of elements of radius r_i in the bundle

j = the number of different radii of the vessels in a bundle

v = the absolute viscosity of the xylem sap (Pa-sec)

P = P(x,t) = the pressure a distance x from the end of the stem, at time t after application of the overpressure (Pa)

Differentiating equation 8.2 with respect to x and lumping all of the parameters into a single constant, k_o , gives:

$$\frac{\partial M_b}{\partial t} = -k_o \frac{\partial^2 P}{\partial x^2} \qquad (8.3)$$

If N is the number of cells per millimeter of the bundle and V the average volume of the cells in the tissue, then

$$M_c = - N \frac{\partial V}{\partial t} \qquad (8.4)$$

V will depend on x, the distance of the cell from the end of the xylem

open to the atmosphere and t, the time after application of the overpressure. Substituting equations 8.3 and 8.4 into equation 8.1 gives:

$$k_o \frac{\partial^2 P}{\partial x^2} = N \frac{\partial V}{\partial t} \qquad (8.5)$$

Flow of water across the membrane of a single cell is defined as the product of cell membrane permeability, the area across which flow occurs, and the difference in potential on opposite sides of the membrane (Slatyer, 1967, equation 6.3). I adapted Slatyer's equation to the model by assuming that water flows from the tissue across only a portion of the total mesophyll cell surface area in the leaf. Assuming that the cell membrane acts as though it separates the cells from the xylem, I assigned the water in the tissue the potential of water inside the cell vacuoles and the water outside the tissue the potential of water in the xylem. This allowed me to write $\partial V/\partial t$, the change in cell volume with time, as:

$$\frac{\partial V}{\partial t} = -L_p A(\psi_{tissue} - \psi_{xyl}) \qquad (8.6)$$

L_p = the permeability of the membrane (mm/sec-Pa)

A = area across which water flows from cell to xylem (mm)

$\psi_{tissue} = \psi_{tissue}(x,t)$ = the water potential of the tissue (Pa)

$\psi_{xyl} = \psi_{xyl}(x,t)$ = the water potential of the water

in the xylem at distance x and time t (Pa)

As mentioned previously, I assumed the potential of the water in the xylem, ψ_{xyl}, is equal to its pressure. The components of ψ_{tissue} are the volume-averaged turgor and osmotic potentials as described by Tyree and Hammel (1972):

$$\psi_{tissue} = \psi_{vat} + \psi_{vaop} + P_c \qquad (8.7)$$

$\psi_{vat} = \psi_{vat}(x,t)$ = the volume averaged turgor potential of the cells (Pa)

$\psi_{vaop} = \psi_{vaop}(x,t)$ = the volume averaged osmotic potential of the cells (Pa)

P_c = the pressure of the cell contents due to the forces exerted on the cell by the chamber (assumed equal to chamber pressure) (Pa)

When they used equation 8.7, Tyree and Hammel assumed that the matrix component of cell water potential was negligible. They described the bulk parameters used in equation 8.7 as follows:

$$\psi_{vat} = \varepsilon\left(\frac{V-V_o}{V_o}\right) \qquad (8.8)$$

$$\psi_{vaop} = \frac{-\overline{\pi}_o V_o}{V} \qquad (8.9)$$

V = the average volume of the cells (mm)

V_o = the average volume of the cells at zero turgor (mm)

ε = the bulk modulus of elasticity of the tissue (Pa)

$-\overline{\pi}_o$ = the average value of the osmotic potential of the cells at zero turgor (Pa) (Osmotic potential is less than zero. It was written in this manner to make it conform to the convention that all parameters, such as $\overline{\pi}_o$, are positive numbers.)

Substituting equations 8.7, 8.8, and 8.9 into equation 8.6 and assuming ψ_{xyl} is equal to P gives:

$$\frac{\partial V}{\partial t} = -L_p A\left(P_c + \varepsilon\left(\frac{V-V_o}{V_o}\right) - \frac{\pi_o V_o}{V} - P\right) \quad (8.10)$$

By making the change of variable $\eta = (V-V_o)/V_o$ equations 8.5 and 8.9 can be expressed in terms of η and P. Linearizing these equations by assuming small values of η and using the binomial expansion, $1/(1+\eta) \cong 1-\eta$, equations 8.5 and 8.10 can now be written in the form:

$$\frac{\partial^2 P}{\partial x^2} = k_1 \frac{\partial \eta}{\partial t} \quad (8.11)$$

$$\frac{\partial \eta}{\partial t} = k_2 P - k_3 \eta - k_4 \quad (8.12)$$

Expressions for the coefficients k_1, k_2, k_3, and k_4 are given in table 8.1.

Equations 8.11 and 8.12 can be solved using one initial condition and two boundary conditions. I assumed the cells surrounding the vascular bundle were of uniform volume and had

Table 8.1. Expressions for the coefficients k_i used in equations (8.11) and (8.12).

(1) $$k_o = \frac{\pi \sum_{i=1}^{j} n r_i^4}{8v}$$

(2) $$k_1 = \frac{NV_o}{k_o}$$

(3) $$k_2 = \frac{L_p A}{V_o}$$

(4) $$k_3 = (\varepsilon + \bar{\pi}_o)\, k_2$$

(5) $$k_4 = (P_c - \bar{\pi}_o)\, k_2$$

(6) $$a_1 = \eta_o + \frac{k_4}{k_3}$$

(7) $$\mu_n = \frac{-k_3}{1 + \frac{k_2 k_1}{\lambda_n^2}}$$

(8) $$\lambda_n = \frac{n\pi}{2\ell}$$

identical water potentials. Thus for a given initial balance pressure, P_c^i, the initial value of η for each cell was identical. In other words, $\eta(x,0) = \eta_o$. I determined the value of η_o using equation 8.12. At equilibrium there is no flow through the bundles so P, the gauge pressure in the xylem vessels, will be zero. Setting $\partial\eta/\partial t$ equal to zero and solving for η gives η_o equal to $-k_4/k_3$. Since the osmotic potential at zero turgor, $-\overline{\pi}_o$, is always the same, η will vary linearly with P_c^i (see the definitions of k_3 and k_4 in table 8.1).

The boundary conditions are on P(x,t), the pressure in the xylem vessels. I assumed that the pressure at the end of the bundle open to the atmosphere (at x=0) was zero. Since no water flows into the bundle at the tip of the leaf (at $x=\ell$), I assumed the spatial derivative of P at that point, $\partial P/\partial x\,|_{x=\ell}$ was zero.

I solved equations 8.11 and 8.12 using the method of separation of variables outlined in Appendix C. The solution gave me the following equations describing P and η as functions of time and distance from the open end of the vascular bundle:

$$\eta(x,t) = -\frac{k_4}{k_3} + \sum_{n=1,3,5,\ldots}^{\infty} \frac{4a}{n\pi} e^{\mu_n t} \sin \lambda_n x \quad (8.13)$$

$$P(x,t) = \frac{-16ak\ell}{\pi} \sum_{n=1,3,5,\ldots}^{\infty} \frac{\mu_n e^{\mu_n t}}{n^3} \sin \lambda_n x \quad (8.14)$$

where:

$$a = \eta_o + \frac{k_4}{k_3}$$

$$\mu_n = \frac{-k_3}{1 + \frac{k_2 k_1}{\lambda_n}}$$

$$\lambda_n = \frac{n\pi}{2\ell}$$

I found the flow rate from the stem by differentiating equation 8.14 with respect to x and substituting $\partial P/\partial x$ into Poiseuille's equation:

$$\frac{dQ}{dt} = k_o \frac{\partial P}{\partial x}\bigg|_{x=0} \qquad (8.15)$$

Integrating equation 8.15 with respect to time and substituting the initial conditions Q=0 when t=0 gave me an expression for Q, the total water which has flowed from the end of the stem at time t:

$$Q = \frac{8ak_1k_o\ell}{\pi^2} \sum_{n=1,3,5,\ldots}^{\infty} \frac{1}{n^2} (1-e^{\mu_n t}) \qquad (8.16)$$

Equation 8.16 is the equation I used to predict the water flow from the vascular bundles in the wheat leaf.

8.3 Determination of Parameters

Before I could use the model of water efflux from wheat leaves, I had to assume values for the parameters which determine the

coefficients shown in table 8.1. The values I used are shown in table 8.2. Zimmermann and Steudle (1978) have summarized hydraulic conductivity measurements on higher plant cells. They reported values ranging from 1.0×10^{-9} to 1.0×10^{-13} mm/sec-Pa. The value which I chose, 1.5×10^{-10} mm/sec-Pa, was determined by Tyree and Cheung (1977) from pressure chamber experiments with beech leaves. It is very close to the value of 2.0×10^{-10} mm/sec-Pa reported by Steudle, et al. (1977) for pressure probe measurements on bladder cells of Mesembryanthemum crystallinum. Husken,et al. (1978) measured a value one third as large for pepper fruit tissue cells (Capsicum anum) using a refined model of the pressure probe. However, I used Tyree and Cheung's value because it was measured on mesophyll cells of a higher plant leaf.

Many of the values listed in table 8.2 were measured from leaf cross sections. The cross sections and paradermal section discussed in chapter 5 showed that the mesophyll cells are irregularly shaped with many "fingers." Measurements of mesophyll cells showed that the "fingers" had a radius of approximately 8.5×10^{-3}mm and were 3.0×10^{-2} mm long. I assumed that each "finger" acted like an individual cell and I calculated the cell volume by assuming that each was a cylinder. I assumed that water passed from the cell through one end of the cylinder. This end had area A. Therefore, I assigned A its minimum possible value. If A were equated to the total surface of the cylinder, the value would be 2.1×10^{-3} mm^2 (9.0 times greater).

I determined N, the number of cells per millimeter of vascular bundle, by estimating the total number of mesophyll cells in the leaf

Table 8.2. Numerical values assigned to the parameters which define the coefficients k_i listed in Table 8.1.

Parameter	Meaning	Value	Source
V	Viscosity of water expressed from the leaf	10^{-3} Pa-sec	Value for water at 20°C
V_o	The volume of a mesophyll cell when the turgor potential first becomes zero	6.9×10^{-6} mm^3	Calculated by assuming the cell was a cylinder with radius 8.5×10^{-3} mm and length 3.0×10^{-2} mm
N	The number of mesophyll cells per millimeter of xylem	3450 cells/mm	Determined by dividing the estimated volume of mesophyll cells by V_o
L_p	The permeability of the membrane surrounding a cell	1.5×10^{-10} mm/Pa-sec	Tyree and Cheung (1977)
A	Area of the portion of the cell surface through which water flows out of the cell	2.3×10^{-4} mm^2	The area of the end of a cylinder with a diameter equal to the diameter of the mesophyll cells
ε	Modulus of elasticity of the cell	0	Only the case where the turgor potential was aero was modeled
$-\bar{\pi}_o$	The osmotic potential of the cell when the turgor potential first reaches zero	-12.5×10^5 Pa	Determined from a pressure^{-1} - volume curve

Table 8.2. Continued.

Parmeters	Meaning	Value	Source
P_c	the chamber pressure at which the test is conducted	17.0×10^5 Pa	this depends on the experiment being modeled
η	the value of the non-dimensional parameter at the beginning of the test	.24	calculated from the initial conditions
ℓ	the length of the leaf	238mm	the measured length of leaf 2-G

and then dividing by the total length of leaf vascular bundles. In chapter 5, I described how I used the method of Wiebel (1969) to determine that mesophyll cells occupied approximately 47 per cent of the leaf volume. Therefore, the calculated volume of mesophyll cells in a leaf was 0.47 times the leaf volume. For leaf 2-G, which had a volume of 406 mm^3, the mesophyll volume was 191 mm^3. There were 35 bundles in the leaf and leaf length was 238 mm. Therefore, the volume of mesophyll cell per millimeter of vascular bundle was 191 mm^3 divided by 238 times 35 or 0.0229 mm^3/mm. By assuming cell volume to be 6.9×10^{-6} mm^3 and then dividing this into 0.0229 mm^3/mm I found N to be 3319 for leaf 2-G. In the model I set N equal to 3450, which was the average value of N for leaves 1-E, 2-E, 2-G, and 3-G.

To evaluate the coefficients in table 8.1, I needed to determine a value for $\Sigma\ nr_i^4$. I used the measurements of vessel radii summarized in table 5.1. I assumed the midrib behaved as a large lateral. Using these values I calculated the values of the constants shown in table 8.3. Because the values of $\Sigma\ nr_i^4$ are different for each bundle type, the values of k_o and k_1 differ among bundles. I also calculated the values of the constants by assuming that water flowed out of the leaf through only the lateral bundles. I assumed that there were 6 large lateral bundles for every 4 small lateral bundles and calculated a weighted average of 4.25×10^{-8} mm^3 for $\Sigma\ nr_i^4$. The value of N changed to 4805 since the number of bundles became 10 rather than 35. The values for this second case are shown in the bottom line of table 8.3.

For the modeling I needed to know the number of bundles of each size. Microscopic examination of leaf 2-G showed that it had 10

Table 8.3. Numerical values for the coefficients k_i in Table 8.1 evaluated using the parameters from Tables 8.2 and 5.1.

Bundle type	Σnr_i^4 mm^4	Values of constants k_i				
		k_o $mm^4/Pa\text{-}sec$	k_1 $Pa\text{-}sec/mm^2$	k_2 $(Pa\text{-}sec)^{-1}$	k_3 $(sec)^{-1}$	k_4 $(sec)^{-1}$
Large lateral	4.94×10^{-8}	1.94×10^{-5}	1230	5.0×10^{-9}	6.25×10^{-3}	2.25×10^{-3}
Small lateral	3.19×10^{-8}	1.25×10^{-5}	1901	"	"	"
Large intermediate	1.89×10^{-10}	7.42×10^{-8}	3.20×10^{5}	"	"	"
Small intermediate	2.60×10^{-11}	1.02×10^{-8}	2.33×10^{6}	"	"	"
Values assuming all flow is through the 10 lateral bundles	4.25×10^{-8}	1.69×10^{-5}	4805	"	"	"

lateral bundles and 25 intermediate bundles. Based on the relative proportions of large and small bundles reported by Kuo, I assumed 6 of the laterals were large and 14 of the intermediates were large.

8.4 Model Predictions

Using the k values in the first four lines of table 8.3, I calculated the values of the water efflux from each of the bundle types by multiplying the flow from a single bundle by the number of bundles of that type. I normalized the values by dividing efflux by leaf volume. Figure 8.3 shows the efflux curves predicted by the model when these k values were used. I called this solution case 1. Virtually all of the water is expressed from the 6 large and 4 small lateral bundles within 15 minutes after application of overpressure. However, the rate of water efflux from the intermediate bundles (the slope of the efflux curve) did not decrease even after 30 minutes. These results suggest that the cell membrane limits efflux from the laterals while the xylem resistance limits efflux from the intermediates.

In the efflux experiments on leaf 2-G (see figure 4.5) all of the water flowed from the leaf in 25 minutes. However, the results shown in figure 8.3 suggest that the water could not flow from the intermediate bundles in this amount of time. Therefore, I infer that the lateral bundles must carry a larger proportion of the flow. In the extreme case, they will carry all the water from the leaf. For case 2, I modified the model by assuming that all of the flow occurred through

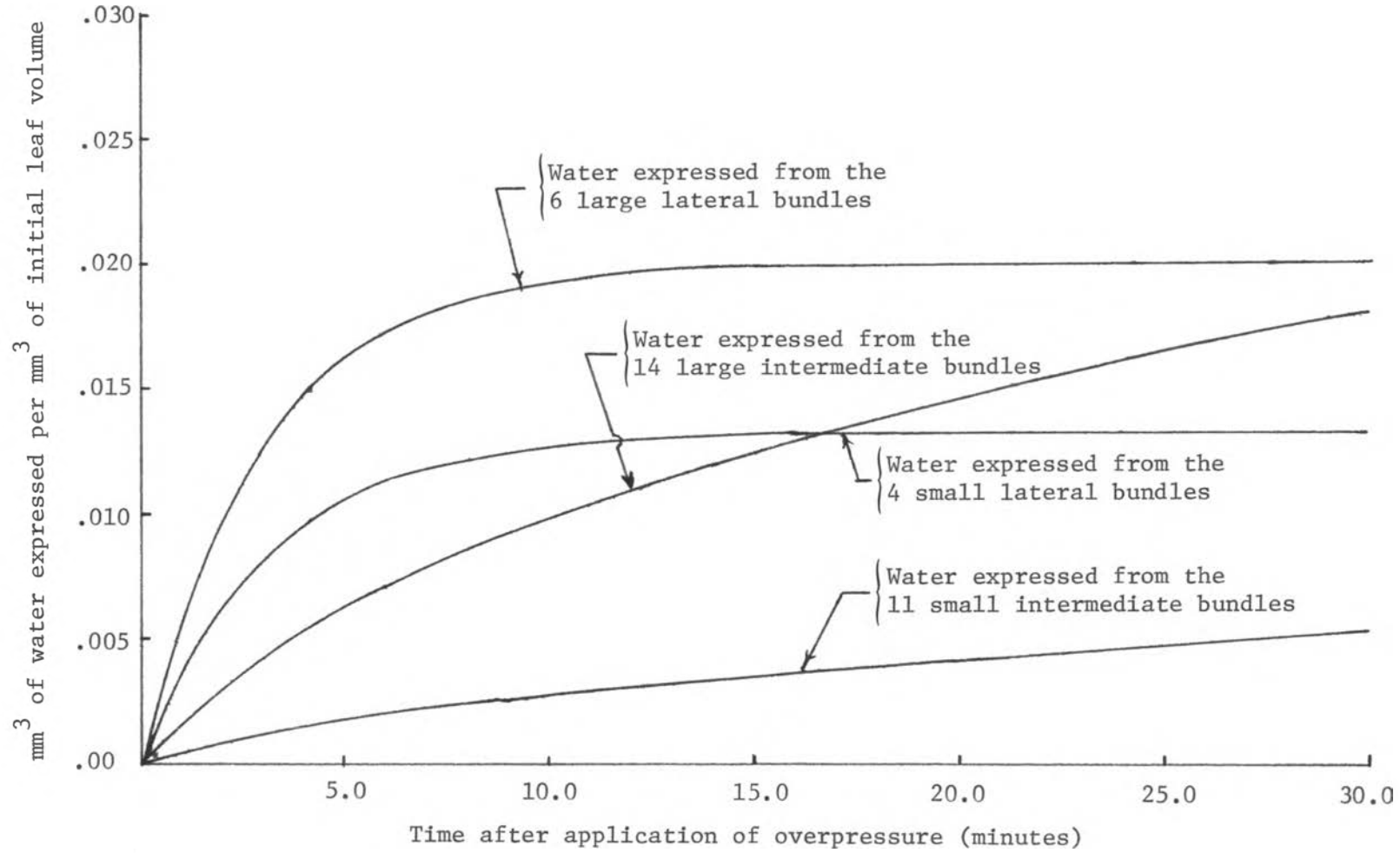

Figure 8.3. Efflux from various sized bundles as predicted by case 1 of the model of water flow through xylem and tissue.

the laterals. This changed the values of k_o and k_1 to the values listed on the bottom line of table 8.3.

Model predictions of efflux from the wheat leaves for the two cases are shown in figure 8.4 along with data points from the efflux experiment. To find the total efflux for case 1, I summed the effluxes from each of the bundle types. The two models represent two extremes which appear to bracket the actual efflux curves. Water driven from the leaf encounters more resistance than that offered by water flow through lateral bundles. Yet the resistance of the intermediate bundles is so great that they could not support the flow rates required to allow all of the water to pass from the leaf in the required time.

There are two possible ways by which I could reconcile the models with the experimental data. First, I could increase the resistance of the cell membrane in case 2. I could justify this either by reasoning that my choice of a membrane permeability was too high or that the water passes through more than one membrane before it gets to the xylem. The latter is supported by the modeling of chapter 7 where I showed that efflux curves predicted by a model of one cell with a low membrane permeability (high resistance) are similar to those in which water passes through several membranes which have a higher permeability (low resistance). The efflux curve for the models in which water flowed through 2 or 3 cells fit experimental data reasonably well. Paradermal sections of wheat leaves such as the one in figure 5.3 show that water flowing through tissue by the vacuolar pathway would have to travel through no more than three membranes

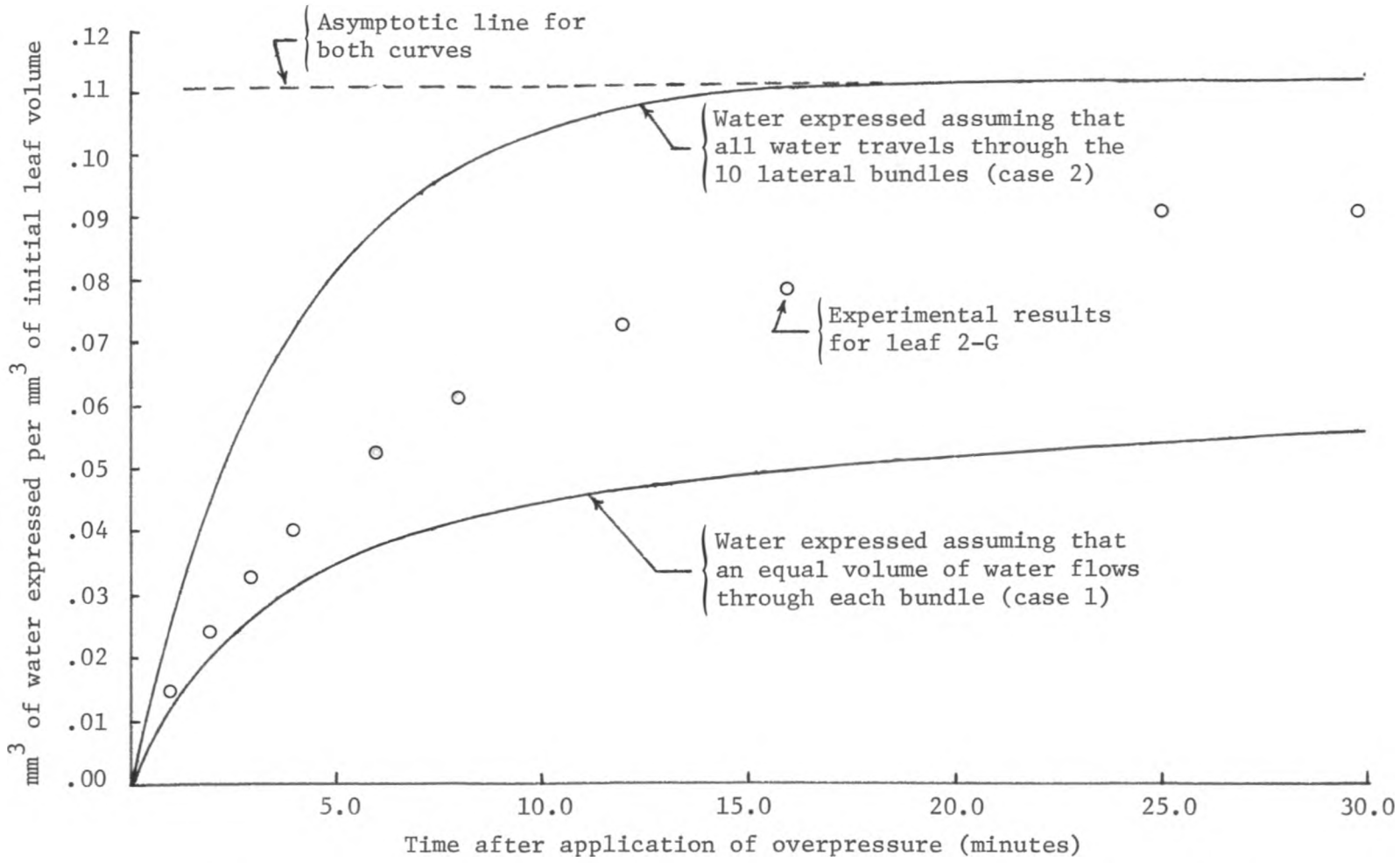

Figure 8.4. Efflux curves predicted by the model of water flow through xylem and tissue. Two cases are shown. In case 1 an equal amount of water flowed through each bundle. In case 2 water flowed through only the 10 lateral bundles. No water flowed through the intermediates. The o's are actual data points for leaf 2-G.

before it reaches xylem vessels. However, this model does not explain the effect of leaf length on efflux.

Secondly, I could reconcile the models with experimental data by assuming that water passes from the leaf through both lateral and intermediate bundles but that a larger proportion of the water flows through the lateral bundles. In such a case water could be transferred to the laterals from the intermediates through the transverse veins. Since the pressure in the laterals will decrease more rapidly than the pressure in the intermediates, the intermediates will be at a higher pressure at any given time after application of the overpressure. Therefore, there will be a gradient along the transverse veins and water will flow from the intermediates to the laterals.

I tested the two cases of the model for the effect of leaf length on efflux. I modeled leaf 2-G and a hypothetical leaf of one-half the length and one half the volume of leaf 2-G. The results for cases 1 and 2 are shown in figure 8.5. Decreasing leaf length changes the shape of the efflux curve predicted by case 1 more than it changes the curve for case 2. This suggests that the xylem resistance of the intermediate bundles and transverse veins can be responsible for at least part of the effect of leaf length on efflux.

To investigate the effect of linearizing equation 8.10, I used it to predict the total volume of water which would be expressed from the leaf. The amount of water expressed from a single cell when chamber pressure is increased from P_c^i to P_c^f can be estimated as follows. At steady state P equals zero. Equating the right hand side of equation 8.10 to zero and solving for V gives the cell volume at P_c^f.

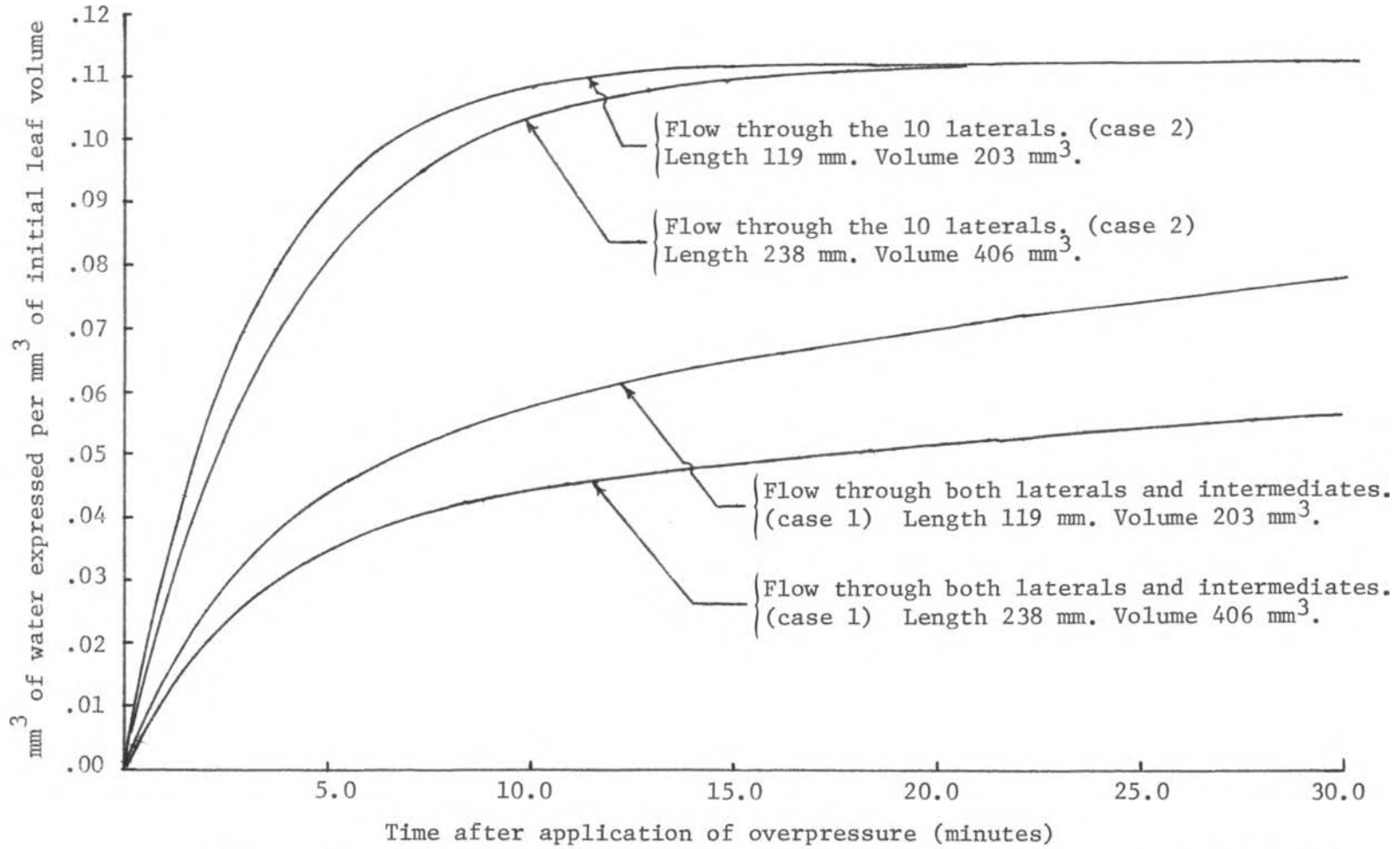

Figure 8.5. Efflux curves predicted by the model of water flow through tissue and xylem, showing the effect of leaf length on efflux for cases 1 and 2. Two solutions are shown for each case. One solution is for a leaf of the same length and volume as leaf 2-G. The second solution is for a leaf with half the length and half the volume of leaf 2-G.

The difference in cell volume when chamber pressures are P_c^i and P_c^f equals the volume of water expressed from the cells when the chamber pressure is increased from P_c^i to P_c^f. Multiplying this value by the number of cells in the leaf gives the total volume of water expressed. For the case solved in this chapter, P_c^i is 14.0 bars and P_c^f is 17.0 bars. The estimated volume of water expressed from the leaf is 0.0741 mm^3 of water per mm^3 of initial leaf volume. By contrast, the asymptotic value of efflux for case 2 is 0.1128 mm^3 of water per mm^3 initial leaf volume as shown by the dashed line in figure 8.4. Although the two curves have different asymptotic values, their shape is similar and therefore my conclusions would be unaffected.

Numerical solution of the non-linearized equations would remove much of the above error. It would also make possible additional modeling. In chapter 4, I described how a series of efflux curves can be obtained for the same leaf. At pressures above the zero turgor value, the total amount of water expressed during an efflux experiment will decrease as the initial balance pressure increases (see figures 4.4 and 4.5). The linearized equations predict that the same amount of water will be expressed regardless of the value of P_c^i. The non-linear equations predict that, as P_c^i increases, less water will be expressed. Therefore, the numerical solution could be used to investigate a series of efflux curves obtained on the same leaf. Finally, the numerical solution would be needed for a study of the time variation of efflux rate.

Equations 8.13 and 8.14 were solved for cases of zero turgor by assuming the cell modulus of elasticity was zero. This was equivalent

to assuming that cells do not develop negative turgor. I have discussed this assumption in section 7.3. The equations could be solved numerically or analytically for cases of non-zero turgor by using an appropriate value of modulus of elasticity and assuming it does not vary as cell volume changes. Results shown in figure 4.3 suggest that, until the turgor is nearly zero, the value of ε for wheat is approximately constant.

Since the shape of the efflux curve predicted by the model is quite close to the shape of the experimental curve, all of the significant resistances in the leaf may have been identified. However, the cell to cell flow model described in chapter 7 also adequately described the efflux curves but was unable to explain the effect of leaf length. Therefore, further experiments could reveal additional resistances.

8.5 Conclusions

The modeling suggests two conclusions. First, the large vascular bundles represent paths of low resistance through which water can travel rapidly through the leaf. The resistance of these bundles is relatively insignificant while the resistance of the intermediates is relatively large. This is one aspect of flow through leaves not apparent from experiments but brought out by this model and by the work of Dimond (1966) and Kuo, et al. (1972). Kuo, et al. (1972) noted the large difference in values of Σnr_i^4 for the lateral and intermediate bundles and suggested that the large vascular bundles are specialized for water transport while the small vascular bundles are

specialized for solute transport through their phloem. If, as Rawlins (1963), Hanson (1977), and Denmead and Millar (1976) suggest, there are water potential gradients along the length of transpiring leaves, such gradients would be more likely to develop in tissue isolated from the lateral bundles. Cross sections of wheat leaves show that there are typically two or three intermediate bundles between lateral bundles. If the transverse veins offer a high resistance to water flow, they could isolate the lateral bundles from the intermediates. If water flow rates through the lateral bundles fluctuate with time because of changes in transpiration rates, the water potentials in the intermediate and lateral bundles may not have time to equalize and gradients along the intermediate bundles may differ from gradients along the intermediates. Preliminary calculations showed that water flow rates during transpiration can be higher than rates during pressure chamber efflux experiments. Under such conditions, the xylem resistance could become even more important and gradients could develop in the lateral bundles.

The results of this model are consistent with the theory of Meidner (1975) that water in the transpiration stream travels from veins through sclerenchyma cells to the epidermis. However, they do not necessarily confirm his theory. The lateral bundles represent paths for water movement through the leaf which have resistances several orders of magnitude smaller than the resistances for flow through intermediate bundles. The schlerenchyma of the lateral bundles extend from the bundles to the epidermis. If the sclerenchyma cells have a low resistance to water flow, then water would readily

flow from stem to epidermis through the lateral bundles and sclerenchyma.

A second conclusion is suggested by the model. The effect of leaf length on water efflux can be at least partially explained by the resistance of the intermediate bundles. A more extensive study of differences in the vascular system of long versus short leaves would be needed to substantiate this conclusion. However, the variation in values of Σnr_i^4 between lateral and intermediate bundles was larger than variations in Σnr_i^4 between leaves for a given bundle type. Therefore, it is unlikely that the variations in Σnr_i^4 for leaves of varying length are great enough to affect the conclusions drawn from the model.

There are several practical implications of this study. When the pressure chamber is used on plants which have networks of fine veins, the overpressure must be applied for longer time periods if all the water is to be expressed. Longer time periods are needed for longer (and perhaps also for larger) leaves. In the case of wheat, I needed up to 40 minutes to express all of the water when a three bar overpressure was applied. All of the water was forced from leaf 1-F in 10 minutes (see figure 4.10), but it took up to 40 minutes to force water from leaf 2-E. Doubling the leaf length increased the efflux time by a factor of 4.

The usual procedure used in running pressure^{-1}-volume tests is to apply an overpressure for several minutes and then to return the chamber pressure to its initial value. If this procedure is followed, water may be expressed from cells around the large vascular bundles

before it is expressed from cells near small vascular bundles. Therefore, upon removal of the overpressure the leaf cells may not be in equilibrium. If another overpressure is applied immediately without allowing time for equilibration of water potential between cells in the leaf, then an error may be introduced into the next water potential determination. From the standpoint of attaining equilibrium among leaf cells, the most desirable method of running overpressure tests would be to apply the overpressure and to allow all of the water to be forced from the leaf.

CHAPTER 9

SUMMARY OF CONCLUSIONS AND RECOMMENDATIONS FOR FUTURE RESEARCH

The following is a summary of the conclusions I have drawn from the experiments and modeling described in this thesis. I have numbered each conclusion and referenced appropriate chapters for each. The section entitled recommendations for future research is a summary of work which could extend the usefulness of the models and further explain efflux of water from leaves placed in the pressure chamber.

9.1 Conclusions

1. If an overpressure is applied to an excised wheat leaf in a pressure chamber, there is a measurable flow of water from the cut end. The time interval during which this flow occurs increases with leaf length (see chapter 4, figure 4.10). For example, in the experiments described in chapter 4, all of the water was forced from leaf 1-F in 10 minutes, but it took up to 40 minutes to express all of the water from leaf 2-E. Increasing the leaf length 1.9 times increased the efflux time by a factor of 4.

2. Leaf mesophyll cells which are inside the chamber do not appear to rupture during pressure^{-1}-volume tests, even when the leaf is subjected to pressures up to 35 bars. However, the relative volume of

airspace in the leaf decreases. The vessel elements do not appear to be permanently deformed (see section 5.4).

3. During a pressure chamber experiment, the epidermal and mesophyll cells in the portion of the leaf in contact with the chamber seal are distorted and disrupted. However, the vessel elements in the vicinity of the chamber seal appear undamaged (see section 5.4.)

4. The efflux of water from a wheat leaf in a pressure chamber can be modeled by assuming water flows from cell vacuole to cell vacuole through the adjacent portions of the membranes of contiguous cells (see section 7.5). This model ignores xylem resistance. It is unable to explain why gradients have been measured along the length of transpiring leaves and it cannot explain the effect of leaf length on efflux described in conclusion number one.

5. The model presented in chapter 8 describes water flow through both tissue and xylem. The results of this model suggest that the resistance to water flow through the intermediate bundles in a leaf is sufficient to limit the rate of efflux of water from a leaf (see sections 8.4 and 8.5). The resistance of the lateral bundles is not sufficient to affect the efflux rate.

6. The model of water flow in tissue and xylem predicts that the resistance to water flow through intermediate bundles is high enough

to at least partially explain the effect of leaf length on efflux described in conclusion number one.

7. Conclusions 5 and 6 have the following implications for the procedures used in pressure chamber experiments.

(a) When a given increment in chamber pressure is applied, the cells in short leaves will reach equilibrium more rapidly than the cells in long leaves.

(b) During most pressure chamber experiments, the chamber pressure is increased for several minutes and then reduced. In many cases, at the time the pressure is reduced, water is still flowing from the cut end of the leaf and the cells may not be in equilibrium. The model in chapter 8 suggests that, at the time when pressure is reduced, the leaf cells may not be in equilibrium. Therefore, the procedure may introduce an experimental error.

9.2 Recommendations for Future Research

1. Results in section 4.3 (figure 4.3) suggest that the relationship between the turgor component of potential and cell volume should be linear. However, the relationship should be placed in equation form so that it can be used in the model of water flow through leaf tissue presented in chapter 7 and the model of water flow through tissue and xylem presented in chapter 8. If the cells were modeled as hollow spheres or cylinders made of a homogeneous, isotropic material, then the relationship between the pressure of the cell contents and the volume of the cell could be investigated using the theory of

elasticity. Cooke, et al. (1976) applied the finite element method in their studies of guard cell deformation. The same method could be used for irregularly shaped cells.

2. Numerical solution of equations 8.5 and 8.10 would enable the following additional investigations.

(a) The effect of initial balance pressure on the efflux of water from the leaf could be studied (see section 8.4). When a given overpressure is applied at a beginning balance pressure near the point on the pressure^{-1}-volume curve where turgor first becomes zero, relatively large amounts of water will be expressed. The same overpressure at a higher beginning balance pressure will express a smaller amount of water. The non-linear equations (equations 8.5 and 8.10) predict this type of behavior. The linearized equations (equations 8.11 and 8.12) do not. Therefore, the numerical solution is needed to explore this type of behavior.

(b) Figures 4.6 through 4.9 are graphs of the natural logarithm of efflux rate as a function of time. All but the first several data points appear to fall on a straight line. In other words, the efflux rate is not log-linear during the first portion of the efflux experiment. When Tyree and Dainty (1973) studied this type of behavior,they devloped a method of continuously measuring efflux rate. If their method could be adapted to wheat leaves, the efflux rates could be measured more accurately and the investigation described in section 4.4 could be extended. Some preliminary work with the model in chapter 8 suggested that the xylem resistance may cause the efflux

rate to deviate from the log-linear behavior. If equations 8.5 and 8.10 were solved numerically, the model could also be used to study the time variation of efflux rate.

3. A more extensive study of the vascular system in long and short leaves might reveal whether differences in anatomy are responsible for the effects of leaf length on efflux time described in conclusion number one.

4. A 3 bar overpressure was used in all of the efflux experiments reported in this thesis. If varying overpressures were used, additional insight into the efflux of water might be gained. When smaller overpressures are used and when the beginning balance pressure is near the point on the pressure^{-1}-volume curve where turgor first becomes zero, the error caused by linearizing equations 8.5 and 8.10 is minimal. In such cases, the analytical solution could be used to investigate the effect of overpressure on efflux. For larger overpressures and beginning balance pressures greater than the zero turgor balance pressure, the numerical solution of the equations would have to be used.

5. Dr. Betty Klepper suggested that the effect of leaf length could be investigated experimentally by taking a long leaf and cutting off a portion near the base. If there are no significant anatomical differences between long and short leaves, then when the long leaves are shortened, they should behave like short leaves.

6. The model of water flow through tissue and xylem described in chapter 8 suggested that the leaf cells will not be in equilibrium if the overpressure is applied for short time intervals and then released. This is a procedure often used in pressure chamber experiments (Cutler, et al., 1980). If the resistance to water flow through the transverse veins and xylem prevents the cells from attaining equilibrium during this time period, then the results of the pressure^{-1}-volume tests could be in error. Pressure^{-1}-volume tests could be conducted on leaves with nearly identical physiological and anatomical characteristics to determine whether the shape of the curve is affected by releasing the overpressure before water stops flowing from the leaf.

7. This study could be extended to other types of leaves. Preliminary experiments with soybean leaves showed that, for a 3 bar overpressure, the time required to force water from a soybean leaf is several times greater than the time required to force water from a wheat leaf. Tanton and Crowdy (1972b) noted that it took longer for chelate to reach the epidermis of bean leaves than the epidermis of wheat leaves. Apparently there is a greater resistance to water movement in the bean leaf. This resistance may be the result of anatomical features. All of the water passing out of the leaf must pass through the vascular bundles in the petiole. If flow rates through these bundles are high, they may offer enough resistance to water flow to limit efflux from the leaf. A study of the dimensions of the vascular bundles in the petiole and leaf would help to identify the significant resistances to

water flow and might reveal which are great enough to affect the efflux of water from the leaf.

8. The rate of water flow through the leaf during transpiration may be as great as or greater than the rate of water flow during a pressure chamber efflux experiment. If there is sufficient resistance to water flow through the xylem to affect the efflux of water during a pressure chamber experiment, there will also be sufficient resistance to affect the water potential distribution along a transpiring leaf. The model presented in chapter 8 could be adapted to modeling transpiration and used to predict whether gradients would develop in transpiring leaves.

REFERENCES

Aifantis, Ellas C. 1977. Mathematical modeling for water flow in plants. pp 1083-1090. In: Xavier Avula (ed.), Proceedings of the First International Conference on Mathematical Modeling, Volume II. University of Missouri, Rolla, Missouri.

Akyurt, M., G. L. Zachariah, and C. G. Haugh. 1972. Constitutive relations for plant materials. Transactions of the American Society of Agricultural Engineers 15:766-769.

Armacost, Richard R. 1944. The structure and function of the border parenchyma and vein-ribs of certain dicotyledon leaves. Proceedings of the Iowa Academy of Science 51:157-169.

Baumeister, T.,(ed.).1967. Standard Handbook for Mechanical Engineers, Seventh Edition. McGraw-Hill Book Company, New York. 2456 p.

Bird, R.B., Warren E. Stewart, and Edwin N. Lightfoot. 1960. Transport Phenomena. John Wiley and Sons, Inc., New York. 780 p.

Block, H.D., E.T. Cranch, P.J. Hilton, and R.J. Walker. 1965. Engineering Mathematics, Volume II. Cornell University, Ithaca, New York.

Boyer, J.S. 1969. Free energy transfer in plants. Science 163:1219-1220.

Boyer, J.S. 1971. Resistances to water transport in soybean, bean, and sunflower. Crop Science 11:403-407.

Boyer, J.S. 1972. Reply to comments on paper entitled "Resistance to water transport in soybean, bean, and sunflower." Crop Science 12:401.

Campbell, G.S. and Melvin D. Campbell. 1974. Evaluation of thermocouple hygrometer for measuring leaf water potential in situ. Agronomy Journal 66:24-27.

Chabot, Brian F. and Jean Fincher Chabot. 1977. Effects of light and temperature on leaf anatomy and photosynthesis in Fragaria vesca. Oecologia (Berl.) 26:363-377.

Chabot, Brian F., Thomas W. Jurick, and Jean F. Chabot. 1979. Influence of instantaneous and integrated light-flux density on leaf anatomy and photosynthesis. American Journal of Botany 66:940-945.

Cheung, Y. N. S., M. T. Tyree, and J. Dainty. 1976. Some possible sources of error in determining bulk elastic modulus and other parameters from pressure-volume curves of shoots and leaves. Canadian Journal of Botany 54:758-765.

Clark, R.N. and E.A. Hiler. 1973. Plant measurements as indicators of crop water deficit. Crop Science 13:466-469.

Cooke, J.R., Josse G. DeBaerdemaeker, Richard H. Rand, and Herbert A. Mang. 1976. A finite element shell analysis of guard cell deformation. Transactions of the American Society of Agricultural Engineers 19:1107-1121.

Crowdy, S.H. and T.W. Tanton. 1970. Water pathways in higher plants. I. free space in wheat leaves. Journal of Experimental Botany 21:102-111.

Cutler, J. M., K.W. Shahan, and P.L. Steponkus. 1979. Characterization of the internal water relations of rice by a pressure-volume method. Crop Science 19:681-685.

Cutler, J.M., K.W. Shahn, and P.L. Steponkus. 1980. Dynamics of osmotic adjustment in rice. Crop Science 72:(in press, May-June issue).

Dawes, D.J. 1971. Biological Techniques in Electron Microscopy. Barnes and Noble, New York, 193 p.

DeBaerdemacker, J. G., L. J. Segerlind, H. Murase, and G. E. Merva. 1978. Water potential effect on tensile and compressive failure stresses of apple and potato tissue. ASAE paper 78-3057. American Society of Agricultural Engineers, St. Joseph, Michigan.

Dengler, N.G. and L.B. MacKay. 1975. The leaf anatomy of beech, Fagus grandifolia. Canadian Journal of Botany 53:2202-2211.

Denmead, O.T. and B.D. Millar. 1976. Water transport in wheat plants in the field. Agronomy Journal 68:297-311.

Dimond, A.E. 1966. Pressure and flow relations in vascular bundles of the tomato plant. Plant Physiology 41:119-131.

Dixon, H.H. 1914. Transpiration and the ascent of sap in plants. Macmillan, London. 216 p.

Esau, Katherine. 1977. Anatomy of Seed Plants, 2nd Edition. John Wiley and Sons, New York. 550 p.

Ferrier, J.M., and J. Dainty. 1977.A new method for measurement of hydraulic conductivity and elastic coefficients in higher plant cells using an external force. Canadian Journal of Botany 55:858-866.

Frank, A.B. and D.G. Harris. 1973. Measurement of leaf water potential in wheat with a pressure chamber. Agronomy Journal 65:334-335.

Gustafson, R. J., G. E. Mase, and L. J. Segerlind. 1977. Continuum theory for gas-solid-liquid media. I. Theory development. Transactions of the American Society of Agricultural Engineers 20:1186-1189.

Gustafson, R. J, and L. J. Segerlind. 1977. Continuum theory for gas-solid-liquid media. II. Modeling by use of the finite element method. Transactions of the American Society of Agricultural Engineers 20:1190-1193,1200.

Hammel, H. T. 1967. Freezing of xylem sap without cavitation. Plant Physiology. 42:55-66.

Hammel, H.T. , and P.F. Scholander. 1976. Osmosis and tensile solvent. Springer-Verlag, New York. 133 p.

Hanson, Andrew D., Charles E. Nelson, and Everett H. Everson. 1977. Evaluation of free proline accumulation as an index of drought resistance using two contrasting barley cultivars. Crop Science 17:720-726.

Helkvist,J.,C.P. Richards and P.G. Jarvis. 1974. Vertical gradients of water potential and tissue water relations in sitka spruce trees measured with the pressure chamber. Journal of Applied Ecology 11:637-667.

Hiler, E.A., C.H.M. Van Bavel, M.M. Hossain, and W.R. Jordan. 1972. Sensitivity of southern peas to plant water deficit at three growth stages. Agronomy Journal. 64:60-64.

Husken, D., Ernst Steudle, and Ulrich Zimmermann. 1978. Pressure probe technique for measuring water relations of cells in higher plants. Plant Physiology 61:158-163.

Kuo, J. and T.P. O'Brien. 1974. Lignified sieve elements in the wheat leaf. Planta(Berlin) 117:349-353.

Kuo, J., T.P. O'Brien, and M.J. Canny. 1974. Pit field distribution, plasmodesmatal frequency, and assimilate flux in the mestome sheath cells of wheat leaves. Planta (Berlin) 121:97-118.

Kuo, J., T.P. O'Brien, and S.-Y. Zee. 1972. The transverse veins of the wheat leaf. Australian Journal of Biological Science 25:721-37.

Lawlor, D.W. 1972. An automatic multichannel thermocouple psychrometer based on an operational amplifier. Journal of Applied Ecology 9:581-588.

Meidner, H. 1975. Water supply, evaporation, and vapour diffusion in leaves. Journal of Experimental Botany 26:666-673.

Molz, F.J. 1972. Comments on the paper entitled "Resistance to water transport in soybean, bean, and sunflower." Crop Science 12:400-401.

Molz, F.J. 1975a. Comments on "Water transport through plant cells and cell walls: theoretical development." Soil Science Society of America Proceedings 39:597.

Molz, F.J. 1975b. Potential distributions in the soil-root system. Agronomy Journal 67:726-728.

Molz, F.J. 1976a. Water transport in the soil-root system: transient analysis. Water Resources Research 12:805-808.

Molz, F.J. 1976b. Water transport through plant tissue: the apoplasm and symplasm pathways. Journal of Theoretical Biology 59:277-292.

Molz, F.J., and J.S. Boyer. 1978. Growth-induced water potentials in plant cells and tissues. Plant Physiology 62:423-429.

Molz, F. J. and George M. Hornberger. 1973. Water transport through plant tissues in the presence of a diffusible solute. Soil Science Society of America Proceedings 37:833-837.

Molz, F.J. and Ernest Ikenberry. 1974. Water transport through plant cells and cell walls:theoretical development. Soil Science Society of American Proceedings 38:699-704.

Molz, F.J., and B. Klepper. 1972. Radial propogation of water potential in stems. Agronomy Journal 64:469-473.

Molz, F.J. and B. Klepper. 1973. On the mechanism of water-stress-induced stem deformation. Agronomy Journal 65:304-306.

Molz, F.J., B. Klepper, and V.D. Browning. 1973. Radial diffusion of free energy in stem phloem: an experimental study. Agronomy Journal 65:219-222.

Molz, F.J., Betty Klepper, and Curt M. Peterson. 1973. Rehydration versus growth-induced water uptake in plant tissue. Plant Physiology 51:859-862.

Molz, F.J., Bryan Truelove, and Curt M. Peterson. 1975. Dynamics of rehydration in leaf disks. Agronomy Journal 67:511-515.

Murase,H., and George Merva. 1977a. Constitutive equations for vegetative media. ASAE paper 77-5513. American Society of Agricultural Engineers, St. Joseph, Michigan.

Murase, H., and G. E. Merva. 1977b. Static elastic modulus of tomato epidermis as affected by water potential. Transactions of the American Society of Agricultural Engineers 20:594-597.

Murase, H. and G. Merva. 1979. Hydraulic Conductivity of vegetative tissue. Transactions of the American Society of Agricultural Engineers 22:877-880.

Nobel, Park S. 1974. Introduction to Biophysical Plant Physiology. W. H. Freeman and Company, San Francisco. 488 p.

O'Brien, T.P. and D.J. Carr. 1970. A suberized layer in the cell walls of the bundle sheath of grasses. Australian Journal of Biological Science 23:275-287.

O'Brien, T.P. and J. Kuo. 1975. Development of a suberized lamella in the mestome sheath of wheat leaves. Australian Journal of Botany 23:783-794.

Palta, J.P. and E.J. Stadelmann. 1977. Effect of turgor pressure on water permeability of Allium cepa epidermis cell membranes. Journal of Membrane Biology 33:231-247.

Parthasurathy, M.V., and Larry H. Klotz. 1976. Palm wood. II. Ultrastructural aspects of sieve elements, tracheary elements and fibers. Wood Science and Technology 10:247-271.

Patrick, J.W. 1972. Vascular system of the stem of the wheat plant. I. mature state. Australian Journal of Botany 20:49-63.

Percival, John. 1921. The wheat plant, a Monograph, Duckworth and Company, London, 463 p.

Philip, J.R. 1958a. The osmotic cell, solute diffusibility, and the plant water economy. Plant Physiology 33:264-271.

Philip, J.R. 1958b. Propogation of turgor and other properties through cell aggregates. Plant Physiology 33:271-274.

Philip, J.R. 1958c. Osmosis and diffusion in tissue: half-times and internal gradients. Plant Physiology 33:275-278.

Philip, J.R. 1958d. Correction to the paper entitled "Osmosis and diffusion in tissue:half-times and internal gradients." Plant Physiology 33:443.

Philip, J.R. 1966. Plant water relations: some physical aspects. Annual Review of Plant Physiology 17:245-268.

Rand, R.H. 1978. A theoretical analysis of carbon dioxide absorption in sun versus shade leaves. Journal of Biomechanical Engineering, Transactions of ASME 100:20-24.

Raven, J.A. 1977. The evolution of vascular land plants in relation to supracellular transport processes. In: H.W. Woolhouse (ed.), Advaces in Botanical Research, Volume 5. Academic Press, New York. p 153-219.

Rawlins, Stephen L. 1963. Resistance to water flow in the transpiration stream. In: Israel Zelitch (ed.), Stomata and Water Relations in Plants, Connecticut Agricultural Experiment Station Bulletin 664. The Connecticut Agricultural Experiment Station, New Haven, Connecticut.

Ritchie, G.A. and Thomas M. Hinkley. 1975. The pressure chamber as an instrument for ecological research. In: A. MacFayden (ed.), Advances in Ecological Research, Volume 9. Academic Press, New York, p 165-254.

Scholander, P.F., H.T. Hammel, Edda Bradstreet, and E.A. Hemmingson. 1965. Sap pressure in vascular plants. Science 148:339-346.

Scholander, P.F., H.T. Hammel, E.A. Hemmingsen, and E.D. Bradstreet. 1964. Hydrostatic and osmotic potentials in leaves of mangroves and some other plants. Proceedings of the National Academy of Science 52:119-125.

Shahan, Kevin W. 1980. Facultative Drought-induced Alternations of Internal Water Relations in Rice. (Oryza sativa L.). Unpublished M.S. Thesis, Cornell University, January, 1980.

Sheriff, D.W. and H. Meidner. 1974. Water pathways in leaves of Hedera helix L. and Tradescantia virginiana L. Journal of Experimental Botany 25:1147-56.

Slatyer, R.O. 1967. Plant Water Relationships. Academic Press, New York 366 p.

Splinter, W. 1979. Energy and the center pivot. Address at the 1979 SAE Winter meeting in Milwakee, Wisconsin. Quoted in: Irrigation Journal. 29(5):42.

Stegman, E.C., L.H. Schiele, and A. Bauer. 1976. Plant water stress criteria for irrigation scheduling. Transactions of the American Society of Agricultural Engineers 19:850-855.

Steudle, E., U. Zimmermann, and U. Luttge. 1977. Effect of turgor pressure and cell size on the wall elasticity of plant cells. Plant Physiology 59:285-289.

Tanton, T.W. and S.H. Crowdy. 1972a. Water pathways in higher plants. II. Water pathways in roots. Journal of Experimental Botany 23:600-618.

Tanton, T.W. and S.H. Crowdy. 1972b. Water pathways in higher plants:III. The transpiration stream within leaves. Journal of Experimental Botany 23:619-625.

Timoshenko, S.P., and J.N. Goodier. 1970. Theory of Elasticity, Third Edition. McGraw-Hill Book Company, New York. 567 p.

Tyree, M.T. 1969. The thermodynamics of short-distance translocation in plants. Journal of Experimental Botany 20:341-349.

Tyree, M.T. 1976. Negative turgor pressure in plant cells: fact or fallacy? Canadian Journal of Botany. 54:2738-2746.

Tyree, M.T., M. Benis, and J. Dainty. 1973. The water relations of hemlock (Tsuga canadensis). III. The temperature dependence of water exchange in a pressure bomb. Canadian Journal of Botany 51:1537-1543.

Tyree, M. T., C. Caldwell, and J. Dainty. 1975. The water relations of hemlock (Tsuga canadensis). V. The localization of resistances to bulk water flow. Canadian Journal of Botany 53:1078-1084.

Tyree, M.T. and Y.N.S. Cheung. 1977. Resistance to water flow in Fagus grandifolia leaves. Canadian Journal of Botany 55:2591-2599.

Tyree, M.T. and J. Dainty. 1973. The water relations of hemlock (Tsuga canadensis). II. The kinetics of water exchange between the symplast and apoplast. Canadian Journal of Botany 51:1481-1489.

Tyree, M. T., J. Dainty, and M. Benis. 1973. The water relations of hemlock (Tsuga canadensis). I. Some equilibrium water relations as measured by the pressure bomb technique. Canadian Journal of Botany 51:1471-1480.

Tyree, M. T. J. Dainty, and D. M. Hunter. 1974. The water relations of hemlock (Tsuga canadensis). IV. The dependence of balance pressure on temperature as measured by the pressure bomb technique. Canadian Journal of Botany 52:973-978.

Tyree, M.T. and H.T. Hammel. 1972. The measurement of the turgor pressure and the water relations of plants by the pressure bomb technique. Journal of Experimental Botany 23:267-282.

U.S. Bureau of the Census. 1978. Table no. 346. Estimated daily water use: 1940 to 1975 and projections to 2000. Statistical Abstract of the United States, 1978.(99th edition). Washington, D.C.

Weatherly, P.E. 1963. The pathway of water movement across the root cortex and leaf mesophyll of transpiring plants. In: A.J. Rutter (ed.) Symposium of the British Ecological Society , John Wiley and Sons, New York.

Weatherly, P.E. 1965. The state and movement of water in the leaf. Symposia of the Society for Experimental Biology 19:157-184.

Wenkert, W., E.R. Lemon, and T.R. Sinclair. 1978. Changes in water potential during pressure bomb measurement. Agronomy Journal 70:353-355.

Wiebe, Herman H. and Rex J. Prosser. 1977. Influence of temperature gradients on leaf water potential. Plant Physiology 59:256-258.

Wiebel, Ewald R. 1969. Stereological principles for morphometry in electron microscope cytology. International Review of Cytology. 26:235-302.

Zimmermann, U., and E. Steudle. 1978. Physical aspects of water relations of plant cells. In: H.W. Woolhouse (ed.) Advances in Botanical Research, Vol 6 , Academic Press, New York.

Appendix A

Pressure^{-1}-volume Data

for

Wheat Leaves

Table A.1 Data For Pressure^{-1}-Volume Curves.* Tests were conducted on 3/13/79 on leaves from wheat plant #16. See table B.4 for the data from efflux experiments conducted on this leaf.

Leaf *	Balance Pressure ψ (bars)	Reciprocal of Balance Pressure $\frac{1}{\psi}$ (bars^{-1})	Cumulative Volume of Water Expressed at the Balance Pressure V_e (mm^3)
1-16	2.8	.357	0.0
	6.4	.156	9.0
	10.8	.0926	29.8
	14.0	.0714	84.3
	14.8	.0676	92.2
	17.8	.0562	122.8
	18.7	.0535	124.4
	21.6	.0463	141.1
2-16	3.2	.312	0.0
	8.8	.114	10.5
	10.2	.0980	12.6
	10.8	.0926	15.9
	11.0	.0909	21.4
	11.5	.0870	28.4
	12.0	.0833	33.7
	12.6	.0794	38.7
	13.2	.0758	43.4
	13.7	.0730	48.5

*The identification system used for the leaves is as follows. The first number indicates the number of the test such as the first or the second. The second number indicates the plant from which the leaf was taken. For example, leaf 1-16 was the first leaf tested from wheat plant #16.

Table A.2 Data For Pressure^{-1}-Volume Curves.† Tests were conducted between 7/27/79 - 8/2/79. See table B.5 and B.7 - B.10 for the data from efflux experiments on leaves 1-D, 2-E, 1-F, 2-G, and 3-G. No efflux experiments were performed on the other leaves.

Leaf†	Balance Pressure ψ (bars)	Reciprocal of Balance Pressure $\frac{1}{\psi}$ (bars^{-1})	Cumulative Volume of Water Expressed at the Balance Pressure V_e (mm^3)
1-C	5.8	.172	0.0
	9.4	.106	0.0
	12.0	.0833	1.5
	13.8	.0725	7.0
	14.8	.0676	18.5
	15.7	.0637	30.6
1-D	7.2	.139	0.0
	13.3	.0752	4.6
	18.2	.0549	28.1
	24.2	.0413	44.7
2-E	3.4	.294	0.0
	7.2	.139	1.4
	10.4	.0962	7.0
	13.2	.0758	41.9
	16.4	.0610	112.7
	19.6	.0510	171.2
	22.6	.0442	211.3
1-F	6.2	.161	0.0
	12.2	.0820	0.2
	15.8	.0633	7.9
	19.3	.0518	21.7
	22.5	.0444	24.4
	25.6	.0391	26.9

(continued)

Table A.2 continued

Leaf†	Balance Pressure ψ (bars)	Reciprocal of Balance Pressure $\frac{1}{\psi}$ ($bars^{-1}$)	Cumulative Volume of Water Expressed at the Balance Pressure V_e (mm^3)
2-F	3.4	.294	0.0
	5.5	.182	1.2
	8.0	.125	4.4
	10.7	.0935	7.7
	12.2	.0820	12.1
	13.3	.0752	18.7
	14.2	.0704	27.9
	15.2	.0658	39.0
	16.2	.0617	46.9
	17.4	.0575	54.0
	18.5	.0541	61.0
	20.2	.0495	65.8
	23.2	.0431	70.2
	25.2	.0397	71.1
	28.2	.0355	71.8
1-G	3.7	.270	0.0
	6.5	.154	3.1
	9.6	.104	5.2
	11.6	.0862	11.9
	12.8	.0781	24.8
	13.8	.0725	37.6
	14.7	.0680	51.9
	15.7	.0637	65.8
	16.8	.0595	78.8
	17.8	.0562	90.5
	18.8	.0532	99.8
	19.9	.0503	109.5
	21.0	.0476	117.6
	22.0	.0455	123.4
	23.3	.0429	131.7
	24.6	.0406	140.0
	25.8	.0388	146.8
	27.2	.0368	152.8
	28.8	.0347	159.2
	30.7	.0326	163.8
	32.2	.0311	168.2
	34.0	.0294	171.6

(continued)

Table A.2 concluded

Leaf†	Balance Pressure ψ (bars)	Reciprocal of Balance Pressure $\frac{1}{\psi}$ ($bars^{-1}$)	Cumulative Volume of Water Expressed at the Balance Pressure V_e (mm^3)
2-G	3.6	.278	0.0
	6.5	.154	2.9
	9.4	.106	5.8
	11.8	.0847	9.6
	13.0	.0769	13.8
	14.0	.0714	22.7
	17.5	.0571	59.7
	20.5	.0488	73.5
	23.3	.0429	83.0
	26.0	.0385	88.7
	27.9	.0358	94.5
	30.1	.0332	96.6
3-G	3.5	.286	0.0
	7.1	.141	0.8
	10.6	.0943	1.6
	12.8	.0781	5.8
	14.3	.0699	11.0*
	17.2	.0582	34.7
	20.3	.0493	50.8
	23.4	.0427	64.3
	25.7	.0389	72.0
	27.8	.0360	77.8
	29.7	.0337	82.4

†The identification system used for the leaves is as follows. The number indicates the number of the test such as the first or the second. The letter indicates the day on which the test was conducted. For example, leaf 1-C was the first leaf tested on 7/27/79. Test dates for all leaves are given in table 4.1.

*A vial was used twice but only weighed after the second time. Therefore, this point was estimated from the regression line fit to the next 5 points.

Table A.3 Data for Pressure^{-1}-Volume Curves.* Tests were conducted between 8/20/79 and 8/21/79. See tables B.11 - B.13 for data from efflux experiments conducted on this leaf.

Leaf*	Balance Pressure Ψ (bars)	Reciprocal of Balance Pressure $\frac{1}{\Psi}$ (bars^{-1})	Cumulative Volume of Water Expressed at the Balance Pressure V_e (mm^3)
1-H	3.4	.294	0.0
	6.4	.156	2.5
	9.0	.111	5.7
	10.0	.0943	7.9
	11.5	.0870	21.9
	14.5	.0690	39.0
	12.6	.0568	43.1
2-H	3.8	.2631	0.0
	7.2	.138	0.0
	9.6	.104	1.7
	11.1	.0901	8.1
	13.7	.0730	22.5
	16.2	.0617	32.5
	17.2	.0581	32.1
	18.0	.0556	34.6
	18.7	.0535	36.0
	19.5	.0513	38.1
	20.6	.0485	40.3
	21.5	.0465	40.8
	22.8	.0439	42.5
	24.7	.0405	43.6
	26.0	.0385	44.7
	27.5	.0364	45.8
	28.8	.0347	46.4
	29.5	.0339	47.6
	30.5	.0328	48.3

(continued)

Table A.3. Continued.

Leaf*	Balance Pressure Ψ (bars)	Reciprocal of Balance Pressure $\frac{1}{\Psi}$ ($bars^{-1}$)	Cummulative Volume of Water Expressed at the Balance Pressure V_e (mm^3)
1-I	2.8	.357	0.0
	5.8	.172	2.8
	8.8	.114	6.4
	10.6	.0943	12.7
	13.6	.0735	24.5
	16.8	.0595	52.9
	18.5	.0541	56.2
	20.0	.0478	63.8
	22.2	.0450	65.9
	23.8	.0420	67.1
	26.2	.0382	69.3
	28.5	.0351	70.1

*The identification system used for the leaves is as follows. The first number indicates the number of the test such as the first or the second. The letter indicates the day on which the test was conducted. For example, leaf 1-H was the first leaf tested on 8/20/79. Test dates for all leaves are given in table 4.1.

Appendix B

Efflux Data

for

Wheat Leaves

Table B.1 The Efflux of Water from a Leaf Taken from Wheat Plant Number 1. The leaf was pressurized in a pressure chamber with a 3.0 bar overpressure. The test was conducted on 3/8/79. The plant was under water stress. No pressure^{-1}-volume experiment was conducted on this plant.

Elapsed Time After Application of a 3 bar Overpressure (min)	Cumulative Water Expressed at Various Initial Balance Pressures (mm^3)		
	With an Initial Balance Pressure of 2.6 bars	With an Initial Balance Pressure of 11.0 bars	With an Initial Balance Pressure of 16.2 bars
0.0	0.0	0.0	0.0
0.5	1.6	3.2	3.0
1.0	2.4	5.7	5.4
1.5	3.2	7.8	7.7
2.0	3.7	10.6	11.9
2.5	3.7	-	-
3.0	-	14.7	15.4
4.0	3.9	18.5	18.4
5.0	-	22.0	22.2
7.0	-	27.1	25.6
10.0	-	34.1	28.8
15.0	-	40.8	31.4
20.0	-	44.5	33.7
25.0	-	47.0	34.6
30.0	-	48.1	-

Table B.2 The Efflux of Water from a Leaf Taken from Wheat Plant Number 4. The leaf was pressurized in a pressure chamber with a 3.0 bar overpressure. The test was conducted on 3/9/79. The plant was under water stress. No pressure^{-1}-volume experiment was conducted on this leaf.

Elapsed Time After Application of a 3 bar Overpressure (min)	Cumulative Water Expressed at Various Initial Balance Pressures (mm^3)		
	With an Initial Balance Pressure of 2.5 bars	With an Initial Balance Pressure of 10.8 bars	With an Initial Balance Pressure of 16.3 bars
0.0	0.0	0.0	0.0
0.5	2.1	2.4	0.5
1.0	3.2	4.3	1.3
1.5	4.1	5.7	1.7
2.0	5.2	7.1	1.8
3.0	6.4	9.6	2.8
4.0	7.5	11.6	4.1
5.0	8.0	13.2	4.9
7.0	8.9	16.6	6.5
10.0	10.0	21.3	8.7
15.0	-	27.2	11.8
20.0	-	32.4	14.4
25.0	-	35.8	16.6
30.0	-	38.1	-
35.0	-	39.4	-

Table B.3 The Efflux of Water from a Leaf Taken from Wheat Plant Number 12. The leaf was pressurized in a pressure chamber with a 3.0 bar overpressure. The test was conducted on 3/12/79. The plant was under water stress. No pressure^{-1}-volume experiment was conducted on this leaf.

Elapsed Time After Application of a 3 bar Overpressure (min)	Cumulative Water Expressed at Various Initial Balance Pressures (mm^3)		
	With an Initial Balance Pressure of 5.0 bars	With an Initial Balance Pressure of 11.3 bars	With an Initial Balance Pressure of 14.5 bars
0.0	0.0	0.0	0.0
0.5	2.6	2.6	2.6
1.0	3.8	4.1	5.3
1.5	3.9	5.4	7.0
2.0	4.0	6.2	8.8
3.0	4.4	8.6	11.5
4.0	4.6	10.5	13.8
5.0	4.7	11.9	15.7
7.0	-	14.6	18.9
10.0	-	18.7	22.6
15.0	-	22.5	27.9
20.0	-	25.1	32.3
25.0	-	26.6	34.9
30.0	-	27.6	36.6
35.0	-	27.6	38.3
40.0	-	-	38.7

Table B.4 The Efflux of Water from a Leaf Taken from Wheat Plant Number 16. The leaf was pressurized in a pressure chamber with a 3.0 bar overpressure. The test was conducted on 3/13/79. The plant was well watered. See table A.1 for the pressure^{-1}-volume experiment conducted on this leaf.

Elapsed Time After Application of a 3 bar Overpressure (min)	Cumulative Water Expressed at Various Initial Balance Pressures (mm^3)			
	With an Initial Balance Pressure of 2.8 bars	With an Initial Balance Pressure of 10.8 bars	With an Initial Balance Pressure of 14.8 bars	With an Initial Balance Pressure of 18.7 bars
0.0	0.0	0.0	0.0	0.0
0.5	3.6	4.1	3.2	0.7
1.0	5.2	7.3	5.5	1.3
1.5	6.5	9.9	7.2	2.2
2.0	7.3	12.5	9.3	3.1
3.0	7.8	17.7	12.3	4.0
4.0	8.7	21.7	14.9	5.0
5.0	8.7	25.6	16.6	5.9
7.0	9.0	31.3	19.7	6.9
10.0	9.0	38.2	22.6	8.2
15.0	-	46.4	25.0	10.6
20.0	-	50.4	26.7	12.9
25.0	-	52.5	28.2	14.9
30.0	-	52.8	29.5	16.1
35.0	-	54.5	30.6	16.7
40.0	-	-	-	16.7

Table B.5 The Efflux of Water from Wheat Leaf 1-D when it was Pressurized in a Pressure Chamber with a 3.0 bar Overpressure. The test was conducted on 7/30/79. The leaf volume was 428 mm^3 and the leaf length was 254 mm. See table A.2 for the pressure^{-1}-volume experiment conducted on this leaf.

Elapsed Time After Application of a 3 bar Overpressure (min)	Cumulative Water Expressed at Various Initial Balance Pressures			
	With an Initial Balance Pressure of 13.3 bars		With an Initial Balance Pressure of 18.2 bars	
	mm^3	mm^3/mm^3 Leaf Vol.	mm^3	mm^3/mm^3 Leaf Vol.
0	0.0	.0	0.0	.0
1	0.6	.0014	7.4	.01729
2	7.1	.01659	11.0	.02570
3	11.8	.02757	13.3	.03107
4	15.4	.03598	14.6	.03411
5	17.7	.04136	14.9	.03481
7	21.7	.05070	-	-
8	-	-	16.6	.03879
9	23.5	.05491	-	-
15	23.5	.05491	-	-
20	23.5	.05491	-	-

Table B.6 The Efflux of Water from Wheat Leaf 1-E when it was Pressurized in a Pressure Chamber with a 3.0 bar Overpressure. The test was conducted on 7/31/79. The leaf volume was 600 mm^3 and the leaf length was 254 mm. No $pressure^{-1}$-volume experiment was conducted on this leaf.

Elapsed Time After Application of a 3 bar Overpressure (min)	Cumulative Water Expressed at Various Initial Balance Pressures					
	With an Initial Balance Pressure of 15.2 bars		With an Initial Balance Pressure of 18.8 bars		With an Initial Balance Pressure of 22.8 bars	
	mm^3	mg/mm^3 Leaf Vol.	mm^3	mg/mm^3 Leaf Vol.	mm^3	mg/mm^3 Leaf Vol.
0	0.0	.0	0.0	.0	0.0	.0
1	9.9	.01650	11.2	.01867	9.9	.0165
2	15.1	.02517	17.5	.02917	13.3	.02217
3	19.1	.03183	19.9	.03317	15.3	.02550
4	21.2	.03533	21.1	.03517	16.3	.02717
5	22.3	.03717	22.6	.03767	16.7	.02783
7	22.9	.03817	23.1	.03850	16.7	.02783
10	22.9	.03817	23.1	.03850	16.7	.02783
15	22.9	.03817	23.1	.03850		.02833

Table B.7 The Efflux of Water from Wheat Leaf 2-E when it was Pressurized in a Pressure Chamber with a 3.0 bar Overpressure. The test was conducted on 7/31/79. The leaf volume was 865 mm^3 and the leaf length was 338.1 mm. See table A.2 for the $pressure^{-1}$-volume experiment conducted on this leaf.

Elapsed Time After Application of a 3 bar Overpressure (min)	Cumulative Water Expressed at Various Initial Balance Pressures					
	With an Initial Balance Pressure of 3.4 bars		With an Initial Balance Pressure of 7.2 bars		With an Initial Balance Pressure of 10.4 bars	
	mm^3	mm^3/mm^3 Leaf Vol.	mm^3	mm^3/mm^3 Leaf Vol.	mm^3	mm^3/mm^3 Leaf Vol.
0	0.0	.0	0.0	.0	0.0	.0
1	-	-	-	-	-	-
2	0.4	.000462	4.4	.005086	6.7	.007746
3	0.9	-	-	-	-	-
4	0.9	.001046	5.0	.005780	12.3	.01422
6	1.4	.001618	5.0	.005780	16.6	.01919
8	-	-	5.6	.006474	21.0	.02428
10	-	-	-	-	23.5	.02717
12	-	-	-	-	-	-
15	-	-	-	-	29.0	.03353
16	-	-	-	-	-	-
18	-	-	-	-	-	-
20	-	-	-	-	32.6	.03769
22	-	-	-	-	-	-
25	-	-	-	-	34.2	.03954
30	-	-	-	-	34.9	.04035
32	-	-	-	-	-	-
35	-	-	-	-	-	-
40	-	-	-	-	-	-

(continued)

Table B.7 concluded

Elapsed Time After Application of a 3 bar Overpressure (min)	Cumulative Water Expressed at Various Initial Balance Pressures					
	With an Initial Balance Pressure of 13.2 bars		With an Initial Balance Pressure of 16.4 bars		With an Initial Balance Pressure of 19.6 bars	
	mm^3	mm^3/mm^3 Leaf Vol.	mm^3	mm^3/mm^3 Leaf Vol.	mm^3	mm^3/mm^3 Leaf Vol.
0	0.0	.0	0.0	.0	0.0	.0
1	8.7	.01006	11.5	.01329	7.8	.0090
2	14.8	.01711	18.1	.02092	13.0	.01503
3	20.8	.02405	23.4	.02705	17.2	.01988
4	25.1	.02902	27.3	.03156	21.5	.02486
6	34.0	.03931	35.2	.04069	26.7	.03087
8	39.8	.04601	40.7	.04705	30.1	.03480
10	-	-	-	-	-	-
12	49.3	.05699	48.2	.05572	35.2	.04069
15	-	-	-	-	-	-
16	-	-	-	-	38.1	.04405
18	59.0	.06821	54.5	.06301	-	-
20	-	-	-	-	-	-
22	-	-	-	-	40.1	.04630
25	65.5	.07572	58.0	.06705	-	-
30	-	-	-	-	-	-
32	68.7	.07942	-	-	-	-
35	-	-	58.5	.06763	-	-
40	70.8	.08184	-	-	-	-

Table B.8 The Efflux of Water from Wheat Leaf 1-F when it was Pressurized in a Pressure Chamber with a 3.0 bar Overpressure. The test was conducted on 8/1/79. The leaf volume was 268 mm^3 and the leaf length was 177.8 mm. See table A.2 for the $pressure^{-1}$-volume experiment conducted for this leaf.

Elapsed Time After Application of a 3 bar Over-pressure (min)	Cumulative Water Expressed at Various Initial Balance Pressures							
	With an Initial Balance Pressure of 12.2 bars		With an Initial Balance Pressure of 15.8 bars		With an Initial Balance Pressure of 19.3 bars		With an Initial Balance Pressure of 22.5 bars	
	mm^3	mm^3/mm^3 Leaf Vol.	mm^3	mm^3/mm^3 Leaf Vol.	mm^3	mm^3/mm^3 Leaf Vol.	mm^3	mm^3/mm^3 Leaf Vol.
0	0.0	.0	0.0	.0	0.0	.0	0.0	.0
1	-	-	4.3	.01609	2.4	.008955	-	-
2	3.6	.01343	7.8	.02910	2.7	.01007	2.2	.008209
3	-	-	10.3	.03843	2.7	.01007	-	-
4	5.4	.02015	11.6	.04328	2.7	.01007	2.5	.009328
6	6.6	.02463	13.3	.04963	2.7	.01007	-	-
8	-	-	13.8	.05149	-	-	-	-
10	7.7	.02872	-	-	2.7	.01007	-	-
12	-	-	13.8	.05149	-	-	-	-
15	-	-	-	-	-	-	-	-
18	-	-	13.8	.05149	-	-	-	-

Table B.9 The Efflux of Water from Wheat Leaf 2-G when it was Pressurized in a Pressure Chamber with a 3.0 bar Overpressure. The test was conducted on 8/2/79. The leaf volume was 406 mm^3 and the leaf length was 238 mm. See table A.2 for the $pressure^{-1}$-volume experiment conducted on this leaf.

Elapsed Time After Application of a 3 bar Over-pressure (min)	Cumulative Water Expressed at Various Initial Balance Pressures							
	With an Initial Balance Pressure of 14.0 bars		With an Initial Balance Pressure of 17.5 bars		With an Initial Balance Pressure of 20.5 bars		With an Initial Balance Pressure of 23.3 bars	
	mm^3	mm^3/mm^3 Leaf Vol.	mm^3	mm^3/mm^3 Leaf Vol.	mm^3	mm^3/mm^3 Leaf Vol.	mm^3	mm^3/mm^3 Leaf Vol.
0	0.0	.0	0.0	.0	0.0	.0	0.0	.0
1	5.9	.01453	3.3	.008128	4.1	.01009	2.5	.006158
2	9.8	.02414	6.5	.01601	7.1	.01749	-	-
3	13.2	.03251	8.9	.02192	-	-	3.8	.009360
4	16.3	.04015	9.8	.02414	9.5	.02340	-	-
6	21.2	.05222	12.2	.03005	9.5	.02340	-	-
7	-	-	-	-	-	-	5.5	.01355
8	24.8	.06108	13.6	.03350	-	-	-	-
10	-	-	-	-	9.5	.02340	-	-
12	29.5	.07266	13.8	.03399	-	-	5.7	.01404
16	31.9	.07857	13.8	.03399	-	-	-	-
25	37.0	.09112	-	-	-	-	-	-

Table B.10 The Efflux of Water from Wheat Leaf 3-G when it was Pressurized in a Pressure Chamber with a 3.0 bar Overpressure. The test was conducted on 8/2/79. The leaf volume was 286 mm^3 and the leaf length was 202 mm. See table A.2 for the pressure^{-1}-volume experiment conducted for this leaf.

Elapsed Time After Application of a 3 bar Overpressure (min)	Cumulative Water Expressed at Various Initial Balance Pressures					
	With an Initial Balance Pressure of 14.3 bars		With an Initial Balance Pressure of 17.2 bars		With an Initial Balance Pressure of 20.3 bars	
	mm^3	mm^3/mm^3 Leaf Vol.	mm^3	mm^3/mm^3 Leaf Vol.	mm^3	mm^3/mm^3 Leaf Vol.
0	0.0	.0	0.0	.0	0.0	.0
1	5.5	.01923	-	-	-	-
2	-	-	6.3	.02378	5.6	.01958
3	13.5	.04720	-	-	-	-
5	17.3	.06049	11.5	.04021	9.5	.03322
8	21.2	.07413	-	-	-	-
9	-	-	14.6	.05105	11.9	.04161
12	23.6	.08252	-	-	-	-
15	-	-	16.1	.05629	13.5	.04720
16	23.7	.08287	-	-	-	-

Table B.11. The efflux of water from wheat leaf 1-H when it was pressurized in a pressure chamber with a 3.0 bar overpressure. The test was conducted on 11/20/79. The leaf volume was 291 mm^3 and the leaf length was 225 mm. See table A.3 for the $pressure^{-1}$–volume experiment conducted on this leaf.

Elapsed Time After Application of a 3 bar Overpressure (min)	Cumulative Water Expressed at Various Initial Balance Pressures			
	With an Initial Balance Pressure of 11.5 bars		With an Initial Balance Pressure of 14.5 bars	
	mm^3	mm^3/mm^3 Leaf Vol.	mm^3	m^3/mm^3 Leaf Vol.
0	0.0	0.0	0.0	0.0
1	4.4	.0151	1.7	.00584
2	7.0	.0241	2.6	.00893
3	7.0	.0241	2.7	.00928
4	7.3	.0251	2.7	.00928
6	10.3	.0354	3.2	.0110
8	13.0	.0447	3.8	.0131
10	13.2	.0453	4.1	.0141
15	15.3	.0526	4.1	.0141
20	17.1	.0588	4.1	.0141

Table B.12. The efflux of water from wheat leaf 2-H when it was pressurized in a pressure chamber with a 3.0 bar overpressure. The test was conducted on 11/20/79. The leaf volume was 272 mm^3 and the leaf length was 248 mm. See table A.3 for the $pressure^{-1}$-volume experiment conducted on this leaf.

Elapsed Time After Application of a 3 bar Overpressure (min)	Cumulative Water Expressed at Various Initial Balance Pressures			
	With an Initial Balance Pressure of 11.1 bars		With an Initial Balance Pressure of 13.7 bars	
	mm^3	mm^3/mm^3 Leaf Vol.	mm^3	mm^3/mm^3 Leaf Vol.
0	0.0	0.0	0.0	0.0
1	6.5	.0239	2.4	.00882
2	8.0	.0294	4.5	.0165
4	12.0	.0441	7.1	.0261
6	13.5	.0496	8.6	.0316
10	13.6	.0500	9.9	.0364
15	14.4	.0529	9.9	.0364
17	----	-----	10.0	.0368

Table B.13. The efflux of water from wheat leaf 1-I when it was pressurized in a pressure chamber with a 3.0 bar overpressure. The test was conducted on 11/21/79. The leaf volume was 315 mm^3 and the leaf length was 246 mm. See table A.3 for the $pressure^{-1}$-volume experiment conducted on this leaf.

Elapsed Time After Application of a 3 bar Overpressure (min)	Cumulative Water Expressed at Various Initial Balance Pressures			
	With an Initial Balance Pressure of 10.6 bars		With an Initial Balance Pressure of 13.6 bars	
	mm^3	mm^3/mm^3 Leaf Vol.	mm^3	mm^3/mm^3 Leaf Vol.
0	0.0	0.0	0.0	0.0
1	0.8	.00254	0.0	0.0
2	1.1	.00349	6.1	.0194
4	3.9	.0124	9.9	.0314
6	5.0	.0159	13.0	.0413
10	7.5	.0238	16.7	.0530
15	8.8	.0279	20.5	.0651
20	10.6	.0337	23.5	.0746
25	11.8	.0375	25.5	.0810
30	----	-----	26.9	.0854
35	----	-----	27.9	.0886
40	----	-----	28.4	.0902

Appendix C

Solution of Equations 8.11 and 8.12

by

Separation of Variables

APPENDIX C

The following is a description of a solution of equations 8.11 and 8.12 using the technique of separation of variables. Equations 8.11 and 8.12 are:

$$P'' = k_1\dot{\eta} \qquad \text{(C-1)}$$

$$\dot{\eta} = k_2P - k_3\eta - k_4 \qquad \text{(C-2)}$$

with boundary conditions:

$$P = 0 \qquad x = 0 \qquad \text{(C-3)}$$

$$P' = 0 \qquad x = \ell \qquad \text{(C-4)}$$

Let:

$$\xi = \eta + \frac{k_4}{k_3} \qquad \text{(C-5)}$$

Changing the variable in the above equations gives:

$$P'' = k_1\dot{\xi} \qquad \text{(C-6)}$$

$$\dot{\xi} = k_2P - k_3\xi \qquad \text{(C-7)}$$

Assume that ξ and P are separable so that they can be written:

$$\xi = F(x)\ R(t) \qquad \text{(C-8)}$$

$$P = H(x)\ G(t) \qquad \text{(C-9)}$$

Substituting (C-8) and (C-9) into (C-6) and (C-7) gives:

$$H''G = k_1F\dot{R} \qquad \text{(C-10)}$$

$$F\dot{R} = k_2HG - k_3FR \qquad \text{(C-11)}$$

From equation (C-11):

$$F(\dot{R} - k_3R) = k_2HG \qquad \text{(C-12)}$$

or:

$$\frac{H}{F} = \frac{\dot{R} - k_3R}{k_2G} \qquad \text{(C-13)}$$

The right-hand side is a function of time only. Therefore, at any given time it will have one value. This suggests that H and F are proportional, differing only by a constant. Since a series solution of the equations is being sought, this constant could be "absorbed" in the expansion of R and G. Therefore, H and F can be equated. Equations (C-10) and (C-11) now become:

$$H''G = k_1 H\dot{R} \qquad \text{(C-14)}$$

$$H\dot{R} = k_2 HG - k_3 HR \qquad \text{(C-15)}$$

Equation (C-14) can be rearranged to give:

$$\frac{H''}{H} = \frac{k_1 \dot{R}}{G} \qquad \text{(C-16)}$$

Let:

$$\frac{H''}{H} = \alpha$$

If α is equal to zero, then H is of the form:

$$H = c_1 + c_2 x$$

If it is greater than zero, then H is of the form:

$$H = c_1 \sinh \sqrt{\alpha} x + c_2 \cosh \sqrt{\alpha} x$$

and if it is less than zero, then H is of the form:

$$H = c_1 \sin \lambda x + c_2 \cos \lambda x$$

where:

$$\alpha = -\lambda^2$$

Since it was assumed that $P = H(x)\, G(t)$, if P or P' is zero for a given value of x and all values of time, then H or H' must also be zero. Therefore:

$$H = 0 \quad \text{when} \quad x = 0$$

and

$$H' = 0 \quad \text{when} \quad x = \ell$$

For the cases where α is equal to or greater than zero, the above conditions can only be satisfied when c_1 and c_2 are both zero. The only nontrivial solution is therefore:

$$H = c_1 \sin \lambda x + c_2 \cos \lambda x \qquad \text{(C-17)}$$

Applying the condition H=0 when x=0 to (C-17) gives:

$$c_2 = 0$$

If H' is zero when $x = \ell$, there is a nontrivial solution ($c_1 \neq 0$) only if:

$$\lambda_n = \frac{n\pi}{2\ell} \qquad \text{(C-19)}$$

Therefore:

$$H_n = c_n \sin \lambda_n x \qquad \text{(C-20)}$$

with λ_n as defined in (C-19)

Substituting (C-20) into (C-14) gives:

$$\frac{k \dot{R}_n}{G_n} = -\lambda_n^2 \qquad \text{(C-21)}$$

or

$$G_n = \frac{-k \dot{R}_n}{\lambda_n^2} \qquad \text{(C-22)}$$

Substituting (C-22) into (C-15) gives:

$$\dot{R}_n = \frac{-k_3}{1 + \frac{k_2 k_1}{\lambda_n^2}} R_n \qquad \text{(C-23)}$$

or

$$\dot{R}_n = \mu_n R_n \,, \qquad \text{(C-24)}$$

where:

$$\mu_n = \frac{-k_3}{1 + \frac{k_2 k_1}{\lambda_n^2}}$$

The solution to equation (C-24) is:

$$R_n = b_n e^{\mu_n t} \qquad \text{(C-25)}$$

From (C-22):

$$G_n = \frac{-k_1 \dot{R}_n}{\lambda_n^2} \qquad \text{(C-26)}$$

Since P and ξ are defined by H, G, and R:

$$P = HG = \sum_{i=1,3,5,\ldots}^{\infty} \frac{-b_n c_n k_1 \mu_n e^{\mu_n t} \sin(\lambda_n x)}{\lambda_n^2} \qquad \text{(C-27)}$$

$$\xi = HR = \sum_{i=1,3,5,\ldots}^{\infty} b_n c_n e^{\mu_n t} \sin(\lambda_n t) \qquad \text{(C-28)}$$

The coefficients $b_n c_n$ can be determined using the initial conditions on η and the relation:

$$\xi(x,o) = \eta(x,o) + \frac{k_4}{k_3} \qquad \text{(C-29)}$$

For a given set of cell properties and for a given initial balance pressure, $\xi(x,0)$ will have a unique value. Call this value "a." At t=0 $e^{\mu_n t}$ is one and equation (C-28) gives:

$$\xi(x,o) = a = \sum_{n=1,3,5,\ldots}^{\infty} b_n c_n \sin(\lambda_n x) \qquad \text{(C-30)}$$

Multiplying both sides of equation (C-30) with $\sin \lambda_m x$, integrating from 0 to ℓ on dx, and using the orthogonality properties of the

trigonometric functions gives an expression for $b_m c_m$:

$$b_m c_m = \frac{4a}{m\pi} \qquad \text{(C-31)}$$

The expressions for P and η can be written by solving (C-5) for η, using (C-27) and (C-28) for P and ξ, and substituting (C-31) for $b_n c_n$. This gives the following expressions for P and η:

$$P(x,t) = \frac{4ak_1}{\pi} \sum_{n=1,3,5,\ldots}^{\infty} \frac{\mu_n}{n\lambda_n^2} e^{\mu_n t} \sin(\lambda_n x) \qquad \text{(C-32)}$$

$$\eta(x,t) = -\frac{k_4}{k_3} + \frac{4a}{\pi} \sum_{n=1,3,5,\ldots}^{\infty} \frac{e^{\mu_n t}}{n} \sin(\lambda_n x) \qquad \text{(C-33)}$$